Th.J. van de Nes

Department of Hydraulics and Catchment Hydrology
Agricultural University, Wageningen

LINEAR ANALYSIS OF A PHYSICALLY BASED MODEL OF A DISTRIBUTED SURFACE RUNOFF SYSTEM

2062322

ABSTRACT

Nes, Th.J. van de, 1973. Linear analysis of a physically based model of a
distributed surface runoff system. Agric. Res. Rep. (Versl. Landbouwk. Onderz.)
799. ISBN 90 220 0458 9, (viii) + 104 p., 5 tbs, 48 figs, 39 refs, Eng. and
Dutch summaries.
Also: Doctoral thesis, Wageningen.

    As part of a model for the rainfall-run-off relation of a catchment, a
linear distributed model of surface run-off is presented in this report.
    This model, without internal boundary conditions, consists of a cascade
of linear conceptual elements. It simulates the complex drainage system by
a network of overland flow and channel-flow elements. These elements obey
the one-dimensional equations for unsteady flow in a channel. Simplification
and linearisation of the dynamic equations lead to diffusion type equations.
Their solution for suitable boundary conditions yield the impulse response
functions, which characterize the operation of the elements. Special attention
is given to the application of the techniques of linear system analysis, such
as moments and spectra. These techniques produce information on the relative
importance of the various conceptual elements. Consequently it is possible
to decide on the necessary detail in the variation in time and space of both
the inflow and structure of the drainage model.
    Results obtained by using the linear model have been compared with results
of a more exact non-linear model and have been encouraging. At the end some
practical applications have been given.

CONTENTS

1.INTRODUCTION

In catchment hydrology one can distinguish two broad classifications of
problems.
i) hydrograph forecasting on a short term basis
ii) discharge frequency prediction on a long term basis
Two major groups of factors affect the run-off from a catchment: hydrometeoro-
logic factors (rainfall, snow and evapotranspiration) make up one group, and the
other group consists of physiographic factors (physical characteristics of the
catchment).
The understanding of hydrological processes requires modelling, which is the
reason why scientific hydrology has always been concerned with mathematical
modelling.
Hydrologists usually differentiate between deterministic and stochastic models.
No final concensies of opinion has however been reached as to which techniques
belong to the fields of either deterministic or stochastic simulation. Broadly
stated the two approaches can be discerned as follows:
A deterministic model is essentially an abstraction of the way a system trans-
forms the input into the output. Both the structure of the model and the choice
of the parameters should reflect some conception of the system's structure and
the principal laws that govern the system's transformation. Consequently the
model parameters are to a certain degree related to physical characteristics
of the system. Because of the role which the parameters play in the subsequent
fitting of the model to the observed system's cause-effect relationship the
deterministic approach is often indicated as "parametric modelling". The de-
terministic model is meant to describe transient responses and it is mainly
used for the generation of hydrographs from precipitation data either for flood
forecasting or water management purposes (Schermerhorn and Kuehl, 1968).
A stochastic model however is meant to generate time series which are statis-
tically indistinguishable from certain measured records. Usually the modelling
of a cause-effect relationship is not the main object and the parameters or
coefficients are mainly of a pure statistical nature. Consequently a stochastic
model is a less appropriate tool for describing actual hydrographs but it can
generate "equally likely" series of smoothly varying responses (Fiering, 1967).
In this report only the deterministic approach is used for hydrograph fore-
casting on a short term basis. The more closely the model approximates the
physical system, the more accurately does it predict. However an increasing
complexity of the model makes it also more difficult to handle. Therefore it-

is necessary to compromise between accuracy and simplicity when developing models.

The advent of the digital computer has allowed in all areas of hydrology the use of more complex models that are closer to the physical systems. In this respect a division can be made into component modelling and integrated system modelling (Dawdy, 1969).

In component modelling the land phase of the hydrologic cycle can be divided into several parts (infiltration, evapotranspiration, aquifer response and surface streamflow routing). The empirical approach to the mathematical process controlling each component is being gradually replaced by a theoretical approach, based on the physical laws governing the component, in an attempt to make the empirical approximations more equivalent to the theoretical physical laws. It must be stressed at this point that even with the theoretical hydro-dynamic approach many simplifications and approximations have to be made. In general for the various flow processes this approach leads to non-linear partial differential equations which for given boundary conditions, can be solved numerically by a digital computer. The various components will be combined in the integrated system modelling. The purpose of developing better conceptual models for the individual components is on the one hand to solve particular problems in hydrology and on the other to improve the overall model of the total system. However the development of the model increases its complexity, which to a certain extent limits the use of the better model. The difficulty is not lack of understanding of the physical processes but firstly not knowing the boundary conditions and their dependence on the interaction of the various flow processes, secondly the problem of accurate measurement of physical characteristics of the catchment and thirdly the impracticability of dealing with detailed variations in time and space.

In the recent years the systems approach was introduced in hydrology (e.g. Nash 1959; Dooge, 1959, 1967; Vemuri et al, 1970) with its powerful systems engineer-ing techniques, so that system analysis has had a strong impact upon the metho-dology of mathematical modelling.

This report shows how the techniques of linear system analysis can be used for the optimization of parameters in a conceptual model for the surface component, consisting of overland flow and channel flow, as a part of a complex simulation model of the rainfall-run-off relation for a catchment. The approach of Dooge, Harley and O'Meara (1967, 1968), who introduced linear conceptual models for the surface run-off based on the hydrodynamics of channel flow is also followed in this report. Summarizing it can be stated that a

combination of the linear systems theory and the hydrodynamic approach in the
study of the surface run-off system seems effective for the following reasons:
1. There is a direct relationship between the physical structure of the system
   and the structure of the model as it describes the system's operation. There-
   fore there is also a relation between physical characteristics and model
   parameters.
2. Powerful techniques from system analysis can be used.
3. Approximate solutions for complex systems are possible.
4. Influence of the initial and boundary conditions can be studied.
5. Necessary compromise between the desires for accuracy, simplicity and
   physical understanding can be reached in this type of approach.

1.1. OBJECTIVES AND SCOPE OF THE STUDY

The complexity of the flow process by which surface run-off flows overland into
small rivulets then into larger channels and finally into a river channel, makes
it difficult to find exact solutions, based on hydrodynamics, because of the
complex boundary conditions. Therefore, simplification is necessary for solving
this complex problem. Recent technological progress in computer facilities has
stimulated the hydrodynamic approach to the surface run-off problem. Cheng Lung
Chen and Ven te Chow (1968) formulated a mathematical model, which describes
the mechanics of surface run-off of a catchment by treating the watershed as
a non-linear distributed system subject to hydrodynamic principles, using the
complete dynamic equation for the one dimensional flow, including the over-
pressure of raindrop impact. The non-linear equations were solved by the method
of characteristics using the explicit scheme for a simplified overland flow
problem. However, for complex systems with a large number of internal boundary
conditions this results in an extremely lengthy computer program that is beyond
the capacity of computers available at present. At the same time Dooge, Harley
and O'Meara (1967, 1968) used a linearized version of the complete dynamic
equation and derived analytical solutions for the upstream inflow and lateral
inflow or overland flow problem. These solutions are used as basic elements
for a linear distributed model of catchment run-off by Bravo, et al (1970).
These linear solutions were introduced into the MIT catchment model as an alter-
native for the kinematic non-linear solution, as developed by Henderson and
Wooding (1964, 1965, 1966). However, this model has some disadvantages. Firstly,
because water is restricted to flowing in one direction only, which physically
is incorrect. Secondly, because the analytical solutions are very complex, which

3

causes difficulties in the calculation.

For these reasons in this paper the dynamic equation is first simplified and then linearised. This leads to a diffusion type equation as proposed by Schön-feld (1948); Hayami (1951); Daubert (1964) and Harley (1967). The latter showed that for the upstream inflow the diffusion type solution leads to very small deviations with respect to the complete linear solution and it can be assumed that the error due to the linearization is much more important.

For the diffusion type equations analytical solutions are derived for the tributary and lateral inflow or overland flow, without restriction for reversed flow in the considered channelreach. In combination with the solution for the upstream inflow a complex distributed conceptual model can be constructed. In combination with the linear systems approach the instantaneous unit hydrograph (IUH), the summation curves (S-curves), shape factors and spectra, expressed in the model parameters, are derived for the various linear elements. These techniques yield information on the relative importance of the various conceptual elements. Consequently, it is possible to decide on the necessary variation in time and space of both the inflow and the degree of detail in the model structure which is needed to provide computed results of sufficient accuracy. This is an interesting aspect of this study because it appears to add a theoretical background to the experimental fact that the run-off process in drainage basins can often be simulated by simple conceptual models with lumped parameters and lumped inputs, such as the model suggested by Nash (1959, 1960).

4

2. THE SYSTEMS APPROACH

The rainfall and run-off relation of a catchment has been described by
classic hydrology in terms of surface run-off, interflow and groundwater flow.
In practice quantitative hydrology usually modifies this concept and considers
the hydrograph to be made up of a direct storm response and a base flow.
In Fig. 2.1 a picture of the simplified catchment model is given, which is
borrowed from Dooge (1967).
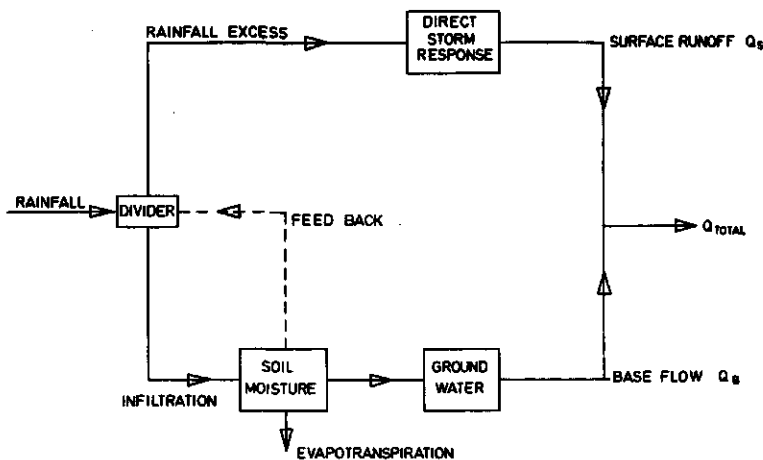
fig. 2.1 Simplified catchment model (Dooge 1967)

This system consists of three subsystems, the subsystem involving the direct
storm response or surface run-off, the subsystem involving groundwater response
and the subsystem soil phase, which has a feedback loop to the separation of
precipitation into precipitation excess and infiltration.
In this report only the first subsystem involving the surface run-off is
considered. Speaking in system terminology the surface run-off system
transforms an input (= inflow or rainfall excess) into an output (= discharge
or storage expressed as water depth). Quoting Dooge (1967): "the rôle of the
system in generating output from input, or in interrelating input and output,
is its essential feature. The output from any system depends on the nature of
the input, the physical laws involved, and the nature of the system itself,
both the nature of the components and the structure of the system according to
which they are connected". (Fig. 2.2)

5
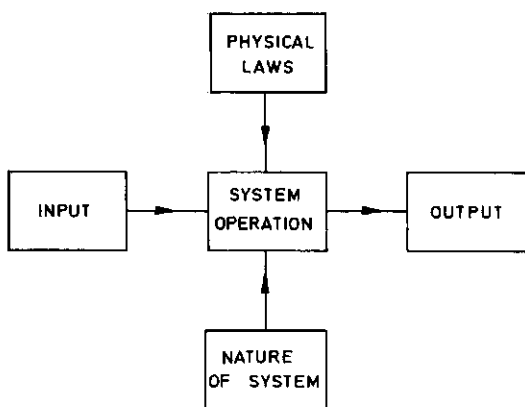
fig. 2.2 Concept of system operation (Dooge 1967)

In the system analysis however the overall operation of the system is examined without taking into account all the complex details of the system or all the complex physical laws involved. Although the system operation depends on the physical laws and the nature of the system, this dependence may be ignored in this approach to the problem. This is represented by the horizontal components in Fig. 2.2.

Thus in unit hydrograph studies, once the unit hydrograph has been derived from records of input and output, it can be used as a prediction tool without reference to the nature of the catchment or the physical laws involved.

In the system synthesis however, where a synthetic unit hydrograph has to be derived, or the validity of the unit hydrograph procedure must be examined, it is necessary to examine the connection between the unit hydrograph, the characteristics of the watershed, and the physical laws governing its behaviour. This relation is represented by the vertical components in Fig. 2.2.

2.1. LINEAR SYSTEMS

The linearisation of the non-linear differential equations with constant coefficients, describing the non-steady channel and overland flow makes it possible to consider the surface run-off problem as a linear time invariant system, which is characterised by the convolution integral

$$y(t) = {_0}\!\int^{t} x(\tau)h(t-\tau) \, d\tau$$

or   (2.1)

$$y(t) = {_0}\!\int^{t} x(t-\tau)h(\tau) \, d\tau$$

This convolution integral expresses the relation between the output $y(t)$, the input $x(t)$ and the instantaneous unit hydrograph (IUH) or the impulse response $h(t)$, which characterises the system operation.

If the input is given as a histogram the convolution integral takes the following discrete form:

$$y(n\Delta t) = \Delta t \sum_{i=0}^{n} p(i+1)h(\Delta t, (n-i)\Delta t) \tag{2.2}$$

where $p(i+1)$ represents the successive volumes of the input and $h(\Delta t, (n-i)\Delta t)$ the finite period (Δt) unit hydrograph (TUH). This can be derived from the summation curve defined as

$$S(t) = {_0}\!\int^{t} h(o,\tau) \, d\tau \tag{2.3}$$

It follows that:

$$h(\Delta t, (n-i)\Delta t) = \{S((n-i)\Delta t) - S((n-i-1)\Delta t)\} / \Delta t \, , \, n > i \tag{2.4}$$

$$h(\Delta t, (n-i)\Delta t) = 0 \quad , \, n < i$$

The shape of the IUH, can be characterised by statistical moments, shape factors (Nash, 1959) and spectra (Eagleson, 1966), expressed in the system parameters.

2.2. STATISTICAL MOMENTS AND SHAPE FACTORS

As shown by Nash (1959) and Diskin (1967) the moments in the linear systems approach are very powerful tools for finding the model parameters from input and output, because the following relations between the moments of input, output and IUH exist.

$$M_1'(y) = M_1'(x) + M_1'(h)$$

$$M_2(y) = M_2(x) + M_2(h) \qquad (2.5)$$

$$M_3(y) = M_3(x) + M_3(h)$$

The relation for the higher moments are more complex.
The moments of a function $f(t)$ relative to the origin are defined as:

$$M_n'(f) = {}_o\!\int^\infty ft^n dt / {}_o\!\int^\infty fdt \qquad (2.6)$$

and relative to the centre of area (first moment)

$$M_n(f) = {}_o\!\int^\infty f(t-M_1')^n dt / {}_o\!\int^\infty fdt \qquad (2.7)$$

The first moment of the IUH relative to the origin gives the lag or the mean, the second, third and fourth moment relative to the mean are the variance, the skewness and the kurtosis respectively.
The Laplace transform of the function $f(t)$, is defined as

$$\tilde{f}(\lambda) = {}_o\!\int^\infty e^{-\lambda t} f(t) \, dt$$

or $\qquad (2.8)$

$$\tilde{f}(\lambda) = {}_o\!\int^\infty f(t)dt - \lambda \, {}_o\!\int^\infty tf(t) \, dt + \frac{\lambda^2}{2!} {}_o\!\int^\infty t^2 f(t) \, dt - \ldots$$

This equation shows how the Laplace transform of the function is related to the moments of that function. So that Eq. (2.8) can be considered as the moment generating function.

$$(-1)^n \left(\frac{d^n \tilde{f}}{d\lambda^n}\right)_{\lambda=o} = {}_o\!\int^\infty f(t) \, t^n dt$$

or

$$M_n'(f) = (-1)^n \left(\frac{d^n \tilde{f}}{d\lambda^n}\right)_{\lambda=o} \cdot / \tilde{f}(o) \qquad (2.9)$$

The IUH for the different conceptual elements are derived by means of the Laplace transform, so with Eq. (2.9) the moments of the IUH can easily be derived.

8

In fact Nash (1960) does not use the moments of the IUH but the shape factors, defined as:

$$S_1 = M_1'(h)$$
$$S_2 = M_2(h)/(M_1'(h))^2$$
$$\vdots$$
$$S_n = M_n(h)/(M_1'(h))^n$$

(2.10)

all of which, except S_1 are dimensionless and therefore less likely to be mutually correlated than $M_1'(h)$, $M_2(h)$, etc., while it has the advantage that scale effects have disappeared, when the IUH of different conceptual models are compared with each other. In our case, where the IUH for the various types of inflow problems are based on two or three model parameters, S_3 and S_2 are used for comparison.

Harley (1967) proposed to use the cumulants for characterising the system, but because the first three moments are equal to the first three cumulants, which are dominant for the shape of the IUH, the cumulants will not be discussed here.

2.3. ATTENUATION COEFFICIENT

If the input and output in the rainfall-run-off process or in flood routing are compared it is clear that the system has a translation i.e. lag and an attenuation. The time lag can be calculated from the first moment of the IUH. It is reasonable to assume that the second moment of the IUH and of the input can together be a good index for the attenuation. It is well known that a peaked wave attenuates much quicker than a long duration wave. Expressing the attenuation of the wave in a coefficient as follows

$$C_A = \frac{M_2(y) - M_2(x)}{M_2(x)} = \frac{M_2(h)}{M_2(x)}$$

(2.11)

By plotting calculated values of this attenuation coefficient C_A against corresponding values of the specific attenuation R_A, defined as:

$$R_A = \frac{x_p - y_p}{x_p} \cdot 100\%$$

(2.12)

where x_p and y_p are respectively the peak values of the input and the output, an empirical relation was obtained. Thus the attenuation coefficient C_A is an index for the specific attenuation.

Because the attenuation coefficient C_A for a conceptual model can be expressed by model parameters and by characteristics of the input (duration and shape) a first quick estimate of the specific attenuation of the peak can be made if the model parameters and duration and shape of the input are known or can be estimated.

As will be shown later conversely this relation can be used to find the model parameters if the specific attenuation is known.

Therefore an iteration procedure is required.

2.4. SPECTRA

Simular to the Laplace transform, which yielded a simple relation between the moments, also the Fourier transforms of input, output and IUH will be shown to be simply related. (Eagleson, 1966)

By this transform the behaviour of the system is replaced from the time domain to the frequency domain - as follows:

$$\hat{h}(\omega) = {}_o\!\!\int^\infty h(t)\ e^{-j\omega t}\ dt \tag{2.13}$$

where the spectralfunction $\hat{h}(\omega)$ in general is complex i.e.

$$\hat{h}(\omega) = r(\omega) + j i(\omega)$$

and is commonly described by an amplitude density spectrum

$$\hat{h}_a(\omega) = \{r^2(\omega) + i^2(\omega)\}^{\frac{1}{2}} \tag{2.14a}$$

and a phase density spectrum

$$\hat{h}_\theta(\omega) = \tan^{-1} \frac{i(\omega)}{r(\omega)} \quad (\text{mod } \pi) \tag{2.14b}$$

where r is the real part, i the imaginary part and ω the frequency in radians per time interval.

Application of the Fourier transform to the convolution integral yields for linear time invariant systems

10

$$\hat{y}(\omega) = \hat{x}(\omega)\hat{h}(\omega)$$

and
$$\hat{y}_a(\omega) = \hat{x}_a(\omega)\hat{h}_a(\omega) \qquad\qquad (2.15)$$

$$\hat{y}_\theta(\omega) = \hat{x}_\theta(\omega) + \hat{h}_\theta(\omega)$$

which in a similar way to moments, interrelates input, output and IUH. This is to be expected because there is a relation between the Fourier transform and the Laplace transform.

By applying the Fourier transform the system seems to act as a low pass filter, which filters out the high frequency energy of the input. The Fourier transform of an impulse (delta input or dirac function) is real and constant over all frequencies. Thus the Fourier transform of the impulse response can be interpreted as the output of a low pass filter, when excited by a signal having a uniform amplitude density (i.e. is flat).

Eagleson, et al (1966) have shown that comparing the spectra of input and IUH leads to conclusions about the sampling interval Δt, with which the input has to be measured, i.e. it gives the duration of the unit storm period. The distribution of the input within this unit storm period does not influence the output. Therefore the assumption is made that the filter has an upper limit ω_c, so that all higher frequencies of the input spectrum will be filtered out. This implies that it is not necessary to measure the higher frequencies, because they do not supply any significant information. The signal pulse of duration Δt of the input behaves as an impulse to the system in question if its amplitude density spectrum is flat for $0 < \omega < \omega_m$, with $\omega_m \geqslant \omega_c$.

For some rainfall spectra it is found, that they are flat for $\omega_m \Delta t \leqslant 1$ radian, so the unit storm period $\Delta t \leqslant \dfrac{1}{\omega_m} < \dfrac{1}{\omega_c}$ $\qquad\qquad (2.16a)$

which is only valid if the band width of the input signal $\omega_p > \omega_c$. However if $\omega_p < \omega_c$ than the whole input spectrum is of interest.

Defining the band width of the input signal

$$0 \leqslant \text{band width} < \omega_p$$

and arbitrarily select a fairly conservative cutoff frequency ω_p such that

$$\hat{x}_a(\omega_p) = 0{,}05 \; \hat{x}_a(0)$$

which represents the 13 db point on the amplitude density curve then

Hamming (1962) has shown that for band-limited functions the time interval Δt can be expressed as follows:

$$\Delta t \leqslant \frac{\pi}{\omega_p} \qquad (2.16b)$$

Comparison of the spectra of the IUH for the different types of inflow problems, shows the influence of the system parameters on the shape of the IUH. If the amplitude-density spectra are nearly the same then the shapes of the IUH are also nearly the same. The time shift between the IUH's follows from the phase density spectra.

The following relation applies:

$$\widehat{\tau_{t_o} h}(\omega) = e^{-j\omega t_o} \hat{h}(\omega)$$

where τ_{t_o} is the translator operator defined as:

$$\tau_{t_o} h(t) = h(t-t_o)$$

and t_o is the translation time.

So
$$\widehat{(\tau_{t_o} h)}_a(\omega) = \hat{h}_a(\omega)$$

and
$$\widehat{(\tau_{t_o} h)}_\theta(\omega) = -\omega t_o + \hat{h}_\theta(\omega)$$

or $\log \{\hat{h}_\theta(\omega) - \widehat{(\tau_{t_o} h)}_\theta(\omega)\} = \log \omega Q + \log \dfrac{t_o}{Q}$

where Q is a characteristic time of the system, as will be shown later.
It follows that for $\omega Q = 1$

$$\hat{h}_\theta(\omega) - \widehat{(\tau_{t_o} h)}_\theta(\omega) = \Delta\hat{h}_\theta(\omega) = \frac{t_o}{Q} \qquad (2.17)$$

so if the characteristic time Q of the system is known the translation time t_o can be calculated.

2.5. GOODNESS OF FIT

In order to determine the goodness of fit between the exact or observed data

12

(real world) and the approximate or computed data (model), from the many objective criteria for error measurements, which are available, a special form of the mean square error of the ordinates is chosen. In statistics (Gringorten, 1960) this error measure is called the coefficient of determination. Nash (1970) has introduced this criterion into the study of run-off models, where he used the term efficiency coefficient R_E:

$$R_E = \{1 - \frac{\Sigma(f - f_1)^2}{\Sigma(f - \overline{f})^2} \} \tag{2.18}$$

Here f stands for the exact or observed data, f_1 the approximate or computed data and $\overline{f}$ the mean of the exact or observed data. The numerator expresses the residual variance and the denominator the initial variance. So if the model and the real world fully agree then $R_E = 1$. If the data of the model equal the mean value of the data in the real world then $R_E = 0$. For optimization procedures of the parameters in a conceptual model the efficiency coefficient is useful as an objective criterion for the goodness of fit.

In this presentation the efficiency coefficient has been used as an objective criterion for the goodness of fit between the linear solution of the approximate linear equation and the solution of the complete non-linear equation for the surface run-off problem. Further it was used to compare the theoretical results with the experiments.

3. MODELLING OF THE SURFACE RUNOFF

As stated by Dooge & Harley (1967) the surface runoff process consists of
three conditions: complex geometry, complex physics and complex inputs
Simplifications from a theoretical and practical point of view are therefore
necessary for a quantitative approach to the problem.
The question is how far it is justified to simplify the surface runoff
process.

### 3.1. A DISTRIBUTED CONCEPT CATCHMENT MODEL

The surface run-off process can be divided into overland flow and channel or
stream flow. In particular overland flow is difficult to model, because it
begins as a thin-sheet flow, but is focused into small rivulets by the surface
irregularities, and then into bigger streams constituting channel flow.
Similar to the work of Bravo, et al (1970) (Fig. 3.1) the catchment is
subdivided into smaller elements, for which either one dimensional overland
flow or one dimensional channel-flow is assumed.
These smaller elements are connected with each other by the channel sections.
Approximating the complex geometry in this way 5 types of elementary problems
can be selected:

a. Overland flow problem, which consists of a plane rectangular, impermeable
   surface, which receives a uniformly distributed rainfall. Theoretically
   this problem is handled as turbulent flow in an infinite, wide rectangular
   channel with uniform slope and resistance and fully lateral inflow.
   The term infinite means that there are no restrictions for flow in upstream
   and downstream directions.

b. Fully lateral inflow problem into a channel reach.
   This can be handled in the same way as the overland flow problem, except
   that the infinite channel reach can also be considered as a prismatic
   rectangular or trapezoidal channel.

c. Partial lateral inflow problem into a channel reach, where the lateral
   inflow takes place over a part of the channel reach.

d. Tributary inflow problem into a channel reach, where the inflow from one
   channel is concentrated at a particular point of a second channel.
   In fact the problems b and c are special cases of problem d.

e. Upstream inflow problem into a semi-infinite channel, where the discharge
   at the upstream end of the channel is given.

14
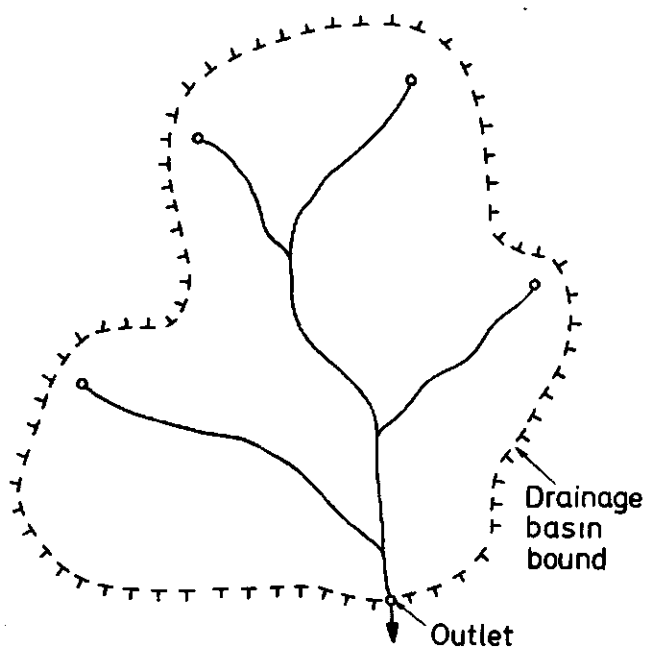
Plan view of typical drainage area
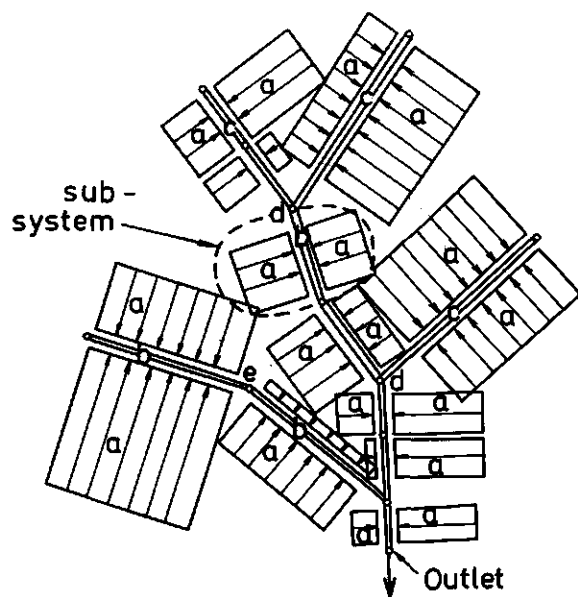
a = overland flow
b = fully lateral inflow
c = partial lateral inflow
d = tributary inflow
e = upstream inflow

fig. 3.1 Equivalent block-diagram of the
surface run-off system for a
catchment (Bravo et al, 1970)

The downstream movement of the wave is studied, forming a classic problem in flood forecasting.

It is assumed that the catchment can be modelled by a suitable combination of these 5 elements. So the complex distributed surface run-off model consists of an appropriate number of elements chosen in accordance with the geometry of the surface run-off system. It is further assumed that one element cascades into the other so that interaction between these elements is excluded. Practically the number of elements, determining the complexity of the system, should be as small as possible. The systems approach seems to be very helpful for this basic problem of integrated system modelling.

3.2. HYDRODYNAMIC CONSIDERATIONS

The hydrodynamic aspects of open channel-flow and overland flow can be found in many handbooks (Ven te Chow, 1959, 1964; Henderson, 1966; Eagleson, 1970), therefore only some points concerning flood routing problems will be given here.

The equations of motion of one dimensional flow in an uniform open channel with lateral inflow can after some simplification be written as follows:

Momentum equation : $S_f = S_o - \dfrac{\partial y}{\partial s} - \dfrac{v}{g}\dfrac{\partial v}{\partial s} - \dfrac{1}{g}\dfrac{\partial v}{\partial t} - D_L$ (3.1)

Continuity equation : $\dfrac{\partial Q}{\partial s} + \dfrac{\partial A}{\partial t} = i(s,t)$ (3.2)

where s and t are distance in flow direction and time respectively, S_o is the bottom slope, y the water depth, v the mean velocity in a cross section of the channel, g the acceleration of gravity, A the cross sectional area of flow, Q the discharge rate (= vA), i the lateral inflow per unit length of channel, S_f the friction slope and the term D_L represents the energy dissipation when the lateral flow mixes with the water already in the channel (Henderson, 1966). The term D_L can be expressed as follows: (Strelkoff, 1970)

$$D_L = \dfrac{v-u_L}{gA}\, i(s,t)$$ (3.3)

where u_L is the s-component of the inflow velocity vector.

Clearly $D_L = 0$, if the lateral inflow $i(s,t)=0$ or if the lateral inflow is in direction of flow and $v=u_L$.

Here it is assumed that the lateral inflow is perpendicular to the direction of

16

flow, which yields $u_L = 0$, so that after introduction of Eq. (3.2) in Eq. (3.3) for D_L, expressed in Q, can be written:

$$D_L = \frac{Q}{gA^2} \left(\frac{\partial Q}{\partial s} + \frac{\partial A}{\partial t} \right)$$ (3.4)

Substitution of Eq. (3.4) in the equation of motion (3.1), expressed in Q yields:

$$S_f = S_o - (1 - F^2) \frac{\partial y}{\partial s} - \frac{2Q}{gA^2} \frac{\partial Q}{\partial s} - \frac{1}{gA} \frac{\partial Q}{\partial t}$$ (3.5)

where F is the local Froude number for which the following relation is valid.

$$F^2 = \frac{Q^2 B}{gA^3}$$ (3.6)

where $B = \frac{\partial A}{\partial y}$ the surface width of the channel.

For lateral inflow $i(o,t) = 0$ (so $D_L = 0$) combining eqs (3.1) and (3.2), expressed in Q, yields the same Eq. (3.5), which means that this equation is valid for the flow with and without lateral inflow. (assuming $u_L = 0$)
For the overland flow problem eqs (3.2) and (3.5) are used, assuming a wide rectangular channel, where discharge q is expressed per unit width of channel. The equations of motion for the one dimensional overland flow therefore can be expressed as follows:

$$S_f = S_o - (1 - F^2) \frac{\partial y}{\partial s} - \frac{2q}{gy^2} \frac{\partial q}{\partial s} - \frac{1}{gy} \frac{\partial q}{\partial t}$$ (3.7)

$$\frac{\partial q}{\partial s} + \frac{\partial y}{\partial t} = i(s,t)/B$$ (3.8)

where q is discharge per unit width of channel, while for the local Froude number the following relation is valid.

$$F^2 = \frac{q^2}{gy^3}$$ (3.9)

Both in the channel-flow and in the overland flow problems the friction slope S_f is difficult to determine.
In this report it is assumed that the flow in both cases is turbulent, where ┼he empirical relation of Chezy or Manning may be used.

The formulas for channel-flow and overland flow are respectively:

Chezy $\quad: S_f = \dfrac{Q|Q|}{A^2 C^2 R}$ $\qquad$ (channel-flow)

$\qquad S_f = \dfrac{q|q|}{C^2 y^3}$ $\qquad$ (overland flow) $\qquad\qquad$ (3.10)

where C is the Chezy coefficient and R is hydraulic radius.

Manning $\quad: S_f = \dfrac{Q|Q|}{A^2 K_m^2 R^{4/3}}$ $\qquad$ (channel-flow)

$\qquad S_f = \dfrac{q|q|}{K_m^2 y^{10/3}}$ $\qquad$ (overland flow) $\qquad\qquad$ (3.11)

where K_m is the Manning coefficient.

In the linear systems approach the complex geometry of the channel reach is simplified by assuming a uniform trapezoidal channel (Fig. 3.2), from which the special cases of a rectangular channel (m=0) or infinite wide rectangular channel (m=0, $B\to\infty$) can be derived.
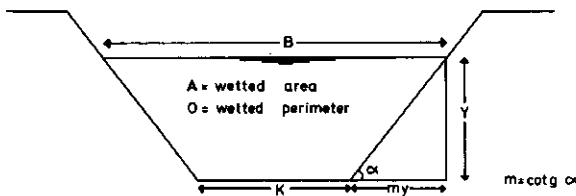
fig. 3.2 Cross section of a channel reach

The complex physics can be simplified by the reasonable assumption that the quasi-steady state approach (the kinematic wave), where $S_f = S_o$, is a good first approximation of Eq. (3.5). Introducing this in the third and the fourth term at the right hand side of Eq. (3.5) (the acceleration terms) which also can be expressed as:

$$\frac{-2Q}{gA^2} \frac{\partial Q}{\partial s} - \frac{1}{Ag} \frac{\partial Q}{\partial t} = -(2v-c) \frac{Bc}{gA} \frac{\partial y}{\partial s} \qquad (3.12)$$

where c is the celerity ($= \dfrac{\partial Q}{\partial A}$ Seddon law)

gives after substitution of Eq. (3.12) in Eq. (3.5) the equation of motion, assuming Chezy friction formula:

18

$$S_f = S_o - \{1 - \frac{F^2}{4} (1 - \frac{2R}{B} \sqrt{1 + m^2})^2\} \frac{\partial y}{\partial s} \qquad (3.13)$$

while assuming Manning's friction formula this gives:

$$S_f = S_o - \{1 - \frac{4}{9} F^2 (1 - \frac{2R}{B} \sqrt{1 + m^2})^2\} \frac{\partial y}{\partial s} \qquad (3.14)$$

The continuity equation, assuming no lateral inflow, can be written as:

$$\frac{\partial Q}{\partial s} + \frac{\partial A}{\partial t} = 0 \qquad (3.15)$$

As will be shown in Section (3.4), the different types of inflow form one of the boundary conditions necessary for solving the differential eqs (3.13) or (3.14) and (3.15).

One way of tackling the problem of the complex geometry of a distributed network and the problem of a complex spatial and secular variation of the input, is the linearisation of the Eq. (3.13) or (3.14).

3.3. LINEARIZED DIFFUSION TYPE EQUATIONS

As proposed already by Schönfeld (1948) linearisation of the Eq. (3.13) or (3.14) can be achieved by considering the flow as a small perturbation on an initial permanent uniform flow. The discharge Q or q can be expanded in a Taylor series, where terms of higher then the first order will be neglected, which is correct only if the perturbation is small.

Starting from Eq. (3.13), based on the Chezy friction formula, the discharge Q can be expressed as follows:

$$Q = CR^{\frac{1}{2}}A(S_o - C_1 S)^{\frac{1}{2}} , Q \geqslant 0 \qquad (3.16)$$

where $C_1 = \{1 - \frac{F^2}{4} (1 - \frac{2R}{B} \sqrt{1 + m^2})^2\}$

and $S = \frac{\partial y}{\partial s}$, the gradient of the water depth.

In general y and $\frac{\partial y}{\partial s}$ are independent functions. (Van de Nes and Hendriks, 1971)

So one can consider Q as a function of the variables y and S (= $\frac{\partial y}{\partial s}$), Q = Q(y,s).

In order to linearize Eq. (3.16) the following notations for the discharge, water depth and slope of the water level are introduced.

$$Q = Q_I + Q_p , \quad y = y_I + y_p \quad \text{and} \quad S = S_I + S_p$$

where the subscript I means initial and p the perturbation, for uniform flow $S_I = 0$. The Taylor series for Q can be expressed as follows:

$$Q = Q_I + (\frac{\partial Q}{\partial y})_I (y - y_I) + (\frac{\partial Q}{\partial S})_I (S - S_I) + \ldots\ldots$$

$$\text{or} \quad Q_p = (\frac{\partial Q}{\partial y})_I y_p + (\frac{\partial Q}{\partial S})_I S_p + \ldots\ldots \tag{3.17}$$

The initial values Q_I, y_I and S_I correspond with the initial values of C and C_1. When writing the Taylor series these values have been considered constant, so that the following relations can be derived:

$$(\frac{\partial Q}{\partial y})_I = \frac{3}{2} v_I B_I \{1 - \frac{2}{3}(\frac{R}{B})_I \sqrt{1 + m^2}\} \tag{3.18}$$

$$\text{and} \quad (\frac{\partial Q}{\partial S})_I = - (C_1)_I \frac{Q_I}{2S_o}$$

Substituting eq. (3.18) into (3.17) it is found that:

$$\frac{Q_p}{B_I} = A_\tau y_p - D \frac{\partial y_p}{\partial s} \tag{3.19}$$

where $A_\tau = \frac{3}{2} v_I \{1 - \frac{2}{3}(\frac{R}{B})_I \sqrt{1 + m^2}\}$ the translation coefficient

$$\text{and} \quad D = \frac{Q_I}{2S_o B_I} \left[1 - \frac{F^2}{4} \{1 - 2(\frac{R}{B})_I \sqrt{1 + m^2}\}^2 \right] \quad \text{the diffusion coefficient} \tag{3.20}$$

For a wide rectangular channel eq. (3.20) gives: (Harley, 1967)

$$A_\tau = \frac{3}{2} v_I$$

$$D = \frac{q_I}{2S_o} (1 - \frac{F_I^2}{4}) \tag{3.21}$$

while for a rectangular channel with width B the following relations can be derived.

$$A_\tau = \frac{3}{2} v_I (\frac{B_I + \frac{4}{3} y_I}{B_I + 2y_I})$$

$$\text{and} \quad D = \frac{q_I}{2S_o} \{1 - \frac{F_I^2}{4} (\frac{B_I}{B_I + 2y_I})^2\} \tag{3.22}$$

20

From the continuity Eq. (3.15) follows:

$$\frac{\partial(Q_I + Q_p)}{\partial s} + B \frac{\partial(y_I + y_p)}{\partial t} = 0 \qquad (3.23)$$

and $\frac{\partial Q_I}{\partial s} = 0$ and $\frac{\partial y_I}{\partial t} = 0$ (steady uniform flow)

therefore Eq. (3.23) gives:

$$\frac{\partial Q_p}{\partial s} + B \frac{\partial y_p}{\partial t} = 0 \qquad (3.24)$$

Combination of the eqs (3.24) and (3.19) produces the two well known linear partial differential equations of parabolic form:

$$\frac{\partial Q_p}{\partial t} = D \frac{\partial^2 Q_p}{\partial s^2} - A_\tau \frac{\partial Q_p}{\partial s} \qquad (3.25)$$

and

$$\frac{\partial y_p}{\partial t} = D \frac{\partial^2 y_p}{\partial s^2} - A_\tau \frac{\partial y_p}{\partial s} \qquad (3.26)$$

Obviously Eq. (3.25) is also valid for q_p (discharge per unit width of channel). These diffusion type equations, which were already given by Schönfeld (1948), Hayami (1951), Daubert (1964) and Harley (1967), form the basic equations of the different type of flood routing problems, as mentioned before.

Linearisation of Eq. (3.14) which is based on the Manning friction formula, leads to the same differential equation. Here the translation coefficient A_τ and the diffusion coefficient D take the following form:

$$A_\tau = \frac{5}{3} v_I \left(1 - \frac{4}{5} (\frac{R}{B})_I \sqrt{1 + m^2}\right) \qquad (3.27)$$

$$D = \frac{Q_I}{2S_o B_I} \left[1 - \frac{4}{9} F_I^2 \{1 - 2(\frac{R}{B}) \sqrt{1 + m^2}\}^2 \right]$$

For a wide rectangular channel this leads to:

$$A_\tau = \frac{5}{3} v_I$$

and

$$D = \frac{q_I}{2S_o} (1 - \frac{4}{9} F_I^2) \qquad (3.28)$$

while for a rectangular channel with width B it gives:

$$A_\tau = \frac{5}{3} v_I \left(\frac{B_I + \frac{6}{5} y_I}{B_I + 2y_I} \right)$$

and   (3.29)

$$D = \frac{q_I}{2S_o} \left\{ 1 - \frac{4}{9} F_I^2 \left(\frac{B_I}{B_I + 2y_I} \right)^2 \right\}$$

So the choice of the friction formula and geometry of the channel determine, which formulae for A_τ and D apply.

As mentioned before the differential equations are accurate if the perturbation is relatively small compared to initial uniform flow. With the linear systems approach the equations will also be used for large perturbations, so that now a constant "reference" discharge Q_o (or q_o) or a constant reference water depth y_o has to be chosen, fixing the parameters A_τ and D.

It should be noted that contrary to the above initial discharge and water depth the reference discharge and water depth are some mean values within the actual range of variation. These only apply to the parameters of the flow equations.

3.4. BOUNDARY CONDITIONS

The solution of the differential eqs (3.25) and (3.26) requires boundary conditions.

For Eq. (3.25) one needs conditions, expressed in discharge, while for (3.26) the conditions must be expressed in water depth. So the boundary conditions determine which of the two equations should be used. Because the flow is considered as a perturbation on an initial uniform flow the initial conditions are:

$$q_p(s,o) = 0$$
                                                                                                    (3.30)
$$y_p(s,o) = 0$$

while the boundary conditions depend on the type of inflow, which may vary in time and space.

As shown before the parameters A_τ and D depend on the physical characteristics of the channel and on a constant reference discharge or water depth. The latter depends on the initial conditions of the system and the range of variation of flow.

The choice of a constant reference discharge or water depth, may be criticized because it entails a crude approximation, especially in the case of the lateral inflow, where the discharge increases with channel distance. A logical choice of reference discharge would be

$$q_o(s) = q_I(s) + {_o\int^s} i(\xi) \ d\xi$$

where $i(\xi)$ would be the average inflow over the period under consideration. A reference discharge which varies with distance can be approximated and brought into the linear systems approach by cutting the channel reach in sections. By this process a histogram of reference discharges along the channel reach can be obtained.

Despite the discontinuities in the reference discharge, the results are not affected, as is shown in Section 4.2.8.

Because of the attenuation of the flood wave for the upstream and tributary inflow problem it is possible to take a decreasing reference discharge with distance. Also here a histogram of reference discharges can be taken, dependent on the behaviour of the flood wave. Construction of a very fine network does not in general increase the accuracy of the solution. In that case it would be better to solve the original non-linear differential equations with the aid of differences schemes, losing however the advantages of linear system analysis. It is interesting to note that chosing a reference discharge dependent on the initial conditions and the inflow, is an essential feature of this quasi-linear system.

The influence of the choice of the reference discharge on the results has therefore been specially investigated. This study shows the influence of the boundary conditions and physical parameters, which are complex and in general not well known, on the results of the rainfall and run-off relation of a catchment.

The result of this hydrodynamic approach is a mathematical model for a quasi-linear time invariant system. The indicial response of this system can be obtained by solving the differential equation with the delta input as a boundary condition.

This means that a unit of volume is added to the channel reach at a point or over a certain distance, depending on the type of inflow problem. In this way synthetic IUH's for the different types of problems will be derived and subsequently the powerful system engineering techniques will be used to analyse the systems behaviour.

Integration of the IUH in time yields the S-curve, from which TUH's can be derived (Eq. 2.4). If the input is given as a histogram or "distribution graph", the output can be calculated, by making use of the convolution integral in discrete form (Eq. 2.2). Because every input can be approximated by a histogram Eq. 2.2 is a very convenient form of the convolution integral, which can be easily programmed for a digital computer, while the computer time is relatively small.

In this paper the theoretical aspects of surface run-off will be studied by applying four types of input to each conceptual element:

a. A long "Thomas wave", (Fig. 3.3) as used by Dooge & Harley (1967), which is expressed as follows:

$$q_p(t) = 75 - 75 \cos \left(\frac{\pi t}{48}\right) \text{ for } 0 < t < 96 \text{ hours}$$

which is superimposed on a baseflow $q_I = 50$. Both are expressed in cusecs per foot width. Transforming this in metric units yields:

$$q_p(t) = 6,975 - 6,975 \cos \left(\frac{\pi t}{48}\right) \text{ m}^3/\text{sec, m'}$$

In order to compare the results of this study with those of Dooge & Harley the British unit system will be used.

This input is approximated by a histogram with an interval of one hour.

b. An intermediate "Thomas wave" (Fig. 3.4) of the following shape:

$$q_p(t) = 75 - 75 \cos \left(\frac{\pi t}{6}\right) \text{ for } 0 < t < 12 \text{ hours}$$

approximated by a histogram with an interval of 15 minutes, which is superimposed on a base flow $q_I = 50$ cusecs per foot width.

Comparison of the results of a. and b. shows the effect of input duration on wave attenuation.

In both cases attention is only given to the discharge. Water depth is not studied. The three aspects, which are studied are: the influence of the reference discharge, the length of the channel and the spatial distribution of the input into the system.

c. A block input (Fig.3.5) expressed as 1 mm/interval, with an interval of 3 hours. In this case the TUH was derived for various types of problem, where water depth was studied. Special attention was also given to the relation
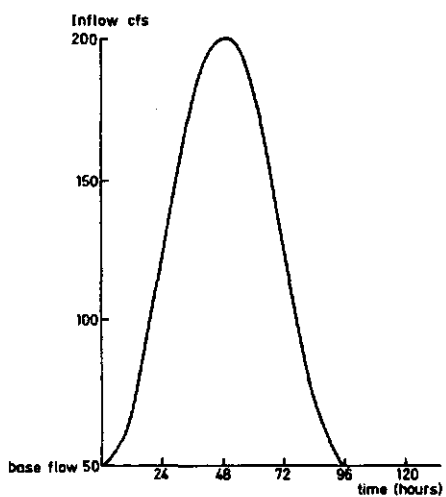
fig. 3.3 "Long Thomas" wave
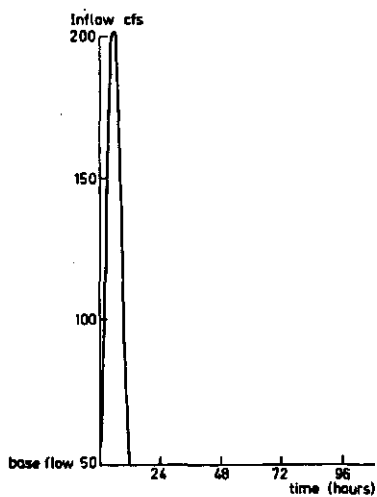
fig. 3.4 "Intermediate Thomas" wave
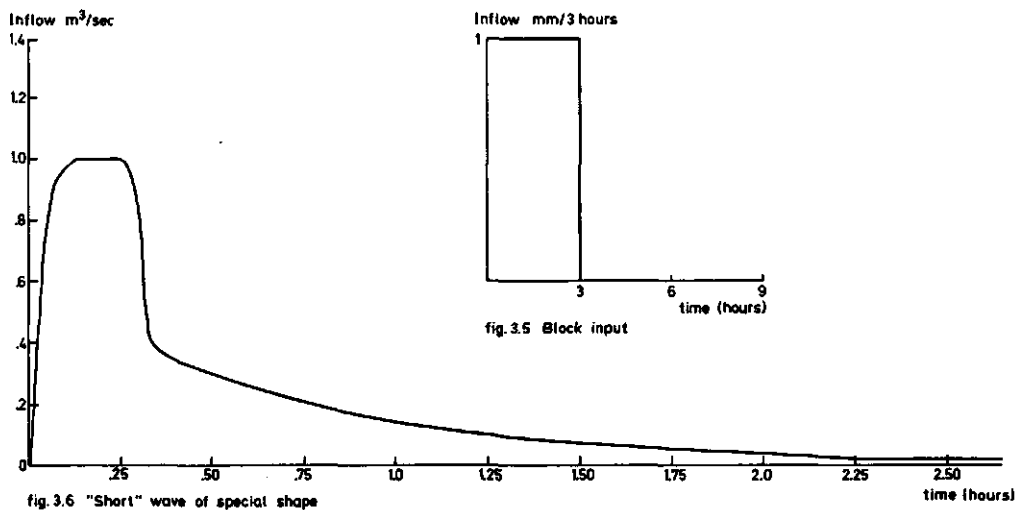
fig. 3.5 Block input

fig. 3.6 "Short" wave of special shape

VARIOUS TYPES OF INFLOWS

25

between water depth and discharge.

d. A short wave with a special shape (Fig. 3.6), where the flat top of the input occurs within 15 minutes and is expressed in m^3/sec. This wave is super-posed on an initial water depth of 0,50 m.

In this case only the water depth is studied. As complete non-linear solutions, based on an implicit difference scheme of Amein (1968), have been derived by Grijsen (1971), it was possible to compare the linear and non-linear solutions.

4. LINEAR CONCEPTUAL ELEMENTS

Complex surface run-off consists roughly of 5 linear elements (Section 3.1).
In this chapter these elements are mathematically formulated in terms of the
linear system theory. Some results on the input-output relation are given for
a channel reach which shows the effects of the spatial and secular variation
in input, of the reference discharge and of the physical characteristics of the
channel.

4.1. INFINITE CHANNEL-LUMPED INPUT

This element, which is studied as the tributary inflow problem can be
considered in two different ways (Fig. 4.1).
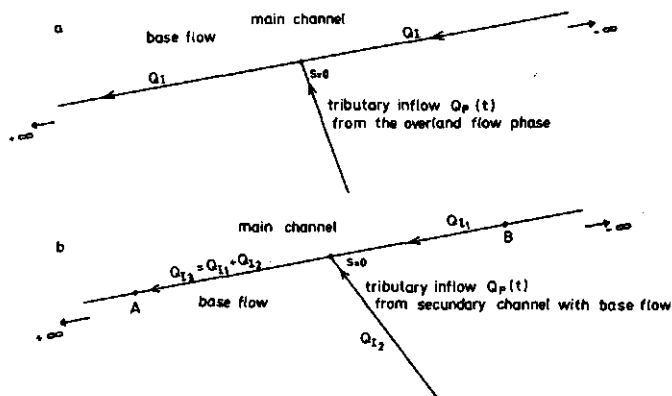
fig.4.1 Concept of the tributary inflow problem

a. First as an infinite channel, in which a constant initial flow occurs over
   the whole channel reach. In one point (s=0) this channel is fed by an known
   inflow, which is cascaded into the channel.
b. Second as an infinite channel with an initial flow, but now this main
   channel is fed at one point by a second channel, which has also an initial
   flow. This causes a discontinuity of the initial flow in the main channel at
   the point, where the second channel enters the main channel.
   From Fig. 4.1 it can be seen that $Q_{I_3} = Q_{I_2} + Q_{I_1}$. If now one is interested

in the discharge at point A, caused by the tributary inflow $Q_p(t)$, then the solution must be superposed on Q_{I_3} and if one is interested at point B the solution must be superposed on Q_{I_1}. The only problem is to find the reference discharge, determining the parameters of the main channel. It will be shown later that a fair estimation of the reference discharge, which depends on the initial flow and the range of variation of flow, can be obtained by applying the following relation.

$$Q_o = Q_I + \frac{Q_p(o)_{peak} + Q_p(s)_{peak}}{N} \quad \text{(4.1)}$$

, where $N = 4$ for the tributary and upstream inflow and $N = 2$ for the fully lateral inflow; where $Q_p(s)_{peak}$ is the peak value at point s.

This agrees with the results given by Bravo et al (1970) and Harley et al (1970).

So for point A: $Q_o = Q_{I_3} + \dfrac{Q_p(o)_{peak} + Q_p(A)_{peak}}{4}$

and for point B: $Q_o = Q_{I_1} + \dfrac{Q_p(o)_{peak} + Q_p(B)_{peak}}{4}$

The same relations are also valid for the reference water depth.
It follows that the peak values in the appropriate points must be known. Such values may be obtained from an empirical relation between the attenuation coefficient and the specific attenuation of a flood. (Section 5.4)

4.1.1. Impulse Response

The impulse response can be found by solving the linear differential equation for the water depth. (Eq. 3.26)

$$\frac{\partial y_p}{\partial t} = D \frac{\partial^2 y_p}{\partial s^2} - A_\tau \frac{\partial y_p}{\partial s} \quad \text{(4.2)}$$

for the following initial- and boundary conditions:

a. $y_p(s,o) = \delta(s)$ (Dirac function)

b. $\lim\limits_{\substack{s \to \infty \\ s \to -\infty}} y_p(s,t) = 0$ (4.3)

c. $\int\limits_{-\infty}^{\infty} y_p(s,t)\, ds = 1$, which follows from the continuity equation.

The physical meaning of $\delta(s)$ is, that a unit volume per unit width of channel is added to the system at time t=o at one point (s=o). There are no restrictions for the flow in upstream and downstream directions (infinite channel). The solution can be found after the transformation:

$$s_1 = s - A_\tau \cdot t \qquad (4.4)$$

which reduces eqs (4.2) and (4.3) to respectively:

$$\frac{\partial y_p}{\partial t} = D \frac{\partial^2 y_p}{\partial s_1^2} \qquad (4.5)$$

and

$$y_p(s_1, o) = \delta(s_1) \qquad (4.6)$$

$\int_o^\infty y_p(s_1, t) \, ds_1 = \frac{1}{2}$, because the solution is symmetrical; so only the case $s_1 > 0$ has to be considered.

$$\lim_{s_1 \to \infty} y_p(s_1, t) = 0$$

The following solution is found with the aid of the Laplace transform method. (Van de Nes and Hendriks, 1971)

$$y_p(s_1, t) = \frac{1}{2\sqrt{\pi D t}} e^{-\frac{s_1^2}{4Dt}} \quad , \quad (s_1, t) \neq (o, o) \qquad (4.7)$$

where $y_p(s_1, o) = \delta(s_1)$

The same is true for $s_1 < o$. Introducing Eq. (4.4) in (4.7)

yields: $$y_p(s, t) = \frac{1}{2\sqrt{\pi D t}} e^{-\frac{(s - A_\tau \cdot t)^2}{4Dt}} \quad , \quad (s, t) \neq (o, o) \text{ and } t > 0 \qquad (4.8)$$

The discharge can be calculated by introducing Eq. (4.8) in Eq. (3.19), which yields:

$$\frac{Q_p}{B_I} = \frac{(s + A_\tau \cdot t)}{4\sqrt{\pi D t^3}} e^{-\frac{(s - A_\tau \cdot t)^2}{4Dt}} \qquad (4.9)$$

For a rectangular channel $\dfrac{Q_p}{B_I}$ can be expressed as

$$q_p(s,t) = \frac{Q_p}{B_I} \tag{4.10}$$

For a trapezoidal channel this expression is approximately true if B_I is chosen as a mean value over the range of the varying surface width of the channel, caused by the inflow.

Because of the particular boundary conditions the eq. (4.8) and (4.9) represent the IUH of waterdepth h_y ($=y_p$) and of discharge h_q ($=q_p$) per unit width of channel, respectively.

In the framework of the systems approach, it is convenient to express both IUH's in a dimensionless form, introducing two dimensionless system parameters:

$$P = \frac{sA_\tau}{2D} \text{ , a dimensionless length parameter}$$

and

$$T = \frac{t}{Q} \text{ , a dimensionless time} \tag{4.11}$$

where $\quad Q = \dfrac{2D}{A_\tau^2}$ is the parameter expressing the characteristic time of the system.

Introducing of Eq. (4.11) into Eq. (4.9) and (4.8) gives:

$$\bar{h}_q = \frac{h_q \cdot Q}{V} = \tfrac{1}{2}\left(\frac{P}{\sqrt{2\pi T^3}} + \frac{1}{\sqrt{2\pi T}}\right) e^{-\frac{(P-T)^2}{2T}} \tag{4.12}$$

and

$$\bar{h}_y = \frac{h_y \cdot s}{V} = \frac{P}{\sqrt{2\pi T}} e^{-\frac{(P-T)^2}{2T}} \tag{4.13}$$

where $\bar{h}_q$ and $\bar{h}_y$ are the dimensionless IUH's of discharge and water depth and V is the unit volume per unit width of channel.

4.1.2. Classification

For the complete linear solution Harley (1967) classified channel reaches as short, intermediate and long. The classification was based on the discharge. For the diffusion type solution a similar classification can be made:

follows: (Fig. 4.2)

fig. 4.2 Dimensionless impulse responses for the tributary inflow problem
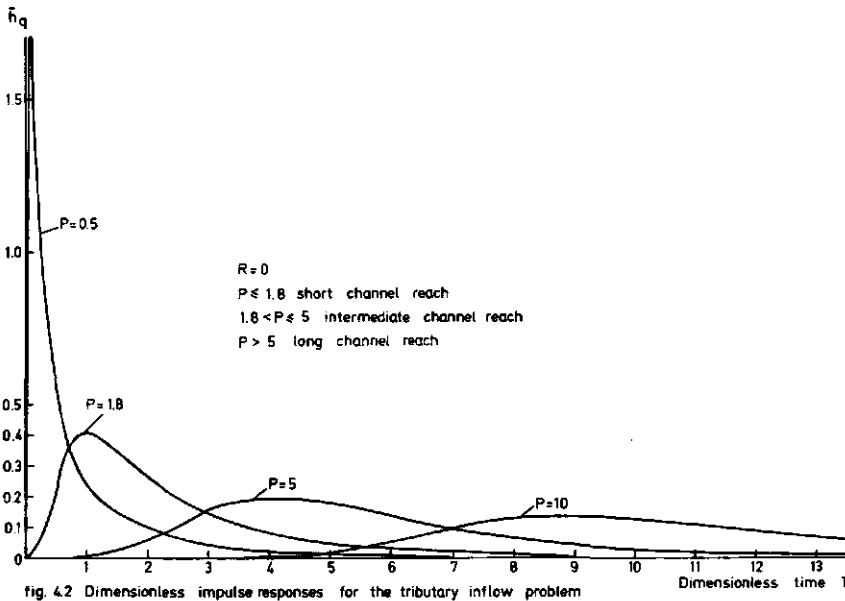
a. A short channel reach, if in the dimensionless IUH the time to peak $T_p < 1$

or $(\dfrac{\partial \overline{h}_q}{\partial T})_{T=1} \leqslant 0$

From this condition it follows, using Eq. (4.12) that $P \leqslant 1,8$

b. An intermediate channel reach, if $T_p > 1$ and $(\overline{h}_q)_{T=1} \geqslant \xi$, where ξ is a small number $(\approx 5 \times 10^{-4})$ from which follows $1,8 < P \leqslant 5$

c. A long channel reach, if $(\overline{h}_q)_{T=1} < \xi$

For practical purposes this means that the rising limb of the dimensionless IUH starts at $T > 1$.

This is valid if $P > 5$.

In combination with the statistical moments and spectra, this classification seems to be useful in analysing the behaviour of the system.

4.1.3. Moments

The moments of the IUH are derived from Eq. (2.9) (Van de Nes and Hendriks, 1971). They can be expressed as follows:

$$M_1'(h_q) = (P + \tfrac{1}{2})Q$$
$$M_2(h_q) = (P + \tfrac{5}{4})Q^2 \qquad (4.14)$$
$$M_3(h_q) = (3P + \tfrac{11}{2})Q^3$$

from which for the shape factors (Section 2.2) follow:

$$S_2 = (P + 5/4)/(P + 1/2)^2 \quad \text{and} \quad S_3 = (3P + 11/2)/(P + 1/2)^3 \qquad (4.15)$$

For the first three moments of the IUH for the water depth was found:

$$M_1'(h_y) = (P + 1)Q$$

$$M_2(h_y) = (P + 2)Q^2 \qquad (4.16)$$

$$M_3(h_y) = (3P + 8)Q^3$$

Comparison of the moments of discharge and water depth shows that water depth fluctuation is more damped then discharge fluctuation. This is in agreement with the hysteresis in the discharge-water depth relation for a flood wave. For large values of P however the moments become equal. Then the relation between water depth and discharge becomes unique. This condition is also characteristic for the kinematic wave, which does not attenuate.

4.1.4. Attenuation coefficient

As defined in Section 2.3. the attenuation coefficient for the discharge

$$C_A = (\frac{P+5/4}{\beta})(\frac{Q}{t_F})^2 \qquad (4.17)$$

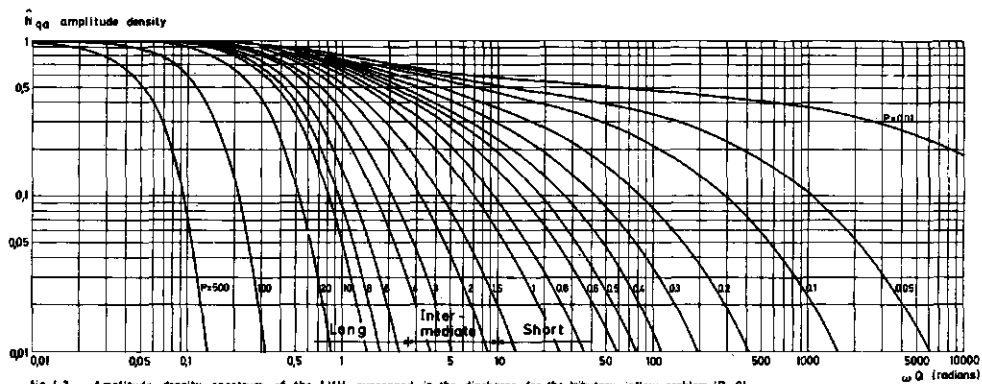βt_F^2 is the second moment $M_2(x)$ of the incoming wave and t_F is the duration of the input.

fig. 4.3   Amplitude density spectrum of the IUH, expressed in the discharge, for the tributary inflow problem (R=0)
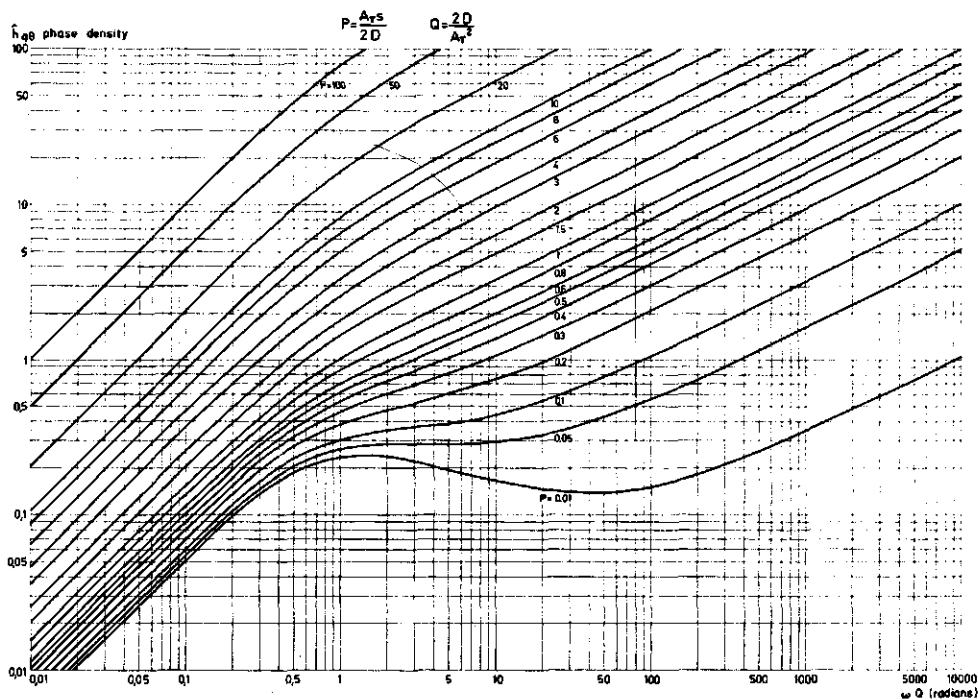

fig. 4.4   Phase density spectrum of the I.U.H., expressed in the discharge, for the tributary inflow problem (R=0)

33

For the 'Thomas wave': $\beta = 1/12 - 1/2\pi^2 \approx 0,033$, while for a block input $\beta = 1/12 \approx 0,083$.

So for a small ratio $\dfrac{t_F}{Q}$ (short wave), a large value of P and or a small value of β the attenuation is more pronounced.

4.1.5. Spectra

The amplitude density spectrum and the phase density spectrum of the IUH of the discharge are derived by Van de Nes and Hendriks, 1971, using the eqs (2.13) and (2.14) given in Section (2.4.).

The amplitude density spectrum can be expressed as follows:

$$\hat{h}_{qa}(\omega) = \tfrac{1}{2}\, e^{P\{1-\alpha(\omega)\}}\left[\frac{2\alpha^2(\omega) + 2\alpha(\omega)}{2\alpha^2(\omega)-1}\right]^{\tfrac{1}{2}} \qquad (4.18)$$

$$\text{for } \omega > 0$$

and the phase density spectrum of the IUH of the discharge is:

$$\hat{h}_{q\theta}(\omega) = -P\beta(\omega) - \tan^{-1}\frac{\beta(\omega)}{\alpha^2(\omega)+\beta^2(\omega)+\alpha(\omega)} \qquad \text{for } \omega > 0 \qquad (4.19)$$

where $\alpha(\omega) = \sqrt{(1 + \sqrt{1 + 4Q^2\omega^2})/2}$

$$(4.20)$$

and $\beta(\omega) = \sqrt{(-1 + \sqrt{1 + 4Q^2\omega^2})/2}$

In the spectra of figs 4.3 and 4.4, the amplitudes and phases are given as function of ωQ for a number of values of P.

The damping effect of the system for an increasing value of P is shown in the spectra, while here Q seems to be only a scale factor.

Also in the frequency domain one can subdivide the area in three parts, which agrees with the channel classification of a short, intermediate and long channel reach, as is shown in the figures.

4.1.6. Summation Curves

Integration of the IUH for the discharge and for the water depth gives the summation curves (S-curves), from which TUH's for any period Δt can be derived. Then the numerical convolution of the input with the TUH is a simple procedure.

34

The responses given in figs 4.5 and 4.6 have been calculated by a digital computer (C.D. 3200) within one minute.

The S-curves for the discharge and the water depth are derived (Van de Nes and Hendriks, 1971):

$$S_q = \tfrac{1}{2} \, \text{erfc} \, (\frac{P-T}{\sqrt{2T}}) \tag{4.21}$$

and

$$S_y = \frac{PQ}{2s} \{ \, \text{erfc} \, (\frac{P-T}{\sqrt{2T}}) - e^{2P} \, \text{erfc} \, (\frac{P+T}{\sqrt{2T}}) \} \tag{4.22}$$

where the complementary error function is defined as:

$$\text{erfc}(z) = 1 - \text{erf}(z) = 1 - \frac{2}{\sqrt{\pi}} \int_o^z e^{-\xi^2} \, d\xi \tag{4.23}$$

and is tabulated. (Abramowitz & Stegun, 1965).

In fact the S-curves are the outputs, due to an input, which has the shape of a step function. This means that a constant unit intensity input starts at time t=o; For $t \to \infty$ the steady state will be reached.

From the eqs (4.21) and (4.22) it follows for $t \to \infty$ that:

$$S_q = 1 \text{ and } S_y = \frac{PQ}{s} \tag{4.24}$$

For the relation of q_p and y_p then it follows:

$$q_p = A_\tau y_p \tag{4.25}$$

which means by comparing Eq. (4.25) with Eq. (3.19) that for $t \to \infty$ the term $\frac{\partial y_p}{\partial s} \to 0$

Because $q = q_I + q_p$, as stated in Section 3.3., it follows for the steady state in a wide rectangular channel with $A_\tau = \frac{3}{2} v_I$:

$$q = v_I y_I + \frac{3}{2} v_I y_p = v_I (y_I + \frac{3}{2} y_p)$$

or $\tag{4.26}$

$$q = v_I y + \tfrac{1}{2} v_I y_p$$

In this linear systems approach to the problem the increase of velocity, due to

35

the increase of water depth is introduced in Eq. (4.26) by the second term on the right hand side.

4.1.7. Response to given waves of inflow

For the long 'Thomas wave', with a duration of 96 hours and the intermediate 'Thomas wave' with a duration of 12 hours, as given in Section 3.4. the response is given for different distances from the point of inflow.
For the long wave distances of 5, 50, 200 and 500 miles are chosen, while for the intermediate wave only 5 and 50 miles are considered.
For comparison with the complete linear solution, as given by Harley (1967) for the upstream inflow problem, the same values have been taken, for the physical characteristics of the channel (4.4.7.).
An original base flow of 50 cfs, in a wide rectangular channel with a bottom-slope S_o = 1 feet/mile and a Chezy friction coefficient C = 50 feet$^{\frac{1}{2}}$/sec is assumed.
The responses given by figs 4.5 and 4.6 show the attenuation of the waves at various distances for a number of reference discharges. For all the calculations the TUH of Eq. 2.4 was used as derived from the summation curves of Eq. 4.21.

4.1.8. Effect of the reference discharge

In the linearized diffusion type equations, as explained in Section 3.3., the estimation of the reference discharge or water depth is important. In figs 4.5 and 4.6 the effect of the reference discharge is shown for various distances of the channel.
In the calculations three values of the reference discharge respectively 100, 150 and 200 cfs were chosen. In some cases the 3 curves were so close together, that only one or two curves could be shown in the same figures.
The system parameter P and Q, as defined by Eq. 4.11, can be calculated from the parameters A_τ and D, as defined for a wide rectangular channel by Eq. 3.21. It follows that P and Q depend on the physical characteristics of the channel and the reference discharge.
Table 1 shows the effect of the reference discharge on the moments of the IUH for the discharge for various distances to the point of inflow; the first moment (time lag) $M_1'(h)$, expressed in hours and the second moment $M_2(h)$, expressed in (hours)^2. These moments are functions of the parameters P and Q.
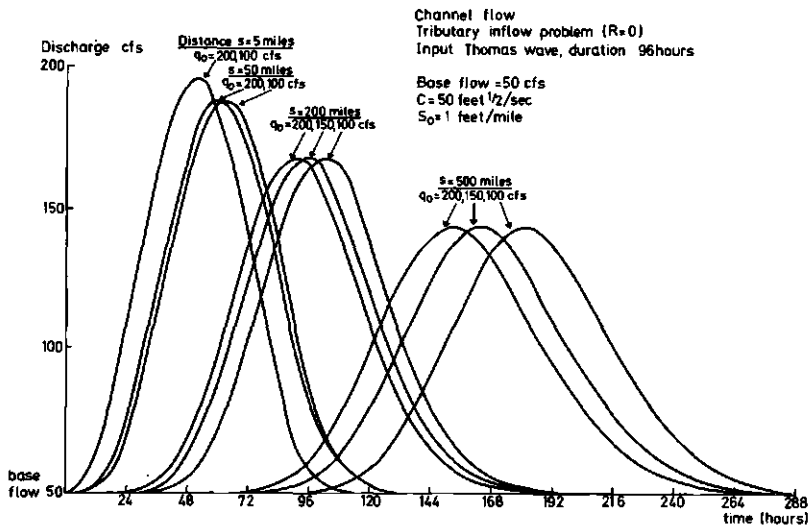
36

fig 4.5 Effect of the reference discharge for different values of the distance s
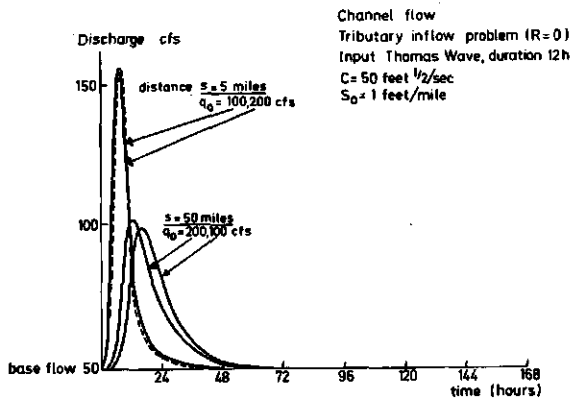for the "Long Thomas" wave

fig 4.6 Effect of the reference discharge
for different values of the distance s
for the "intermediate Thomas" wave

37

Table 1 - Effect of the reference discharge

q_o (cfs)	Q (hours)	s = 5 miles			50 miles			200 miles			500 miles		
		P	M'_1(h)	M_2(h)	P	M'_1(h)	M_2(h)	P	M'_1(h)	M_2(h)	P	M'_1(h)	M_2(h)
100	4.9	0.273	3.79	36.92	2.73	15.83	96.6	10.92	55.96	245.5	27.3	136.2	693.0
150	5.6	0.208	3.96	46.62	2.08	14.45	106.5	8.32	49.39	306.0	20.8	119.3	705.2
200	6.2	0.172	4.17	54.68	1.72	13.76	114.4	6.88	45.75	313.3	17.2	109.7	711.1

Table 1 shows that an increasing reference discharge causes an increasing Q and a decreasing P. For the short reach (s = 5 miles) the first and second moment are increasing, while for the larger distances the first moment is decreasing and the second moment is increasing. The increasing first moment for the short reach is due to the increasing storage in the channel section upstream of the inflow point, causing a slower recession in the tail of the IUH. This is also why the second moments for all values of P are increasing with an increasing reference discharge. For the short reach the relative variation of the second moment is large, while for the long reach the relative variation of the first moment is large. It is clear from Fig. 4.5 that for the 'long' Thomas wave the attenuation effect is negligible for all values of P and the lag effect becomes important only for large values of P.

For the intermediate 'Thomas' wave (Fig. 4.6) in a short reach (5 miles) both effects are small, despite the relative large value and variation of the second moment, whereas the intermediate reach (50 miles) shows some translation and attenuation. Obviously the actual translation and attenuation also strongly depend on the shape of the inflow wave.

Summarising these observations it can be stated that for both inflows into the short channel reach ($P < 1.8$) the reference discharge has hardly any effect. This will be further clarified in Section 5.5. In the intermediate channel reach $1.8 < P < 5$ for the long wave, there is only a little translation, while for the intermediate wave there is some translation and attenuation but it is not very pronounced. In the long channel reach ($P > 5$) an important translation only occurs with the long 'Thomas' wave.

From this example it follows that the reference discharge is not an important factor for a short channel reach. In a long reach however it does effect the translation.

4.1.9. Comparison with a complete non-linear solution

In the department of Hydraulics and Catchment Hydrology research is in progress

on the non-linear theory of channel-flow and overland flow. (Grijsen, 1971)
As some results for a special case are available, the linear solution may be
compared with the non-linear. Conclusions can then be made about the accuracy
of the linear solution and the optimum value of the reference discharge.
The non-linear solution is based on the complete non-linear differential eqs
(3.1) and (3.2), using an implicit difference scheme (Amein, 1968). This
special case, which was solved can be described as follows:
An infinite wide channel or a rectangular channel with width B = 1.75 m, has
a bottomslope S_o = 0.0001, and a Manning friction coefficient K_m = 31 $m^{1/3}$/sec.
This channel is fed in one point (s = 0) by an 'short wave', expressed in
m^3/sec, per 1.75 m width of channel (Fig. 4.6), which is superposed on an
initial uniform water depth of 0.50 m.
The responses, expressed in the water depth, have been calculated for different
values of distance. In Fig. 4.7 the results are only given for s = 0 and
s = 1000 m, which lie within the most interesting range, because this 'short
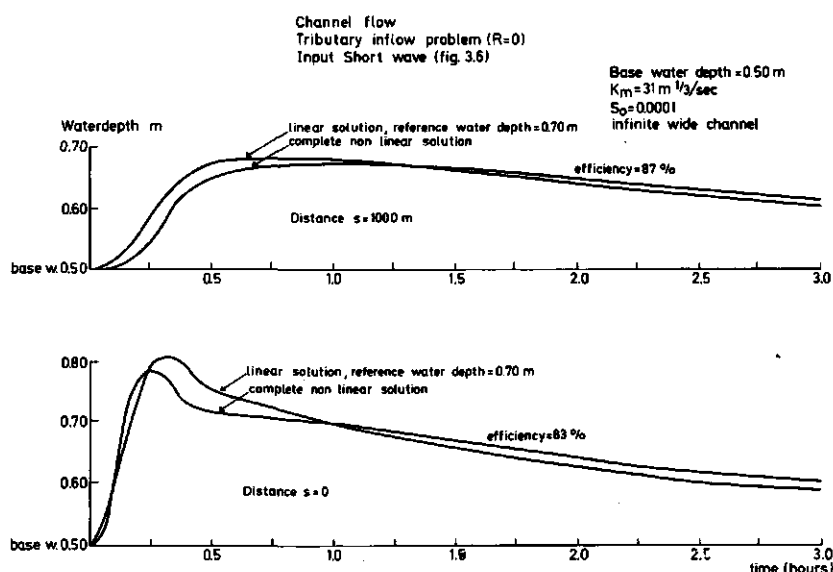wave' attenuated very rapidly.

fig. 4.7 Comparison of linear with complete non linear solution

For a number of reference water depths the linear solution was calculated by
using the S-curve for the water depth (Eq. 4.22) and the convolution integral
in discrete form (Eq. 2.2). A reference water depth of 0.70 m seemed to provide
the best fit. This solution has been presented in Fig. 4.7.

For this 'short wave', especially for s = 0, the effect of the reference water depth on the response is important.

The figures show a fair agreement of the linear solution and the complete non-linear solution. Since this simplification and linearisation of the dynamic equation apparently do not lead to great errors they seem acceptable for practical purposes.

The results also seem to justify the design rule for the reference water depth y_o as suggested in Section 4.1.:

$$y_o = \frac{y_p(o)_{peak} + y_p(s)_{peak}}{4} + y_I \qquad (4.27)$$

The goodness of fit between the linear and non-linear solution can be expressed by the efficiency coefficient R_E defined as (Section 2.5):

$$R_E = \{1 - \frac{\Sigma(f-f_1)^2}{\Sigma(f-\overline{f})^2}\} \; 100\% \qquad (4.28)$$

Here f stands for the data of the non-linear solution, f_1 for the data of the linear solution and $\overline{f}$ for the mean of the data for the non-linear solution.

In the above examples of the linear diffusion type models for distances of s = 0 and s = 1000 m respectively as compared to the non-linear model, showed efficiency coefficients of 83% and 87% respectively.

For optimization procedures of the reference discharge and the system parameters P and Q by a digital computer, the efficiency coefficient is useful as objective criteria for the goodness of fit.

A specific study on the errors due to simplification of the dynamic equation and due to the linearisation of this simplified dynamic equation is in progress.

4.2. INFINITE CHANNEL – DISTRIBUTED INPUT

This element, also called the partial lateral inflow problem, is illustrated in Fig. 4.8. In this case an infinite uniform channel is fed by an inflow, which is uniformly distributed over a distance ℓ, from upstream point s = 0 to downstream point s = ℓ, while the responses can be calculated for $\geq \ell$. No attention is paid to responses, for s < 0, which are relevant for the study of the backwater effect. The inflow may be the result of the overland flow phase or the result of the groundwater flow phase. From the description of the

problem it is clear that the tributary inflow problem is a special case, where $\ell = 0$.
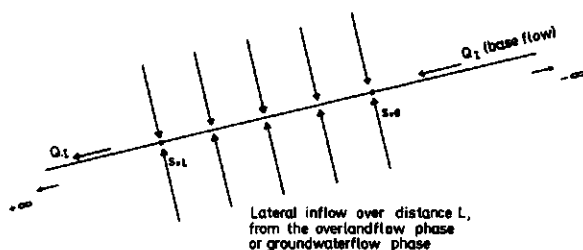
fig 4.8 Concept of the partial lateral inflow problem

4.2.1. Impulse Response

As compared to the tributary inflow problem, using the same differential equation, only the first condition differs as follows:

$$y_p(s,o) = \frac{1}{\ell} \qquad \text{for } 0 \leqslant s \leqslant \ell$$

and   (4.29)

$$y_p(s,o) = 0 \qquad \text{for} \qquad s > \ell \quad \text{and} \quad s < 0$$

which means an instantaneous addition at time $t = 0$ per unit width of channel of a unit volume uniformly distributed over a distance ℓ of the channel reach. The solution can be derived from the solution of the tributary inflow problem, by integrating over the distance:

$$y_p(s,t) = \frac{1}{\ell} \int_{s-\ell}^{s} y_{p_1}(\sigma,t) \, d\sigma \qquad (4.30)$$

where $y_{p_1}(\sigma,t)$ is the solution for the water depth of the tributary inflow problem, given by Eq. (4.8).
Substitution of Eq. (4.8) gives for the water depth of the partial lateral inflow (Van de Nes and Hendriks, 1971):

$$y_p(s,t) = \frac{1}{2\ell} \left\{ \text{erf} \left(\frac{s - A_\tau t}{2\sqrt{Dt}} \right) - \text{erf} \left(\frac{s - \ell - A_\tau t}{2\sqrt{Dt}} \right) \right\} \qquad (4.31)$$

The discharge can be found after introducing Eq. (4.30) into Eq. (3.19) thus:

41

$$q_p(s,t) = \frac{A_\tau}{2\ell} \{ \text{erf}(\frac{s-A_\tau t}{2\sqrt{Dt}}) - \text{erf}(\frac{s-\ell-A_\tau t}{2\sqrt{Dt}}) \}$$

$$+ \frac{1}{2\ell} \sqrt{\frac{D}{\pi t}} \{ e^{-\frac{(s-\ell-A_\tau t)^2}{4 Dt}} - e^{-\frac{(s-A_\tau t)^2}{4 Dt}} \} \tag{4.32}$$

In the terminology of the systems approach and introducing a new dimensionless inflow length parameter $R = \frac{\ell}{s}$ the eqs (4.31) and (4.32) expressing the IUH's can be written in dimensionless form in the same way as has been done for the tributary inflow problem:

$$\bar{h}_q = \frac{h_q Q}{\Psi} = \frac{1}{2PR} \{ \text{erf}(\frac{P-T}{\sqrt{2T}}) - \text{erf}(\frac{P(1-R)-T}{\sqrt{2T}}) \}$$

$$+ \frac{1}{2PR} \frac{1}{\sqrt{2\pi T}} \{ e^{-\frac{(P(1-R)-T)^2}{2T}} - e^{-\frac{(P-T)^2}{2T}} \} \tag{4.33}$$

and

$$\bar{h}_y = \frac{h_y s}{\Psi} = \frac{1}{2R} \{ \text{erf}(\frac{P-T}{\sqrt{2T}}) - \text{erf}(\frac{P(1-R)-T}{\sqrt{2T}}) \} \tag{4.34}$$

where the meaning of the symbols is the same as for the tributary inflow problem. It can be proved that for the case $R \to 0$, the solutions for the tributary inflow follows from eqs (4.33) and (4.34).

4.2.2. Classification

Using the same criteria for classification, as has been done for the tributary inflow problem, it follows that the classification also depends on the third system parameter R:

a. For discharges the classification of the channel reach as a short reach is given in Table 2 for a number of R values:

Table 2 : Condition for the short channel reach.

R	0.01	0.1	0.2	0.3	0.4	0.5	0.6	0.7	0.8	0.9	0.99	1.0
P	$\leqslant 1.8$	1.9	2.0	2.1	2.3	2.4	2.6	2.9	3.2	3.6	4.5	∞

42

Dimensionless impulse responses for the lateral inflow problem (R=0.5)

$R = 0.5$
$P \leqslant 2.4$ short channel reach
$2.4 < P \leqslant 10$ intermediate channel reach
$P > 10$ long channel reach

fig. 4.9a Dimensionless impulse responses for the fully lateral inflow problem (R=1)

$R = 1$
Short channel reach for all values of P

43
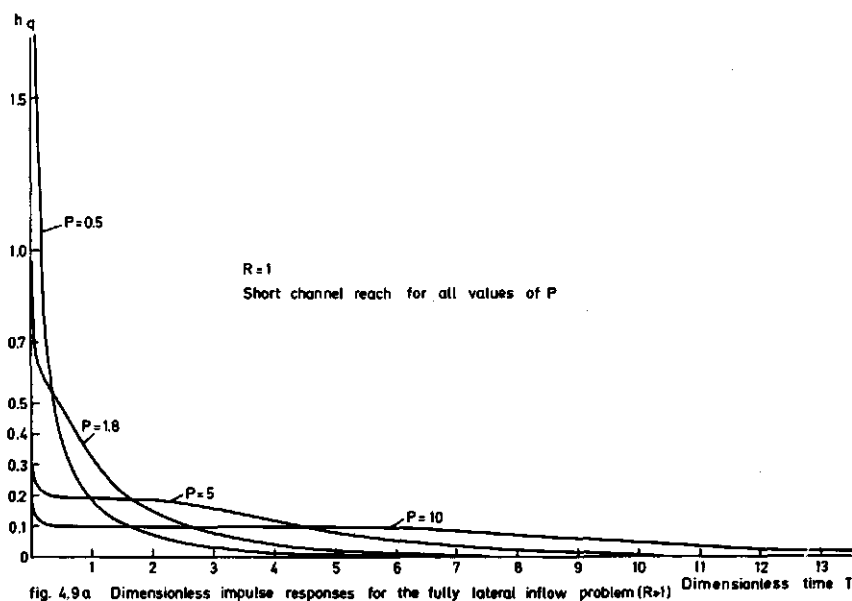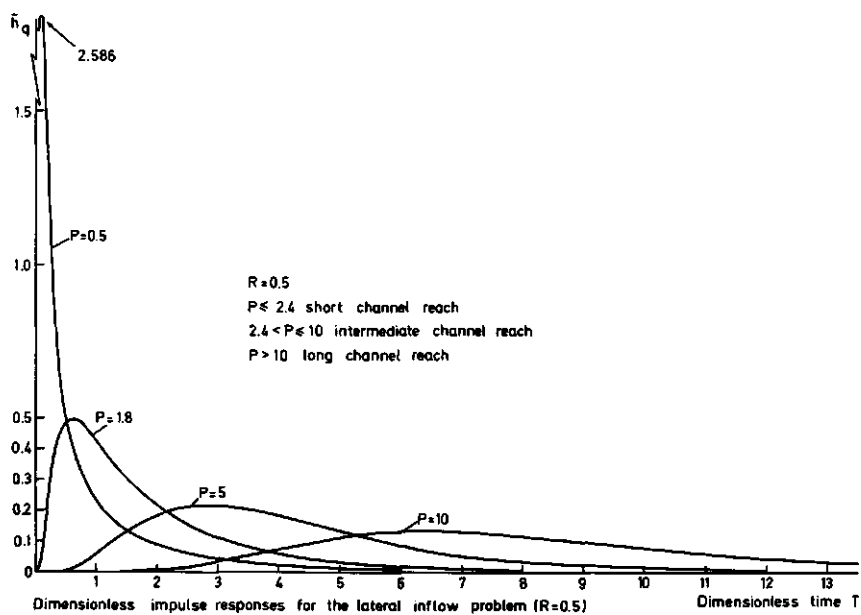
From Table 2 it follows that for $R = 0.01$, the same condition is found as for the tributary inflow problem, while for $R = 1$ the channel reach is short for every value of P, because then the peak occurs at time $t = 0$. It is interesting to note that for $R = 0.99$ the value of P is relatively small ($P \leqslant 4.5$).

b. For an intermediate channel reach, the following conditions are valid:

For $0 < R \leqslant 0.2$ $\qquad$ $P_{short} < P \leqslant 5$ $\qquad$ ($\xi < 3 \times 10^{-3}$)

and $0.2 < R \leqslant 0.5$ $\qquad$ $P_{short} < P \leqslant 10$ $\qquad$ ($\xi < 4 \times 10^{-3}$)

and $0.5 < R \leqslant 0.9$ $\qquad$ $P_{short} < P \leqslant 25$ $\qquad$ ($\xi < 6 \times 10^{-3}$)

where P_{short} are the values given in Table 2 for the appropriate values of R. It can be seen that for increasing values of R the value of P has to be increased considerably, before the channel can be classified as an intermediate reach.

c. For a long channel reach the following conditions apply:

For $0 < R \leqslant 0.2$ $\qquad$ $P > 5$

$\quad 0.2 < R \leqslant 0.5$ $\qquad$ $P > 10$

$\quad 0.5 < R \leqslant 0.9$ $\qquad$ $P > 25$

For larger values of R the value of P becomes very large, with $P \to \infty$, if $R \to 1$. In Fig. 4.9a for $R = 1$ and $R = 0.5$ the dimensionless IUH for the discharge are shown for various values of P.

4.2.3. Moments

The moments of the IUH of the discharge are derived from Eq. 2.9 (Van de Nes and Hendriks, 1971) and can be expressed as follows:

$$
\begin{aligned}
M_1'(h_q) &= (1 - \tfrac{1}{2}R)PQ \; + \tfrac{1}{2}\,Q \\
M_2(h_q) &= (1 - \tfrac{1}{2}R)PQ^2 + \frac{1}{12}\,R^2P^2Q^2 + \frac{5}{4}\,Q^2 \\
M_3(h_q) &= (1 - \tfrac{1}{2}R)3PQ^3 + \tfrac{1}{4}\,R^2P^2Q^3 + \frac{11}{2}\,Q^3
\end{aligned}
\tag{4.35}
$$

from which the shape factors as defined in 2.2 follow:

$$S_2 = \frac{(4-2R)P + 1/3\ R^2P^2 + 5}{(2-R)^2P^2 + (4-2R)P + 1} \quad \text{and } S_3 = \frac{(1-\frac{1}{4}R)\ 24P + 2R^2P^2 + 44}{\{1 + (2-R)P\}^3} \quad (4.36)$$

In Fig. 4.9b S_3 is given as a function of S_2 for a number of values of R. For $R = 0$ the shape factors of the tributary inflow problem is found. It is remarkable that for $0 < R < 0.5$ the shape factor diagrams are very near to each other. This means that the shape of the IUH for these values of R is about the same, although a time lag, dependent on the value of P may occur.

fig. 4.9b Shape factor diagram for the lateral inflow problem
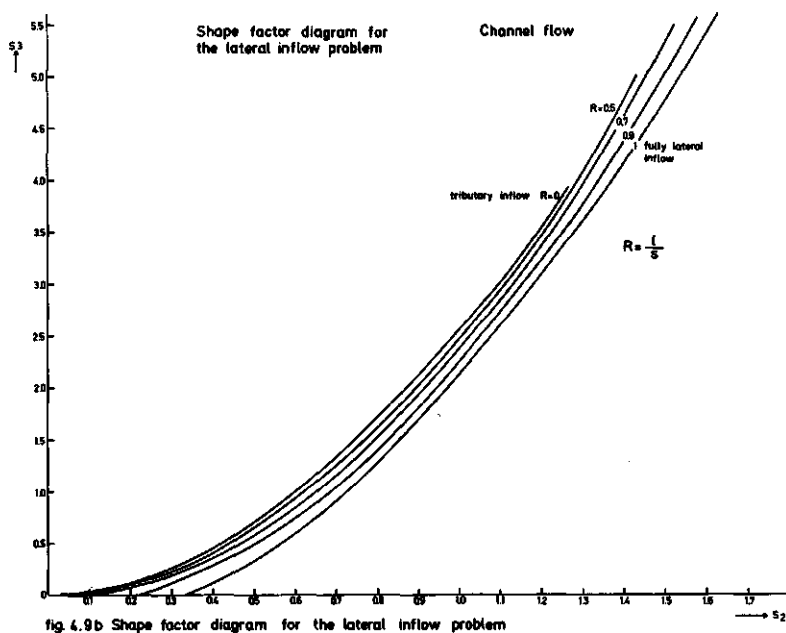
The first three moments of the IUH for the water depth are:

$$M_1'(h_y) = (1 - \tfrac{1}{2}R)PQ + Q$$
$$M_2(h_y) = (1 - \tfrac{1}{2}R)PQ^2 + \frac{1}{12}R^2P^2Q^2 + 2Q^2 \qquad (4.37)$$
$$M_3(h_y) = (1 - \tfrac{1}{2}R)3PQ^3 + \tfrac{1}{4}R^2P^2Q^3 + 8Q^3$$

Here again it follows that for large P-values the moments and therefore the IUH for the discharge becomes equal to the corresponding moments and the IUH for the water depth.

45

4.2.4. Attenuation coefficient

As defined in Section 2.3. the attenuation coefficient for the discharge is:

$$C_A = \left\{ \frac{P + 5/4 + \frac{1}{2} RP \ (1/6 \ RP - 1)}{\beta} \right\} \left(\frac{Q}{t_F}\right)^2 \tag{4.38}$$

where β is dependent on the shape of the input and t_F is the duration of input. Comparing Eq. 4.38 with Eq. 4.17 shows that

$$\text{for} \qquad 1/6 \ RP - 1 > 0 \quad \text{or} \quad 1 \geqslant R > 6/P \tag{4.39}$$

the attenuation for this lateral inflow is greater than the attenuation for the tributary inflow.
For $R < 6/P \leqslant 1$ the attenuation of the system is smaller than the attenuation of the tributary inflow.
The results of calculations in Section 5. illustrate this effect.

4.2.5. Spectra

The amplitude density spectrum and phase density spectrum of the IUH of the discharge are derived by Van de Nes and Hendriks, 1971.
The amplitude density spectrum can be expressed as follows: (4.40)

$$\hat{h}_{qa}(\omega) = \frac{e^{P(1-\frac{1}{2}R)(1-\alpha(\omega))}}{2PR} \left[\frac{2(1+\alpha(\omega))\{\cosh PR(1-\alpha(\omega)) - \cos PR\beta(\omega)\}}{(\alpha(\omega)-1)(2\alpha^2(\omega)-1)} \right]^{\frac{1}{2}}$$

and the phase density spectrum:

$$\hat{h}_{q\theta}(\omega)\big|_X = -P(1-\tfrac{1}{2}R)\beta(\omega) - \tan^{-1} \frac{\alpha(\omega) + \beta^2(\omega)}{\beta(\omega)(\alpha(\omega)-1)}$$

$$+ \tan^{-1} \{\tan \tfrac{1}{2}PR\beta(\omega) \ \coth \tfrac{1}{2}PR(\alpha(\omega) -1)\} \tag{4.41}$$

for $\omega > 0$ and $PR\beta(\omega) \in X = [0,\pi)$

and $\hat{h}_{q\theta}(\omega)\big|_X$ is the restriction of $\hat{h}_{q\theta}$ to X

In the case that $PR\beta(\omega) \in X_k = [(2k-1)\pi,(2k+1)\pi), \ k = 1, 2, \ldots\ldots$
it follows:

$$\hat{h}_{q\theta}(\omega)\big|_{X_k} = \hat{h}_{q\theta}(\omega)\big|_X + k \ \pi \quad, \ k = 1, 2, \ldots\ldots \tag{4.42}$$

fig. 4.10 a   Amplitude density spectrum of the I U H , expressed in the discharge, for the lateral inflow problem [R=0.3]

fig. 4.11a Phase density spectrum of the I U H, expressed in the discharge, for the lateral inflow problem [R=0.3]
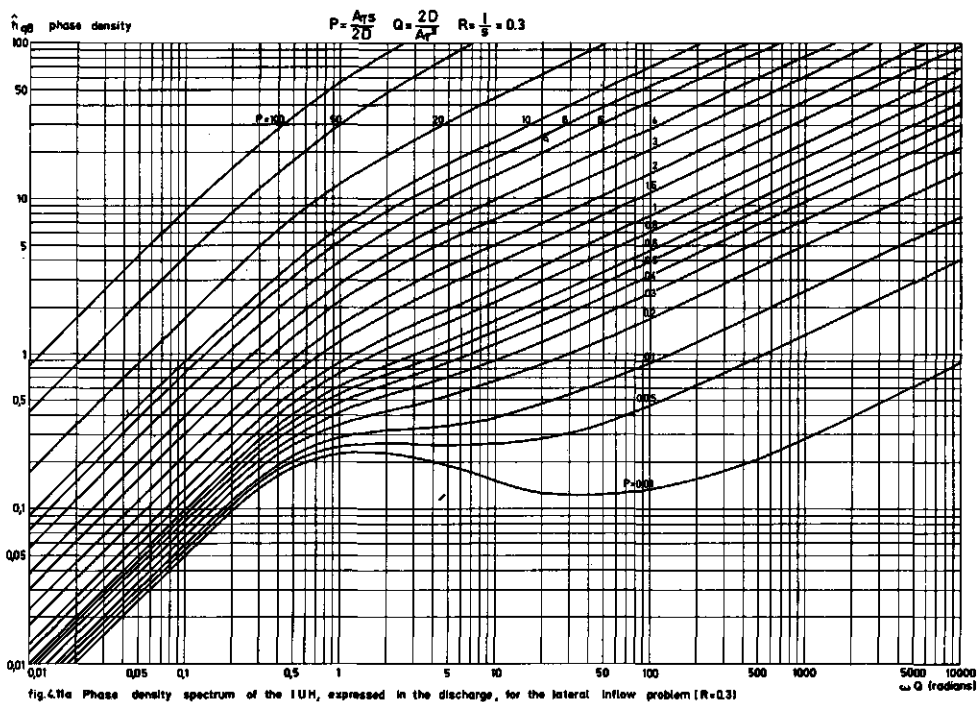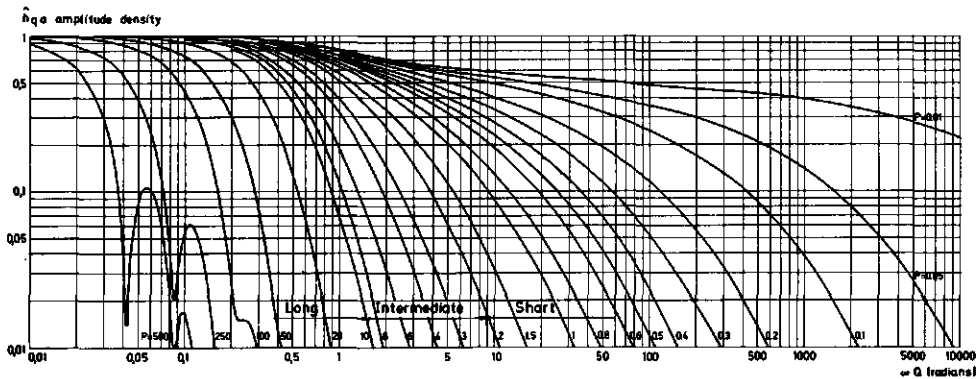
fig 4.10 b   Amplitude density spectrum of the IUH , expressed in the discharge, for the lateral inflow problem (R=0.5)

$$P = \frac{A_T S}{2D} \qquad Q = \frac{2D}{A_T^2} \qquad R = \frac{1}{s} = 0.5$$
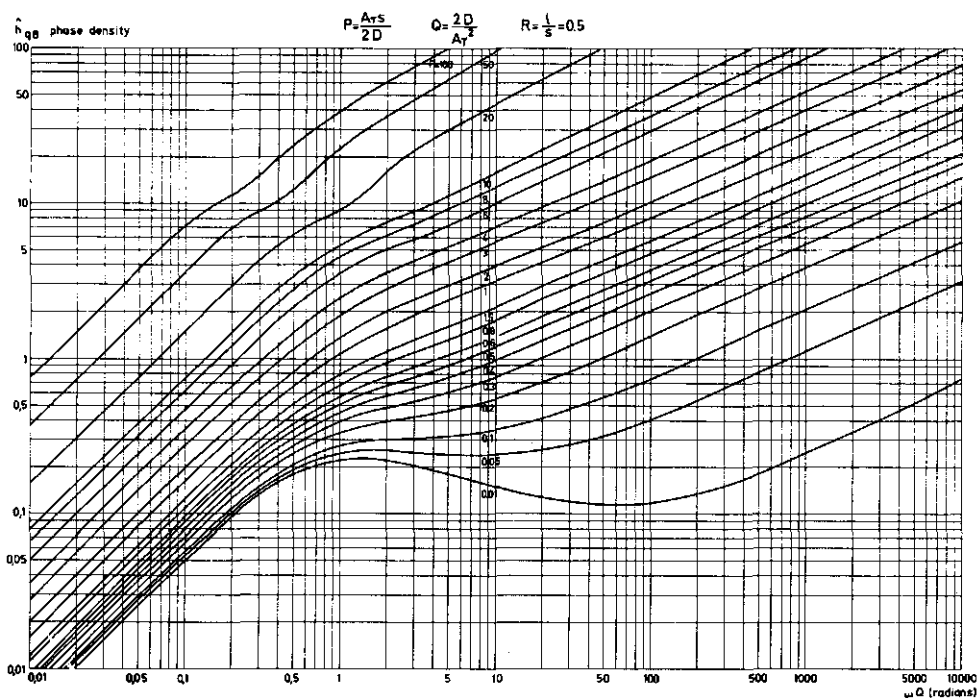
fig 4.11 b Phase density spectrum of the IUH , expressed in the discharge, for the lateral inflow problem (R=0.5)

48

$\hat{n}_q a$ amplitude density

fig.4.10c Amplitude density spectrum of the IUH, expressed in the discharge, for the lateral inflow problem (R=0.7)

$\hat{n}_q\phi$ phase density

$$P = \frac{A_T S}{2D} \qquad Q = \frac{2D}{A_T^2} \qquad R = \frac{1}{S} = 0.7$$

fig.4.11c Phase density spectrum of the IUH, expressed in the discharge, for the lateral inflow problem (R=0.7)

49

fig. 4.10 d Amplitude density spectrum of the IUH, expressed in the discharge, for the lateral inflow problem (R=0.9)

$$P = \frac{A_T s}{2D} \qquad Q = \frac{2D}{A_T^2} \qquad R = \frac{1}{s} = 0.9$$

fig. 4.11 d Phase density spectrum of the IUH, expressed in the discharge, for the lateral inflow problem (R=0.9)

fig. 4.10e Amplitude density spectrum of the IUH, expressed in the discharge, for the lateral inflow problem (R=1)
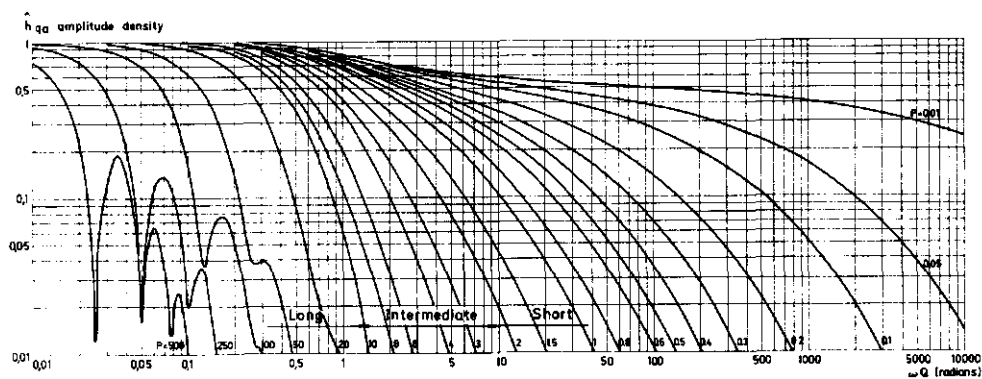
$$P = \frac{A_{TS}}{2D} \quad Q = \frac{2D}{A_T^2} \quad R = \frac{1}{S} = 1$$

fig. 4.11e Phase density spectrum of the IUH, expressed in the discharge, for the lateral inflow problem (R=1)

51

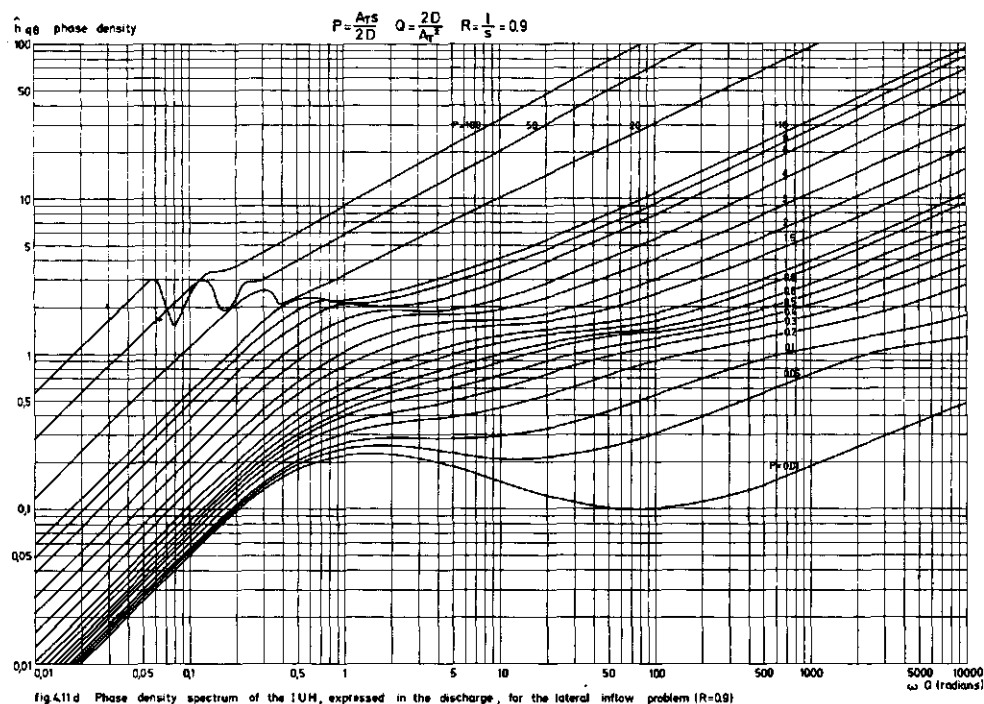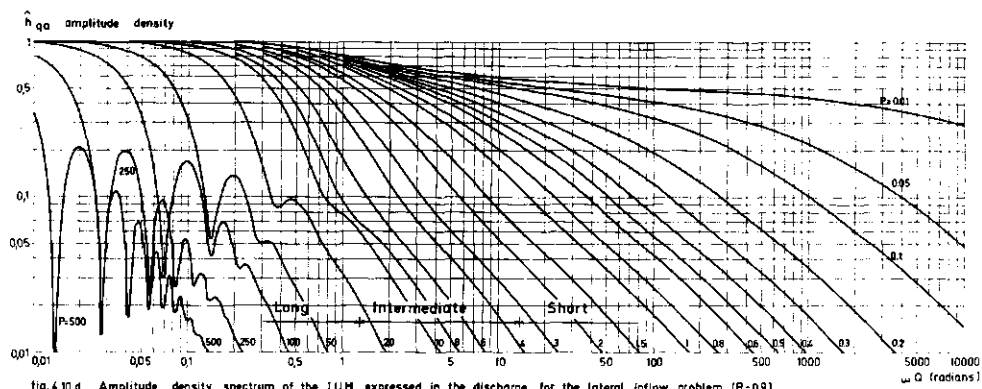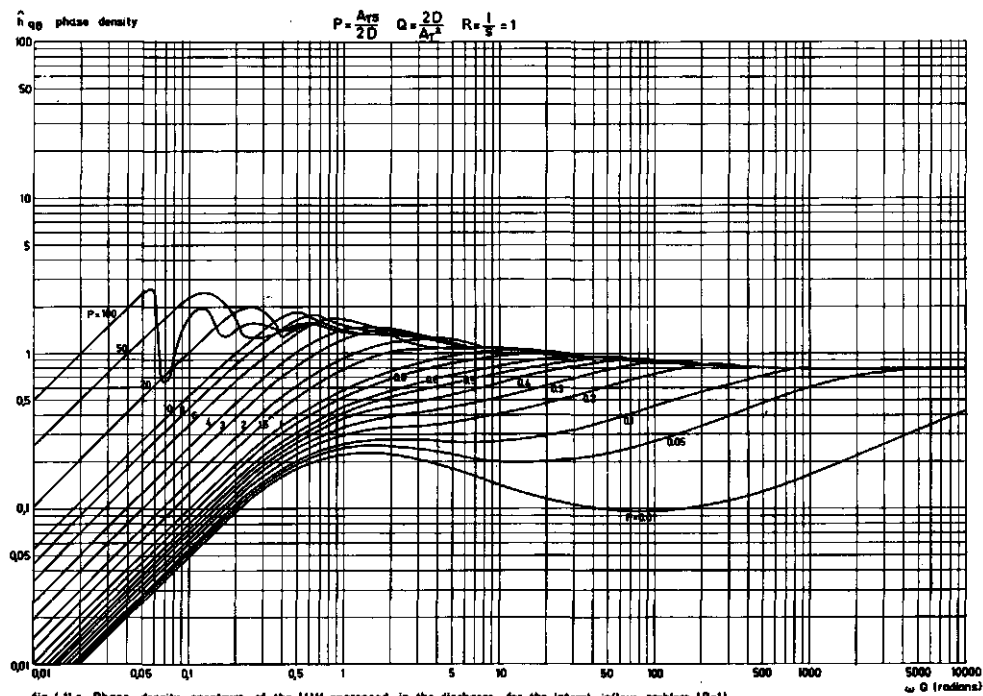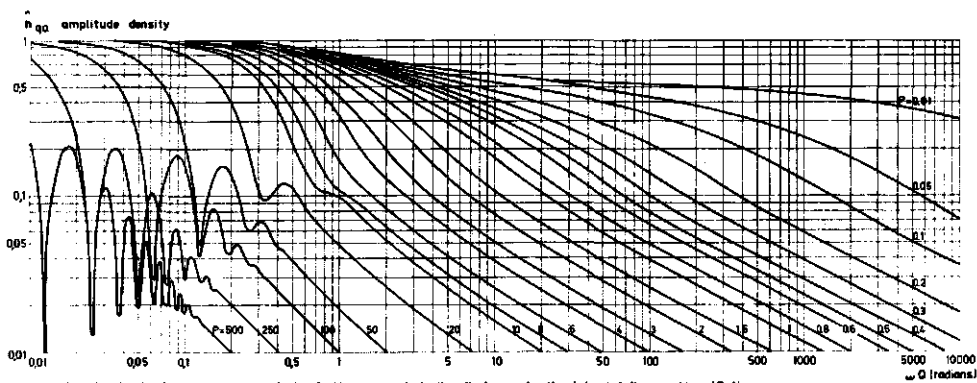For a number of combined R and P values, both spectra are presented in the figs 4.10 and 4.11.

In the amplitude density spectra oscillations for large value of P occur. The value of P, where the oscillations start, depends on the value of R. For an increasing value of R the oscillations start at a lower value of P. The reason for these oscillations is that in the IUH, a nearly horizontal part occurs. This is shown by the results of the corresponsing calculations (see Section 4.2.7.). The same phenomenon can be observed in the phase density spectra. Referring to the criterion $R \lesssim 6/P$ for the relative attenuation (Section 4.2.4.) comparing the spectra shows the same criterion for the filtering effect on the lateral inflow as compared with the tributary inflow.

The phase density spectra show that the translation for a certain value of P becomes more important for decreasing values of R.

In Section 5.2., where the different types of problems are compared this comparison of spectra is more detailed.

4.2.6. Summation curves

The S-curves for the discharge and the water depth are derived by integration of the eqs 4.32 and 4.31 for two different conditions of R. (Van de Nes and Hendriks, 1971).

a. For $0 < R \leqslant 1$ or $s \geqslant \ell$:

$$S_q = \frac{1}{2RP} \sqrt{2T} \{ -\eta \ \text{erf} \ \eta - \frac{1}{\sqrt{\pi}} e^{-\eta^2} + \eta_\ell \text{erf} \ \eta_\ell + \frac{1}{\sqrt{\pi}} e^{-\eta_\ell^2} \} + \frac{1}{2} \quad (4.43)$$

$$S_y = \frac{Q}{Rs} \sqrt{\frac{T}{2}} \{ -\eta \ \text{erf} \ \eta - \frac{1}{\sqrt{\pi}} e^{-\eta^2} + \frac{1}{2\sqrt{2T}} (\text{erfc} \ \eta - e^{2P} \ \text{erfc} \ \xi) \} +$$

$$- \frac{Q}{Rs} \sqrt{\frac{T}{2}} \{ -\eta_\ell \ \text{erf} \ \eta_\ell - \frac{1}{\sqrt{\pi}} e^{-\eta_\ell^2} + \frac{1}{2\sqrt{2T}} (\text{erfc} \ \eta_\ell +$$

$$- e^{2P(1-R)} \ \text{erfc} \ \xi_\ell) \} + \frac{PQ}{2s} \quad (4.44)$$

where $\eta = \frac{P-T}{\sqrt{2T}}$, $\xi = \frac{P+T}{\sqrt{2T}}$

$$\quad (4.45)$$

and $\eta_\ell = \frac{P(1-R)-T}{\sqrt{2T}}$, $\xi_\ell = \frac{P(1-R)+T}{\sqrt{2T}}$

b. For $R > 1$ or $0 \leqslant s < \ell$:

$$S_q = \frac{1}{2RP} \sqrt{2T} \{ -\eta \text{ erf } \eta - \frac{1}{\sqrt{\pi}} e^{-\eta^2} + \eta_\ell \text{erf } \eta_\ell + \frac{1}{\sqrt{\pi}} e^{-\eta_1^2} \} +$$

$$+ \frac{1}{R} - \tfrac{1}{2} \tag{4.46}$$

$$\dot{S}_y = \frac{Q}{Rs} \sqrt{\frac{T}{2}} \{ -\eta \text{ erf } \eta - \frac{1}{\sqrt{\pi}} e^{-\eta^2} + \frac{1}{2\sqrt{2T}} (\text{erfc } \eta - e^{2P} \text{ erfc } \xi) \} +$$

$$- \frac{Q}{Rs} \sqrt{\frac{T}{2}} \{ - \eta_\ell \text{ erf } \eta_\ell - \frac{1}{\sqrt{\pi}} e^{-\eta_\ell^2} + \frac{1}{2\sqrt{2T}} (\text{erfc } \eta_\ell +$$

$$- e^{2P(1-R)} \text{erfc } \xi_\ell) \} + \frac{PQ}{s} (\frac{1}{R} - \tfrac{1}{2}) + \frac{Q}{2Rs} (1 - e^{2P(1-R)}) \tag{4.47}$$

where η, ξ, η_ℓ and ξ_ℓ are defined as given before.

The solutions for the S-curves were derived for the condition that the system is fed by a constant intensity of inflow, expressed in a unit of volume per time, per unit width of channel over a distance ℓ.

If the intensity of inflow to the channel reach is expressed in units of water depth per time over the drainage area D_a, it follows that: unit water depth per time = 1 x D_a unit volumes per time. This volume of water is uniformly distributed over the surface area of the channel $C_a (= B.\ell)$.

Introducing the storage capacity of the channel as:

$$\mu_c = \frac{C_a}{D_a} \tag{4.48}$$

it follows that in the expressions for the S-curves of the water depth the term $Rs(=\ell)$ may be replaced by μ_c. Expressing the intensity of inflow in units of depth per time over the drainage area does not effect the S-curves for the discharge.

For $t \to \infty$ it follows from the eqs (4.43) and (4.44) for the condition $R \leqslant 1$:

$$q_p = A_\tau y_p \frac{\mu_c}{\ell} \quad \text{(steady state)} \tag{4.49}$$

Under condition $R > 1$ or $0 \leqslant s < \ell$ the discharge and water depth over the

distance ℓ of the channel reach vary as:

$$\lim_{T \to \infty} S_q = \frac{1}{R} \tag{4.50}$$

and
$$\lim_{T \to \infty} S_y = \frac{PQ}{\mu_c} + \frac{Q}{2\mu_c} (1 - e^{2P(1-R)}) \tag{4.51}$$

From the eqs 4.50 and 4.51 it follows for $R \to \infty$ ($s = 0$), expressed in parameters A_τ and D.

and
$$S_q = 0$$
$$S_y = \frac{D}{\mu_c A_\tau^2} (1 - e^{-\frac{A_\tau}{D} \ell}) \tag{4.52}$$

This means, according Eq. 3.19 that then $(y)_{s=0} = \frac{D}{A_\tau} (\frac{\partial y}{\partial s})_{s=0}$

It can be concluded from eqs 4.50 and 4.51 that $t \to \infty$ the first term on the right hand side of the equation shows the linear increase of the discharge and water depth with distance, while the second term in the equation of the water depth shows the relative non-linear increase, which decreases with the distance. For $R = 1$ this term vanishes completely. It should be noted that the shape of the water depth profiles depends on the choice of the constant reference discharge or water depth.

4.2.1. Response to given waves of inflow

The four types of input, described in Section 3.4. have been used for demonstrating the various aspects of this type of problem (figs 3.3, 3.4, 3.5 and 3.6):
Fig. 4.12 gives the discharge and water depth profiles for a blockinput of 3 hours and for a number of values of the time t.
In this example the following data were used:
A reference water depth $y_o = 1$ m, $K_m = 25$ m$^{1/3}$/sec, $S_o = 0.0001$, $\mu_c = 0.02$ and $\ell = 25\,000$ m.
For the fully lateral inflow problem ($R = 1$) Fig. 4.13 illustrates the effect of the dimensionless length parameter P on the discharge and the water depth. Here the above data were used. It shows that the peak discharge, expressed in water depth, decreases with channellength. Naturally if the peak discharge were expressed in unit volumes per unit of time, it would increase.

54
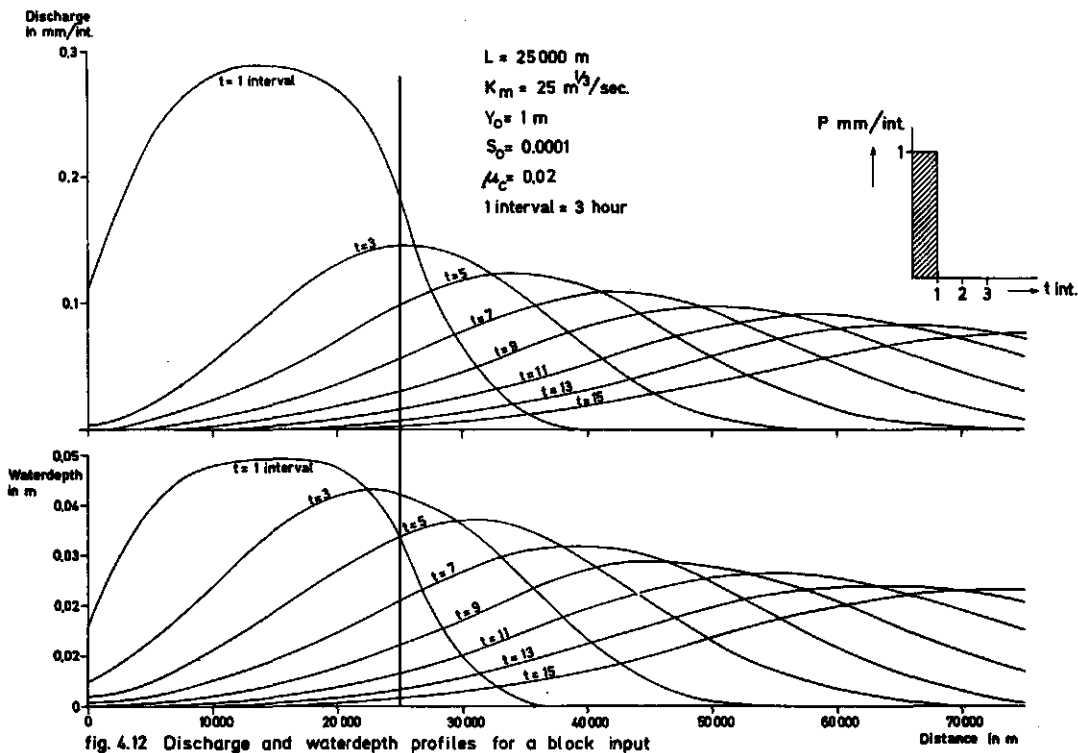
fig. 4.12 Discharge and waterdepth profiles for a block input

The peak of discharge occurs at the end of the block input. The peak of the water depth increases and is delayed by an increase of channellength. Further the water depth is plotted against the discharge, showing the decrease of the gradient of the water depth $(\frac{\partial y_p}{\partial s})$ with increasing length of the channel reach. In Fig. 4.14 for three values of P the effect of R is demonstrated for a constant value of Q

For comparison some results of the upstream inflow problem have been given. This problem will be fully dealt with in Section 4.4.

It shows that for a small value of P (= 0.74), the solution of the fully lateral inflow (R = 1) problem is very close to the upstream inflow problem, while the tributary inflow problem differs considerably. For a larger value of P (= 3.7), tributary, upstream and partial lateral (R =0.2) inflow problems are close to each other, but differ considerably with the fully lateral inflow problem. The same is true for the case P = 7.4.

TUH Discharge
mm/int.

L = 5000 m (P= 0,74)
L = 10 000 m (P = 1,48)
L = 15 000 m (P = 2,22)
L = 20 000 m (P = 2,96)
L = 25 000 m (P = 3,7)
L = 50 000 m (P = 7,4)

K_m = 25 $m^{1/3}/sec.$
Y_0 = 1 m
S_0 = 0,0001
R = 1
Q = 1,65 interval
1 interval = 3 hour

t intervals

Waterdepth
in m

t = 5
10
L = 50 000 m
15
20
2
1
6
4
8
10
5

3 2
L = 25 000 m
1/2
t = 1 interval
2

2
L = 10 000 m
t = 1/2
t = 1

Discharge mm/int.

Waterdepth
in m

L = 50 000 m
L = 25 000 m
L = 20 000 m
L = 15 000 m
L = 10 000 m
L = 5000 m

μ_c = 0.02

Input mm/int.

1 2 3   t intervals

t intervals

fig. 4.13 Effect of the dimensionless length parameter P

TUH mm/int. Discharge

$K_m = 25\ m^{1/3}/sec.$

$Y_0 = 1\ m$

$S_0 = 0.0001$

$S = 5000\ m$

$A_T = 0.37\ m/sec.$

$D = 1248\ m^2/sec.$

$P = \dfrac{A_T S}{2D} = 0.74$

$Q = \dfrac{2D}{A_T^2} = 1.65\ interval$

1 interval = 3 hour

$R = \begin{cases} 0 \\ 0.2 \end{cases}$

R = 1

—————— Lateral inflow

- - - - - Upstream inflow

input mm/int.

1 2 3   t int.

0   2   4   6   8   10   12   14   16   18   t intervals

TUH mm/int.

R = 1

R = 0.2

$R = \begin{cases} 0 \\ 0.02 \end{cases}$

S = 25000 m

P = 3.7

Q = 1.65 interval

—————— Lateral inflow

- - - - - Upstream inflow

0   2   4   6   8   10   12   14   16   18   20   22   24   t intervals

TUH mm/int.

S = 50000 m

P = 7.4

Q = 1.65 interval

—————— Lateral inflow

- - - - - Upstream inflow

R = 1

R = 0.1

$R = \begin{cases} 0 \\ 0.02 \end{cases}$

0   2   4   6   8   10   12   14   16   18   20   22   24   26   28   30   32   t intervals

fig. 4.14 Effect of the spatial distribution of inflow for three values of P

57

The effect of the reference water depth and the bottom slope is shown in Fig. 4.15, for the fully lateral inflow problem $(R = 1)$.

TUH Discharge
mm/int.
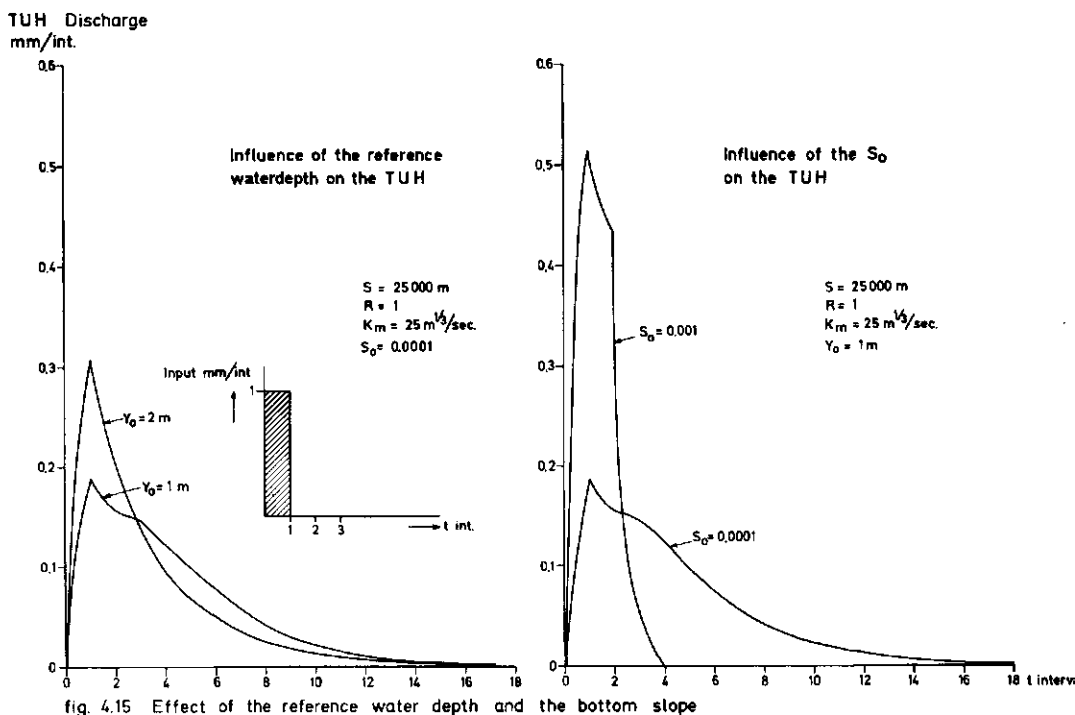
fig. 4.15   Effect of the reference water depth and the bottom slope

For a long and intermediate 'Thomas' wave and using the same physical data as for the tributary problem, the responses are given for $R = 1$ in the figs 4.16 and 4.17.
For all the calculations the TUH of Eq. 2.4 was used as derived from the summation curves of eqs 4.43, 4.44, 4.46 and 4.47.

4.2.8. Effect of reference discharge

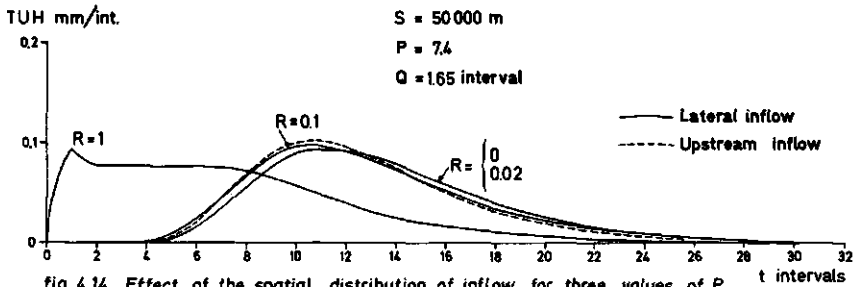Table 3 shows the effect of the reference discharge on the system parameters P and Q and on the first and the second moments of the IUH, for the examples with the 'Thomas' wave, given in the figs 4.16 and 4.17 for the fully lateral inflow problem $(R = 1)$. In this case the 'Thomas' wave inflow is uniformly distributed over the whole reach of the wide rectangular channel.

58
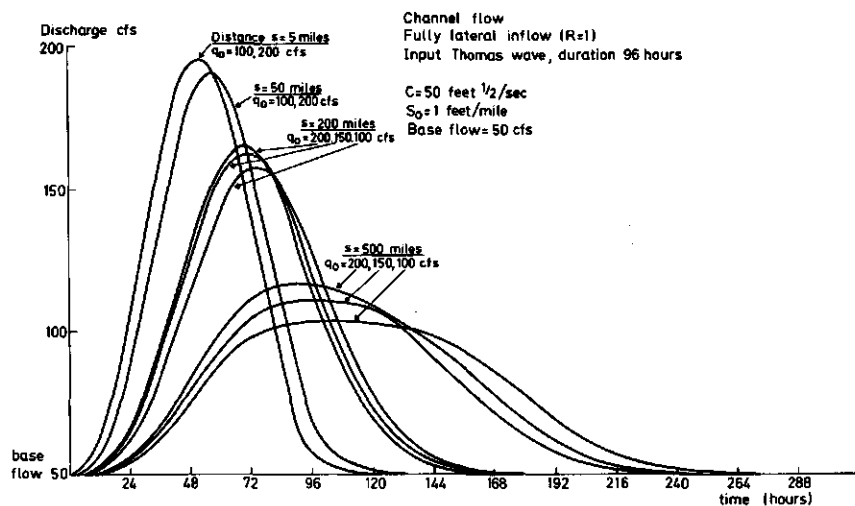
fig 4.16 Effect of the reference discharge for different values of the distance s
for the "Long Thomas" wave
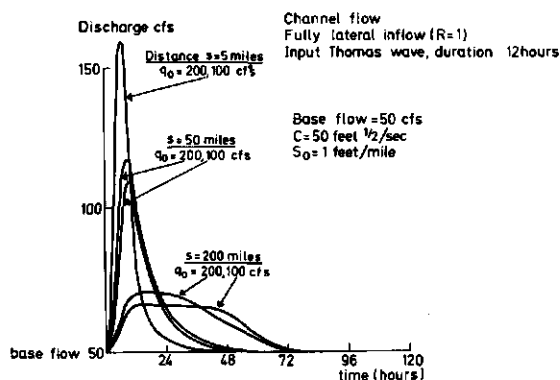
fig 4.17 Effect of the reference discharge
for different values of the distance s
for the "intermediate Thomas" wave

59

Discharge cfs

Input Thomas wave
duration 96 hours

Fully lateral inflow (R=1)
Comparison of constant reference
discharge with varying reference discharge

$C = 50$ feet $^{1/2}$/sec
$S_0 = 1$ feet/mile

constant reference discharge

varying reference discharge

base flow

distance s=200miles

constant reference discharge (100 cfs)
variable reference discharge

base flow 50

time (hours)
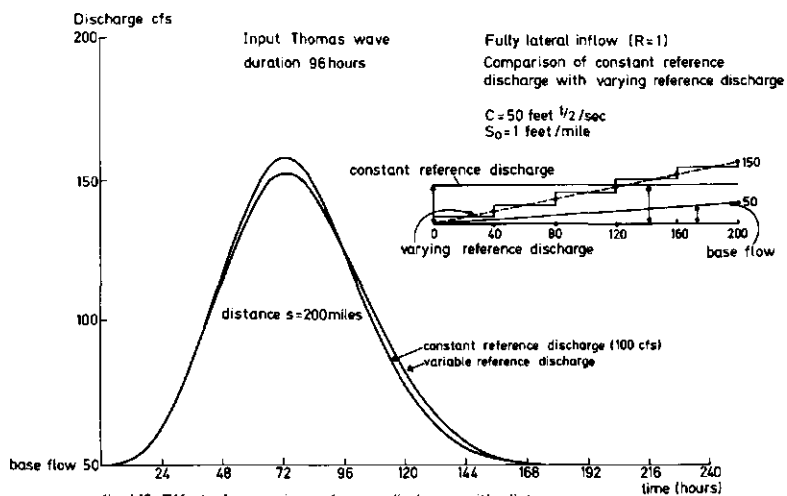
fig. 4.18 Effect of a varying reference discharge with distance
for the "Long Thomas" wave

Channel flow
Lateral inflow over a distance of 1000m
Input Short wave (fig. 3.6)

Base water depth=0.50 m
$K_m = 31 m^{1/3}$/sec
$S_0 = 0.0001$
infinite wide channel

Waterdepth m

linear solution, reference water depth =0.70 m
complete non linear solution

efficiency = 89 %

Distance s = 0

base w. 0.50

linear solution, reference water depth = 0.70 m
complete non linear solution

efficiency = 88 %

Distance s = 500m

base w. 0.50

time (hours)

fig 4.19 Comparison of linear with complete non linear solution

60

Table 3 : Effect of reference discharge for $R = 1$.

Q_o(fs)	Q	5 miles			50 miles			200 miles			500 miles		
		P	M_1'	M_2	P	M_1'	M_2	P	M_1'	M_2	P	M_1'	M_2
100	4.9	0.273	3.12	33.42	2.73	9.14	77.64	10.92	29.20	399.4	27.3	69.3	1848.0
150	5.6	0.208	3.38	42.57	2.08	8.62	83.12	8.32	26.09	350.6	20.8	61.0	1495.9
200	6.2	0.172	3.63	51.45	1.72	8.43	90.53	6.88	24.43	331.9	17.2	56.4	1326.2

The system parameters P and Q are the same as in the case of the tributary
inflow problem ($R = 0$), however the moments are not the same, which is shown
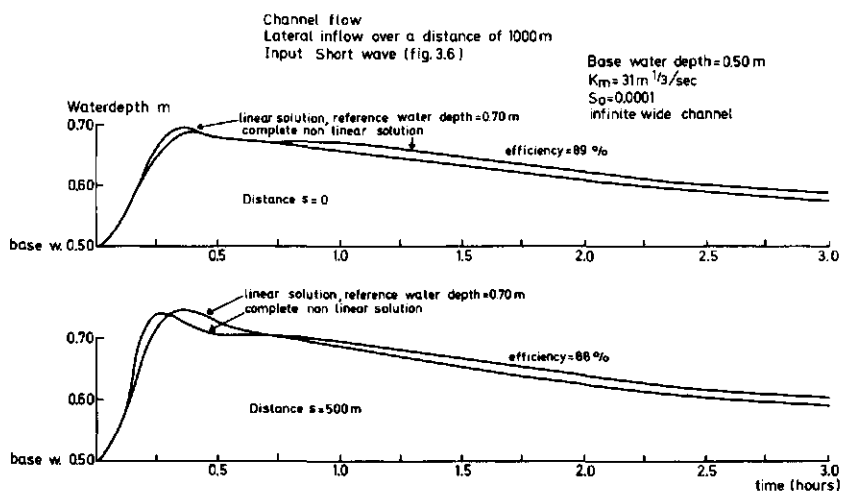in the equation for the moments and in the given responses. From Table 3 it can
be seen that for the 5 mile reach, the first moment increases about 15% to an
increase of reference discharge of 100%, while for the longer channel reaches
the value of M_1' decreases. This phenomenon has been discussed in Section 4.1.8.
In comparison with the tributary inflow problem (Table 1, p45) the values and
variation of the first moment are smaller. However the values and variation of
the second moment are larger for the longer reaches. Fig. 4.5 shows the
dominant translation of a tributary inflow, whereas Fig. 4.16 illustrates the
dominant attenuation of a fully lateral inflow. The figs 4.6 and 4.17 show a
less pronounced difference for an inflow of short duration.
For these inputs it is found that the variation of the reference discharge does
not greatly influence the response.
As mentioned in Section 3.4 for the lateral inflow problem, where the discharge
is increasing with distance, the assumption of a constant reference discharge
over the whole channel reach may be critisized. Therefore in Fig. 4.18 the
response, due to the long Thomas wave, in the 200 miles reach, using a constant
reference discharge (100 cfs) is compared with the response that would occur
with a uniform increase of reference discharge towards the end of the reach.
This uniform increase is approximated by a stepwise increase of the reference
discharge from 0 to 150 cfs.
The results show that the introduction of a varying reference discharge has a
small effect.

4.2.9. Comparison with a complete non-linear solution

The comparison of the linear with the complete non-linear solution is based on
the same inflow and the same channel as used for the tributary inflow (Section
4.1.9), with the only difference that the inflow (short wave) is now uniformly
distributed over 1000 m. The responses, expressed in the water depth, are

calculated for the distances s = 0 and s = 500 m.

Fig. 4.19 shows that a reference water depth of 0.70 m provides a fair agreement between linear and non-linear solutions with an efficiency coefficient of 90%.

4.3. OVERLAND FLOW PROBLEM

As mentioned in Section 3.1. the overland flow problem is considered as turbulent flow in an infinite, wide rectangular channel, although this turbulency is not essential for the diffusion approach.

The assumption of turbulent flow in particular, is arbitary because it is possible that laminar flow may also occur, in some places.

Bravo, et al (1970) found that the solution of O'Meara (1968), based on the linearisation of the complete dynamic equation was not stable for large values of t. Therefore an approximate linear solution for the overland flow problem was derived by integration of the solution of the upstream inflow problem with respect to distance. This approximation is not physically correct because it implies that the flow at any point of the reach of lateral inflow would not be influenced by the inflow of precipitation downstream from that point.

Therefore an alternative solution of the overland flow problem, is suggested which is based on the linear diffusion type differential equation, as derived in Section 3.3., with no restrictions for the upstream effect of inflow.

The solution for this problem is a special case of the partial lateral inflow problem (Section 4.2) by taking $R = 1$ and assuming an infinite wide rectangular channel. Therefore only the mathematical expressions for the IUH's, their moments and spectra and the S-curves will be given here.

Some results of laboratory experiments of overland flow are given in Section 7.3.

4.3.1. Impulse response

The IUH for the discharge and the water depth can be derived in dimensionless form from the eqs (4.33) and (4.34) by taking $R = 1$:

$$\overline{h}_q = \frac{h_q Q}{\Psi} = \frac{1}{2P} \left\{ \text{erf} \left(\frac{P-T}{\sqrt{2T}} \right) + \text{erf} \left(\sqrt{\frac{T}{2}} \right) \right\} +$$
$$+ \frac{1}{2P} \frac{1}{\sqrt{2\pi T}} \left\{ e^{-\frac{T}{2}} - e^{-\frac{(P-T)^2}{2T}} \right\} \tag{4.53}$$

62

$$\overline{h}_y = \frac{h_y s}{V} = \frac{1}{2} \left\{ \text{erf } (\frac{P-T}{\sqrt{2T}}) + \text{erf } (\sqrt{\frac{T}{2}}) \right\} \tag{4.54}$$

4.3.2. Classification

From Table 2 in Section 4.2.2., it follows that for all values of P this overland flow should be classified as flow through a short channel reach because the time to peak of the IUH for the discharge is zero and therefore smaller than Q.

4.3.3. Moments

The moments of the IUH for the discharge follow from Eq. 4.35):

$$M_1'(h_q) = \frac{1}{2} Q (P+1)$$

$$M_2(h_q) = \frac{1}{2} Q^2(1/6 P^2 + P + 5/2) \tag{4.55}$$

$$M_3(h_q) = \frac{1}{2} Q^3(\frac{1}{2} P^2 + 3P + 11)$$

so that for the shape factors (Fig. 4.9b):

$$S_2 = \frac{1/3 \, P^2 + 2P + 5}{(P+1)^2} \quad \text{and} \quad S_3 = \frac{2P^2 + 12P + 44}{(P+1)^3} \tag{4.56}$$

The moments of the IUH for the water depth follow from Eq. (4.37):

$$M_1'(h_y) = \frac{1}{2} Q (P+2)$$

$$M_2(h_y) = \frac{1}{2} Q^2(1/6 P^2 + P + 4) \tag{4.57}$$

$$M_3(h_y) = \frac{1}{2} Q^3(\frac{1}{2} P^2 + 3P + 16)$$

4.3.4. Attenuation coefficient

The attenuation coefficient can be derived from Eq. (4.38):

$$C_A = \frac{(1/12 \, P^2 + \frac{1}{2}P + 5/4)}{\beta} (\frac{Q}{t_F})^2 \tag{4.58}$$

where β depends on the shape of the input and t_F is the duration of the input.

4.3.5. Spectra

The amplitude-density and the phase-density spectra of the IUH for the discharge can be derived from the eqs 4.40, 4.41 and 4.42. For the overland flow problem ($R = 1$, figs 4.10 and 4.11) this results in:

$$\hat{h}_{qa}(\omega) = \frac{e^{\frac{P}{2}(1-\alpha(\omega))}}{2P} \left[\frac{2(1+\alpha(\omega))\{\cosh P(1-\alpha(\omega)) - \cos P\beta(\omega)\}}{(\alpha(\omega)-1)(2\alpha^2(\omega)-1)} \right]^{\frac{1}{2}} \quad (4.59)$$

$$\hat{h}_{q\theta}(\omega)\Big|_X = -\tfrac{1}{2}P\beta(\omega) - \tan^{-1}\frac{\alpha(\omega) + \beta^2(\omega)}{\beta(\omega)(\alpha(\omega)-1)} +$$

$$+ \tan^{-1}\{ \tan \tfrac{1}{2}P\beta(\omega)\coth \tfrac{1}{2}P(\alpha(\omega) - 1)\} \quad (4.60)$$

This expression is valid for $\omega > 0$ and $P\beta(\omega) \in X = [0,\pi)$
whereas for $\omega > 0$ and $P\beta(\omega) \in X_k = [(2k-1)\pi, (2k+1)\pi)$, $k = 1,2\ldots$

the phase density spectrum of the IUH for the discharge is:

$$\hat{h}_{q\theta}(\omega)\Big|_{X_k} = \hat{h}_{q\theta}(\omega)\Big|_X + k\pi \quad (4.61)$$

$\alpha(\omega)$ and $\beta(\omega)$ were defined by Eq. 4.20.

4.3.6. Summation curves

The S-curves for the discharge and the water depth for $s = \ell$ or $R = 1$ can be derived from the eqs (4.43) and (4.44):

$$S_q = \frac{1}{2P}\sqrt{2T}\ \{-\eta\ \mathrm{erf}\ \eta - \frac{1}{\sqrt{\pi}}e^{-\eta^2} + \sqrt{\frac{T}{2}}\ \mathrm{erf}\ \sqrt{\frac{T}{2}} + \frac{1}{\sqrt{\pi}}e^{-\frac{T}{2}}\} + \tfrac{1}{2} \quad (4.62)$$

$$S_y = \frac{Q}{s}\sqrt{\frac{T}{2}}\ \{\ -\eta\ \mathrm{erf}\ \eta - \frac{1}{\sqrt{\pi}}e^{-\eta^2} + \frac{1}{2\sqrt{2T}}\ (\mathrm{erfc}\ \eta - e^{2P}\mathrm{erfc}\ \xi)\} +$$

$$- \frac{Q}{s}\sqrt{\frac{T}{2}}\ \{\ - \sqrt{\frac{T}{2}}\ \mathrm{erf}\ \sqrt{\frac{T}{2}} - \frac{1}{\sqrt{\pi}}e^{-\frac{T}{2}} + \frac{1}{2\sqrt{2T}}\ \left[(1+\mathrm{erf}\sqrt{\frac{T}{2}}) - \mathrm{erfc}\sqrt{\frac{T}{2}}\right]\} +$$

$$+ PQ/2s \quad (4.63)$$

η and ξ were defined Eq. (4.45).

4.4. SEMI-INFINITE CHANNEL - LUMPED INPUT

This system element, which is studied as the upstream inflow problem, was considered by Harley (1967). For the completeness of this report some of his work, concerning the diffusion type solution will also be included.
In this case a semi-infinite uniform channel is fed by an inflow at the upstream end (s = 0), where no flow can occur in an upstream direction. Comparison of the upstream and tributary inflow problems for the latter shows the effect of storage in the channel reach, upstream of the point of inflow.

4.4.1. Impulse response

The impulse response is found by solving the linear differential equation, expressed in the discharge per unit width of channel.

$$\frac{\partial q_p}{\partial t} = D \frac{\partial^2 q_p}{\partial s^2} - A_\tau \frac{\partial q_p}{\partial s} \tag{4.64}$$

for the following boundary conditions:

$$\text{a. } q_p(0,t) = \delta(t) \qquad \text{Dirac function}$$

$$\tag{4.65}$$

$$\text{b. } q_p(s,0) = 0 \qquad \text{for } s > 0$$

The physical meaning of $\delta(t)$ is, that a unit volume per unit width of channel is instantaneously added to the system at the upstream end (s = 0) of the channel.

Laplace transforms are used to find the following solution (Van de Nes and Hendriks, 1971):

$$q_p(s,t) = \frac{s}{2\sqrt{\pi D t^3}} e^{-\frac{(s-A_\tau t)^2}{4Dt}} \tag{4.66}$$

The IUH for the water depth is derived by introducing Eq. 4.66 in the continuity Eq. 3.24:

$$y_p(s,t) = \frac{e^{-\frac{(s-A_\tau t)^2}{4Dt}}}{\sqrt{\pi D t}} - \frac{A_\tau}{2D} e^{\frac{A_\tau s}{D}} \text{ erfc } \left(\frac{s+A_\tau t}{2\sqrt{Dt}}\right) \tag{4.67}$$

In dimensionless form the IUH's for the discharge and the water depth can be written as follows:

$$\bar{h}_q = \frac{h_q Q}{\Psi} = \frac{P}{\sqrt{2\pi T^3}} e^{-\frac{(P-T)^2}{2T}} \tag{4.68}$$

$$\bar{h}_y = \frac{h_y s}{\Psi} = P \left\{ \frac{2}{\sqrt{2\pi T}} e^{-\frac{(P-T)^2}{2T}} - e^{2P} \operatorname{erfc} \left(\frac{P+T}{\sqrt{2T}}\right) \right\} \tag{4.69}$$

P, Q and T were defined by Eq. 4.11.

4.4.2. Classification

Using the criteria introduced in Section 4.1.2. classification based on the discharge, can be derived from Eq. 4.68.

a. short channel reach (Tp $\leqslant$ 1), if $P \leqslant 2$

b. intermediate channel reach (Tp > 1) and $(\bar{h}_q)_{T=1} \geqslant \xi$, where ξ is a small number ($\approx 8\times10^{-4}$) if $2 < P \leqslant 5$.

c. long channel reach, where $(\bar{h}_q)_{T=1} < \xi$ if $P > 5$.

The results are simular to these found for the tributary inflow problem, with the exception of the short reach ($P \leqslant 1,8$).

4.4.3. Moments

The moments of the IUH for the discharge and water depth are derived by Harley, 1967:

$$M_1'(h_q) = PQ$$
$$M_2(h_q) = PQ^2 \tag{4.70}$$
$$M_3(h_q) = 3PQ^3$$

from which for the shape factors follow :

$$S_2 = \frac{1}{P} \quad \text{and} \quad S_3 = \frac{3}{P^2} \quad \text{or} \quad S_3 = 3S_2^2 \tag{4.71}$$

66

For the first three moments of the IUH for the water depth was found
(Van de Nes and Hendriks, 1971):

$$M_1'(h_y) = (P + \tfrac{1}{2})Q$$

$$M_2(h_y) = (P + 3/4)Q^2 \qquad\qquad (4.72)$$

$$M_3(h_y) = (3P + 5/2)Q^3$$

Comparison of the moments for the discharge with the moments of the water
depth leads to the same conclusions, as drawn for the tributary inflow problem.
(Section 4.1.3.). Further for large values of P(a long channel reach), the
moments of the tributary inflow problem approximate the moments of the upstream
inflow problem. This means that the upstream boundary for a long channel has no
significant effect on the responses.

4.4.4. *Attenuation coefficient*

As defined in Section 2.3. the attenuation coefficient for the discharge is:

$$C_A = \frac{P}{\beta} (\frac{Q}{t_F})^2 \qquad\qquad (4.73)$$

where β depends on the shape of the input t_F is the duration of the input.
For the short reach the attenuation coefficient differs considerably from the
C_A for the tributary inflow problem, whereas for the long reach they are nearly
the same.

4.4.5. *Spectra*

The amplitude density spectrum and the phase density spectrum of the IUH for the
discharge are derived by V.d. Nes and Hendriks 1971, using the eqs (2.13) and (2.14).
The amplitude density spectrum of the IUH can be expressed as follows:

$$\hat{h}_{qa}(\omega) = e^{P(1-\alpha(\omega))} \qquad \text{for } \omega > 0 \qquad\qquad (4.74)$$

and the phase density spectrum:

$$\hat{h}_{q\theta}(\omega) = - P\beta(\omega) \qquad \text{for } \omega > 0 \qquad\qquad (4.75)$$

$\hat{h}_{q\alpha}$ amplitude density

fig. 4.20   Amplitude density spectrum of the IUH, expressed in the discharge, for the upstream inflow problem

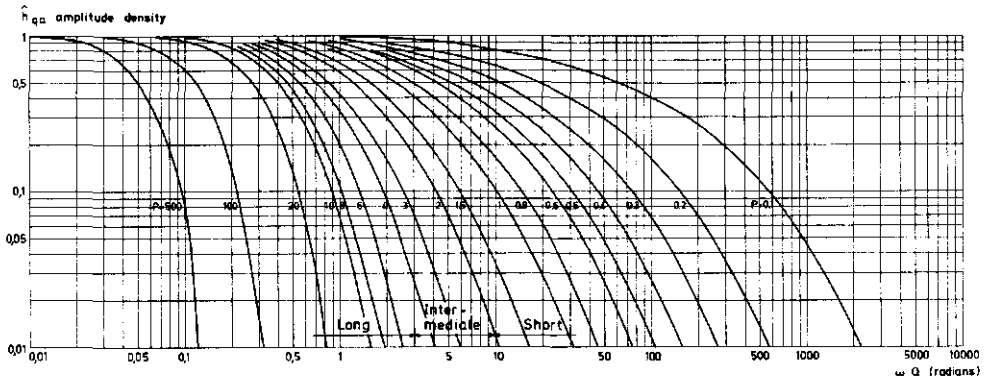$\hat{h}_{q\theta}$ phase density

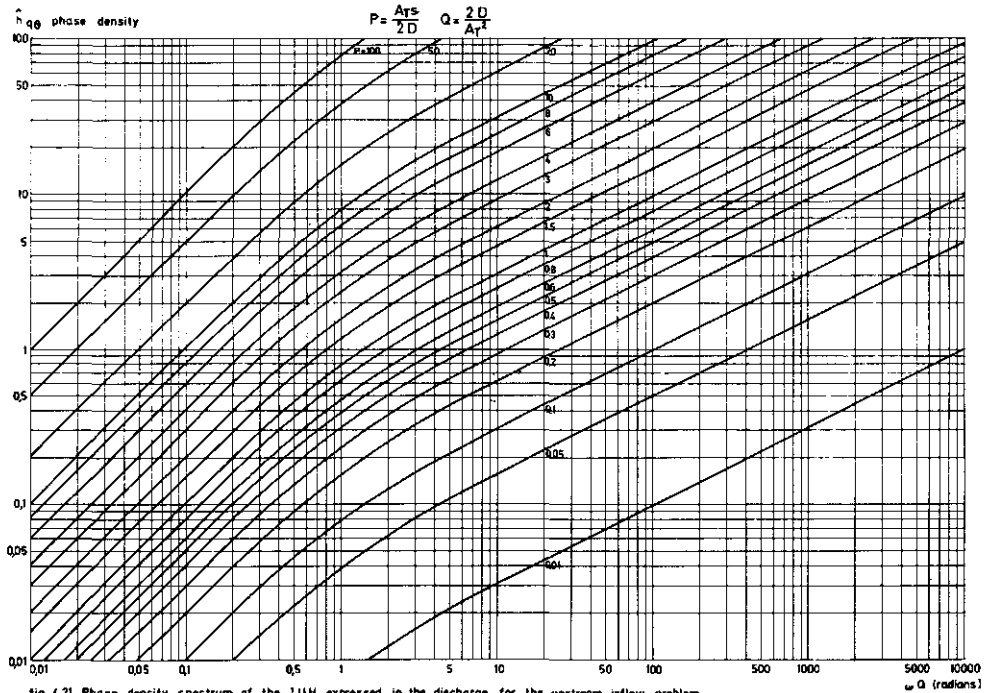$$P = \frac{A_{TS}}{2D} \qquad Q = \frac{2D}{A_T^2}$$

fig. 4.21 Phase density spectrum of the IUH, expressed in the discharge, for the upstream inflow problem

In the spectra of figs 4.20 and 4.21 the amplitudes and phases are given as functions of ωQ for a number of values of P.

The spectra show the damping effect of the system for increasing values of P. Q seems to be only a scale factor. Also in the frequency domain one can subdivide the area in three parts, which agree with the channel classification of a short, intermediate and long channel reach, as is shown in the figures.

4.4.6. Summation curves

The S-curves for the discharge and the water depth can be derived from the eqs 4.66 and 4.67 by integration with respect to time. (Van de Nes and Hendriks, 1971):

$$S_q = \tfrac{1}{2} \left\{ \text{erfc } (\frac{P-T}{\sqrt{2T}}) + e^{2P} \text{ erfc } (\frac{P+T}{\sqrt{2T}}) \right\} \tag{4.76}$$

and

$$S_y = \frac{PQ}{s} \left\{ - (P + T + \tfrac{1}{2}) e^{2P} \text{ erfc } (\frac{P+T}{\sqrt{2T}}) + \tfrac{1}{2} \text{ erfc } (\frac{P-T}{\sqrt{2T}}) + \right.$$

$$\left. + \sqrt{\frac{2T}{\pi}} e^{-(\frac{P-T}{\sqrt{2T}})^2} \right\} \tag{4.77}$$

Similar to the tributary inflow problem the following relations are valid for the steady state $(t \to \infty)$:

$$q_p = A_T y_p \tag{4.78}$$

and

$$q = v_I y + \tfrac{1}{2} v_I y_p \tag{4.79}$$

In this linear systems approach, the increase of velocity, due to the increase of water depth is introduced in Eq. 4.79 by the second term at the right hand side.

4.4.7. Response to given waves of inflow

For the long and intermediate 'Thomas wave' with a duration of 96 and 12 hours respectively, the response is given for various distances from the point of inflow. For the long wave, distances of 5,50, 200 and 500 miles are chosen, while for the intermediate wave only reaches of 5 and 50 miles are considered.

For the physical characteristics of the channel the same values have been
chosen as for the other inflow problems: an original baseflow of 50 cfs,
bottom slope S_o = 1 ft/mile, a Chezy coefficient $C = 50 \text{ ft}^{\frac{1}{2}}/\text{sec}$ in a wide
rectangular channel. In figs 4.22 and 4.23 the responses are given for the
discharge per unit width of channel, based on the eqs 4.76, 2.4 and 2.2.
Both figures show the attenuation and translation of the floodwave. The
attenuation for the intermediate wave is much greater than for the long wave.
Harley (1967) has also presented the responses for the same data, based on the
complete linearized dynamic equation.
By comparison of the linear diffusion type solution with the complete linear
solution only a small difference is found, which cannot be shown in figs 4.22
and 4.23. In the given examples the Froude number $F \approx 0.1$. This agrees with
the statement of Dooge and Harley (1967), that for the upstream inflow problem
the diffusion type of solution is accurate in comparison with the complete
linear solution if $F \sim 0.5$.

4.4.8. Effect of reference discharge

In the linearized theory, as explained in Section 3.3., the estimation of the
reference discharge or water depth is important. In figs 4.22 and 4.23 the
effect of the reference discharge is shown for various distances. The same
values of the reference discharge were chosen as for the other inflow problems
(100, 150 and 200 cfs). In some cases the three curves were so close together,
that only one or two curves could be shown in the same figure.
Table 4 shows the effect of the reference discharge on the system parameters P
and Q (hours) and on the first moment of the IUH for the discharge, expressed
in hours and the second moment, expressed in $(\text{hours})^2$.

Table 4 : Effect of reference discharge.

q_o (cfs)	Q (hours)	5 miles			50 miles			200 miles			500 miles		
		P	$M'_1(h)$	$M_2(h)$	P	$M'_1(h)$	$M_2(h)$	P	$M'_1(h)$	$M_2(h)$	P	$M'_1(h)$	$M_2(h)$
100	4.9	0.273	1.33	6.63	2.73	13.38	66.29	10.92	53.31	265.2	27.3	133.8	662.9
150	5.6	0.208	1.16	6.65	2.08	11.64	66.50	8.32	46.59	266.0	20.8	116.5	665.1
200	6.2	0.172	1.06	6.63	1.72	10.66	66.27	6.88	42.66	265.2	17.2	106.6	662.7

Comparison of Table 4 with Table 1 for the tributary inflow problem shows a
large difference for the short channel reach. For such short reaches the values
of the moments are much smaller for upstream inflow, while the variation of the
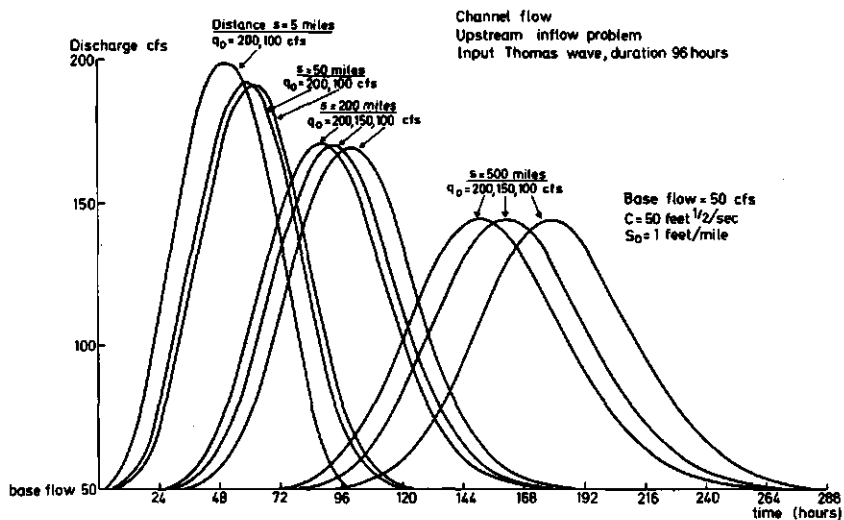
fig 4.22 Effect of the reference discharge for different values of the distance s
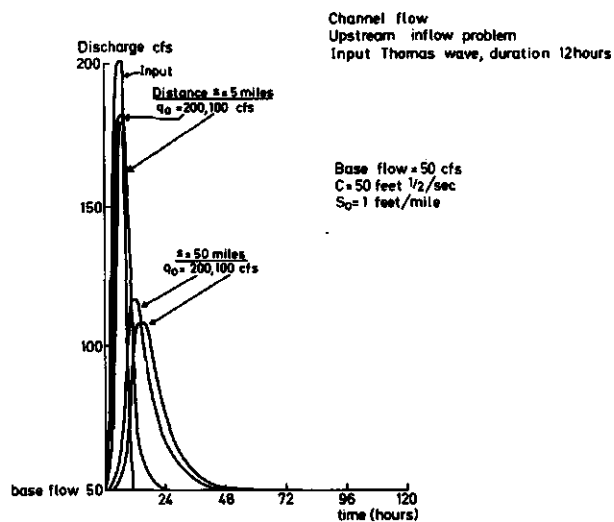for the "Long Thomas" wave

fig 4.23 Effect of the reference discharge for different
values of the distance s
for the "intermediate Thomas" wave

71

first moment with the reference discharge is larger and the variation of the
second moment smaller. For the long channel reaches both the first and the
second moments converge, showing the diminishing effect of the upstream
boundary. Table 4 shows that an increase of the reference discharge increases
the translation. This effect dominates the attenuation for all values of P.
From Fig. 4.22 it is clear that for the long Thomas wave the reference dis-
charge does not significantly effect the attenuation for all values of P,
while the translation becomes important for large values of P. In the case of
the intermediate 'Thomas' wave, where the moments of the IUH have a more
pronounced effect on the shape of the responses, Fig. 4.23 shows both
translation and attenuation in a 50 miles reach.
Summarising the results it can be stated that in short channel reaches ($P \leqslant 2$)
the reference discharge has hardly any effect for both types of inflow. In the
intermediate channel reach ($2 < P \leqslant 5$) there is some translation of the long
'Thomas' wave, whereas the intermediate wave shows both some translation and
attenuation. In the long channel reach ($P > 5$) only the long 'Thomas' wave
shows translation. For the intermediate wave it may be assumed (there are no
results available) that the attenuation becomes less important and the transla-
tion becomes more important. From this example it follows that the reference
discharge is not an important factor for a short channel reach. In a long
reach however it does effect the translation.

4.4.9. Comparison with a complete non-linear solution

The comparison of the linear with the complete non-linear solution is based on
the same inflow and the same channel as used for the tributary inflow (Section
4.1.9.), with the only difference that the inflow at point $S = \acute{o}$ has no effect
in the upstream direction. The responses, expressed in the water depth, are
calculated for the distances $s = o$ and $s = 1000$ m for an infinite wide channel
and for a rectangular channel with a width of 1.75 m. Figs 4.24 and 4.25 show
that a reference water depth of 0.75 m provides a fair agreement between
linear and non-linear solution, with an efficiency coefficient of 90%. For a
wide rectangular channel the coefficients A_τ and D are calculated from Eq. 3.28.
For a channel of limited width Eq. 3.29 must be used.
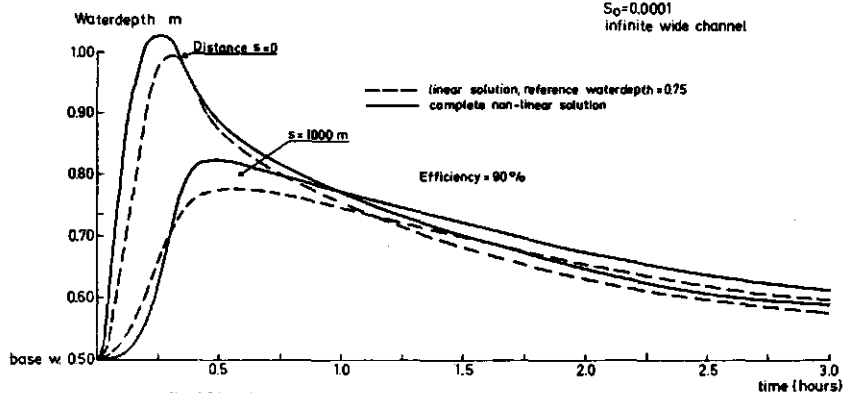
fig. 4.24   Comparison of linear with complete non-linear solution
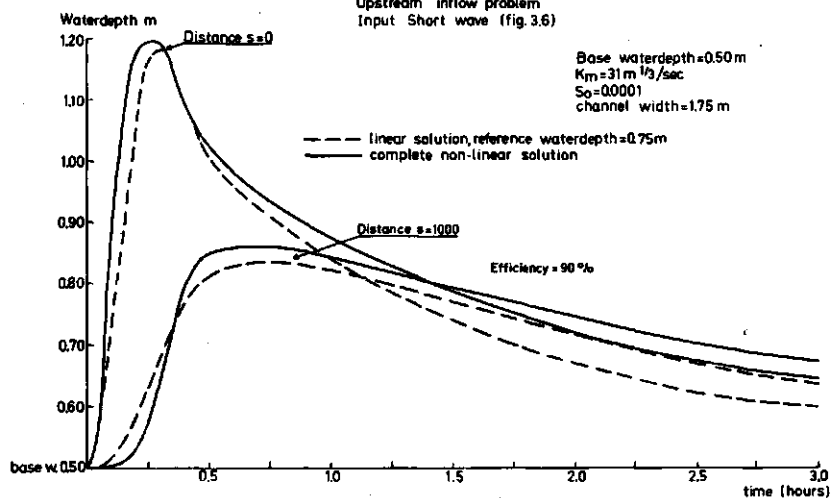
fig 4.25   Comparison of linear with complete non-linear solution

73

5. COMPARISON OF THE DIFFERENT CONCEPTUAL ELEMENTS

Introductory note: In the following the word 'distance' indicates the length of channel downstream from the local (upstream or tributary) inflow or the length of channel downstream from the upstream end of a distributed (fully or partial lateral) inflow.

In Section 4 the effect of the channel length and the reference discharge as expressed in the system parameters P and Q, and of the type of inflow has been studied for the different types of elementary inflow problems. It was found that the linear solutions agreed reasonably well with the complete non-linear solutions.

In this Section however, the effect of the spatial distribution of inflow of both an intermediate and a long 'Thomas' wave is studied separately. This implies that the model parameters P and Q are considered as constants. The independence of P and Q from the spatial inflow distribution will be shown to be a reasonable assumption.

This effect which results from computational experiments will then be inferred from the characteristics of the impulse responses for the tributary, lateral and upstream inflow problem.

5.1. RESPONSE TO GIVEN WAVES OF INFLOW

Fig. 5.1. shows the response at a distance of 50 miles and a reference discharge of 100 cfs (P = 2.73 and Q = 4.9 hours) to the long 'Thomas' wave input.

Comparison of the responses for the tributary inflow (R = 0), the fully lateral inflow (R = 1) and the upstream inflow shows only a small time lag of about 10 hours.

For a distance of 5 miles (P = 0.273), no results are given, as the curves are very close together, which means that for the short reach and a long 'Thomas' wave input the spatial distribution of the inflow does not influence the response significantly.

In Fig. 5.2 the responses are given for a distance of 200 miles (P = 10,92), besides the response is given for the partial lateral inflow problem (R = $\frac{1}{2}$). For the tributary, upstream and partial lateral inflow it is found that this channel is to be classified as a long reach, whereas for the fully lateral inflow the channel is to be classified as a short reach.

74

Channel flow
Reference discharge = 100 cfs
Distance s = 50 miles

P = 2,73
Q = 4,9 hour

Base flow = 50 cfs
C = 50 feet $^{1/2}$/sec, S_0 = 1 feet/mile
Input Thomas wave
duration 96 hours

fig 5.1 Effect of the spatial distribution of the "Long Thomas"
wave input for the 50 miles channel reach

Channel flow
Reference discharge = 100 cfs
Distance s = 200 miles

Base flow = 50 cfs
C = 50 feet $^{1/2}$/sec
S_0 = 1 feet/mile

Input Thomas Wave,
duration 96 hours

P = 10,92
Q = 4,9 hours

fig. 5.2 Effect of the spatial distribution of the "Long Thomas" wave
input for the 200 miles channel reach

75

The results for the upstream and tributary inflow problem appear to be close together. As compared with the tributary inflow the result of the partial lateral inflow ($R = \frac{1}{2}$) only shows a translation (12.5 hours). The result for the fully lateral inflow however shows both some attenuation and a translation of about 30 hours. It is interestimg to note that for $R = \frac{1}{2}$ the attenuation of the partial lateral inflow (RP = 5.46) is smaller, while the attenuation of the fully lateral inflow (RP = 10.92) is larger than the attenuation of the tributary inflow. This is in agreement with the Eq. 4.39, which states that for $R > \frac{6}{P}$ the attenuation of the lateral inflow is larger than the attenuation of the tributary inflow.

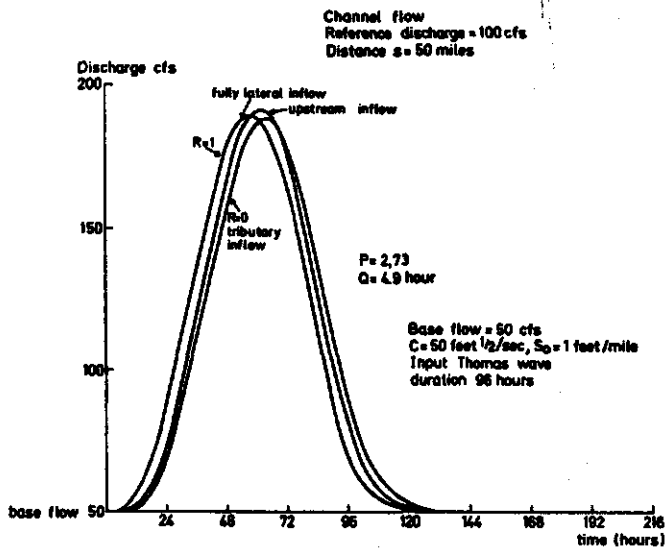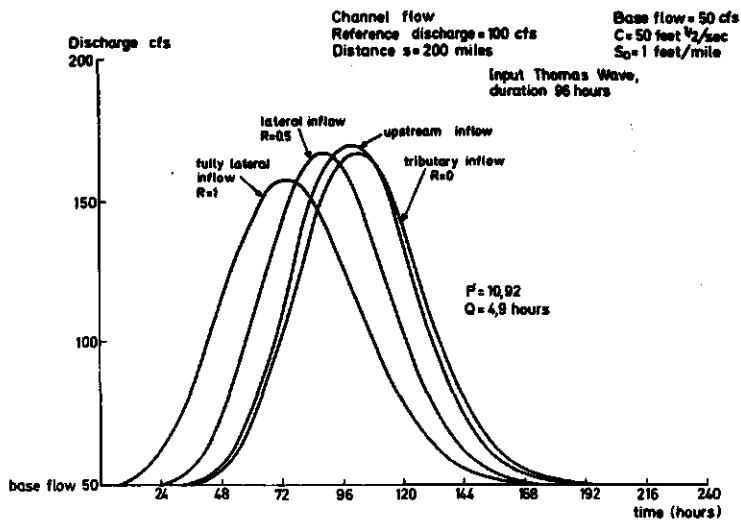In Fig. 5.3 the responses are given for the distance of 500 miles (P = 27.4).
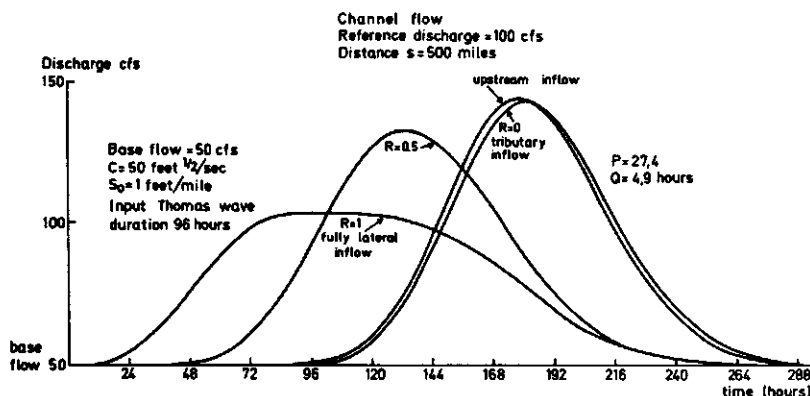
fig. 5.3 Effect of the spatial distribution of the "Long Thomas" wave input for the 500 miles channel reach

The responses of the tributary and upstream inflow are close to each other, but the partial lateral inflow (R = 0.5) shows a translation of about 48 hours and some attenuation. The results of the fully lateral inflow and the tributary inflow differ considerably.

For the long channel reach therefore the conclusion can be drawn that the responses of the partial lateral inflow for $0 < R < 0.5$ have nearly the same shape as the responses of the tributary and upstream inflow, only the translations differ. For $1 > R > 0.5$ also an important attenuation occurs.

For the intermediate channel reach it may be concluded that for all types of inflow the shapes of the response are nearly identical. For $1 > R > 0.5$ the translation of the partial lateral inflow decreases with R.

For the intermediate 'Thomas' wave the results for a distance of 5 miles (P = 0.274) are given in Fig. 5.4.

76

Figure 5.4 (left):

Discharge cfs
200

Channel flow
Refence discharge = 100 cfs
Distance s = 5 miles

upstream inflow

R = 1 fully lateral inflow

R = 0 tributary inflow

150

P = 0.274
Q = 4.9 hour

Base flow = 50 cfs
C = 50 feet $^{1/2}$/sec
S_0 = 1 feet/mile
input Thomas wave
duration 12 hours

100

base flow 50

24   48   72   96
time (hours)
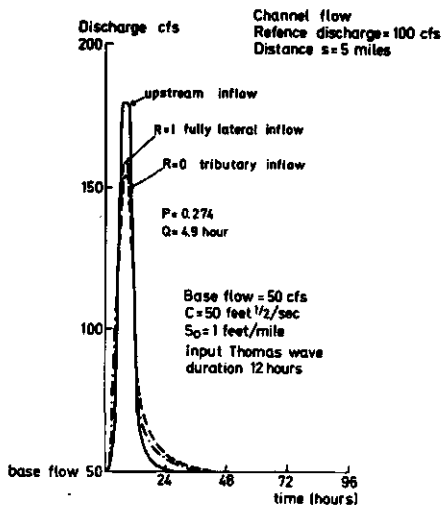
fig. 5.4 Effect of the spatial distribution of the "intermediate Thomas" wave input for the 5 miles channel reach

Figure 5.5 (right):

Channel flow
Reference discharge = 100 cfs
Distance s = 50 miles

Discharge cfs

fully lateral inflow R = 1   P = 2.73
upstream inflow   Q = 4.9 hours
tributary inflow R = 0

100

Base flow = 50 cfs
C = 50 feet $^{1/2}$/sec
S_0 = 1 feet/mile
Input Thomas wave
duration 12 hours

base flow 50

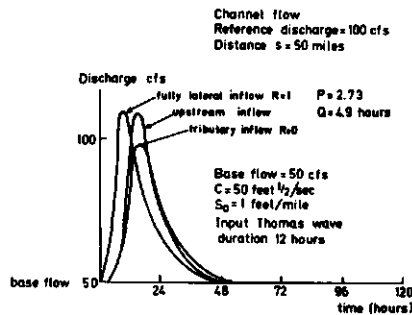24   48   72   96   120
time (hours)

fig. 5.5 Effect of the spatial distribution of the "intermediate Thomas" wave input for the 50 miles channel reach

It shows a difference in attenuation for the tributary and upstream inflows. The responses of the fully lateral ($R = 1$) and the tributary inflow are close together. For the distance of 50 miles ($P = 2.74$) Fig. 5.5 shows that the responses of the tributary and upstream inflows are close together, whereas a translation of the fully lateral inflow occurs. Compared with the 5 miles reach the difference between the responses to the fully lateral and tributary inflow has increased.

For the long channel reach no results are given. However a persisting tendency is found for the responses of the tributary and upstream inflows to become identical for increasing values of P. Also an increasing difference between the responses of the fully lateral and tributary inflow is apparent.

Therefore the conclusion can be drawn that for the short channel reach the spatial variation of the inflow, has little effect on attenuation. For the intermediate reach this variation also effects the translation. For the long reach the responses to the partial lateral inflow for $0 < R < 0.5$ have the same shape as the responses for the tributary and upstreams inflow, only the translations differ. For $1 > R > 0.5$ also an important attenuation occurs. Summarising the results, for large values of P (the long reach) the difference between the responses to the tributary and upstream inflow becomes negligible, the responses of the tributary and the partial lateral inflow differ

77

considerably for $1 > R > 0.5$ and for $R < 0.5$ only a translation effect remains. For small values of P(the short channel reach) the responses of the tributary and lateral inflow are close together, while the difference between the responses of upstream and tributary inflow increases for waves of shorter duration.

For intermediate values of P (intermediate channel reach) comparison of the responses of the different types of inflow shows only a little difference in attenuation and translation.

5.2. MOMENTS

Understanding difference in responses of the different types of inflow, as shown in the figures, can be derived from the shape factor diagrams of the IUH's for the different inflow problems. In Fig. 4.9bof Section 4.2.3. the shape factor diagrams are given for the lateral inflow problem for different values of R, while in Fig. 5.6 the shape factor diagrams are given for the upstream, tributary and fully lateral inflow problem ($R = 1$).

The diagram shows that in the lateral inflow problem (Fig. 4.9) for $0 < R < 0.5$ the shape factors are close together. This means that the shapes of the IUH are nearly the same, only a translation may occur. For $0.5 < R < 1$ the differences are increasing. In general it can be concluded that for $0 < R < 1$ the band of shape factors is narrow, showing a not very pronounced effect of the lateral inflow distribution on the shape of the IUH. Fig. 5.6 also shows that for the short reach the lines for the tributary and the fully lateral inflows converge, while there is an increasing difference between the tributary and upstream inflow problems. For the long reach (large values of P) however the lines representing the upstream and tributary inflow problems converge.

The conclusions drawn from the shape factor diagrams and from the responses to the different types of inflow (Section 5.1) appear to be identical.

It should be noted that the shape factors do not provide any information on the translation.

5.3. SPECTRA

In the figs 5.7 and 5.8 the amplitude density spectra and the phase density spectra of the IUH's are given for the tributary, lateral (with varying value of R) and the upstream inflow problem for values of $P = 0.1$; 1.0; 10 and 100 respectively.
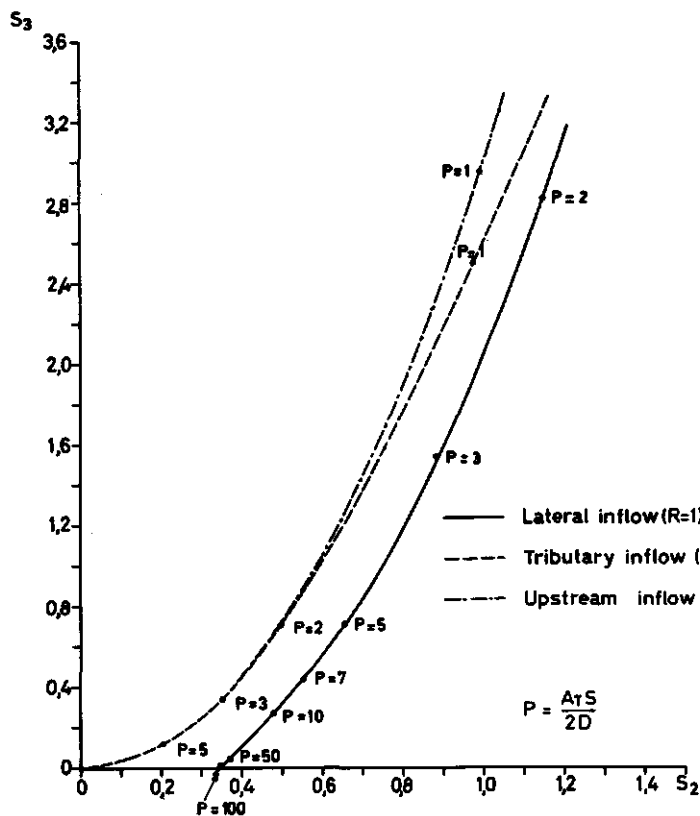
fig. 5.6 Effect of the spatial distribution of the inflow on shape factors

After Eagleson et al (1966) it is assumed that significant variations in the shape of the IUH are only expressed in relative amplitudes greater than 0.1. Fig. 5.7 shows for $P = 0.1$ (the short channel reach) relatively small variations of the spectra for different values of R. For this small P value however there is a large difference between the tributary and upstream inflow problems. For increasing values of P these amplitude spectra converge. In the range of $1 < P < 10$ (about the intermediate channel reach) all spectra converge. In the range of $10 < P < 100$ (long channel reach) the spectra for the IUH of the lateral inflow diverge from the spectra for the tributary and upstream inflow with increasing values of R.

This means that in the intermediate channel reach the shape of the IUH's is not

fig. 5.7 Effect of the spatial distribution of the inflow on the amplitude density spectrum

PHASE DENSITY SPECTRUM

fig. 5.8 Effect of the spatial distribution of the inflow on the phase density spectrum
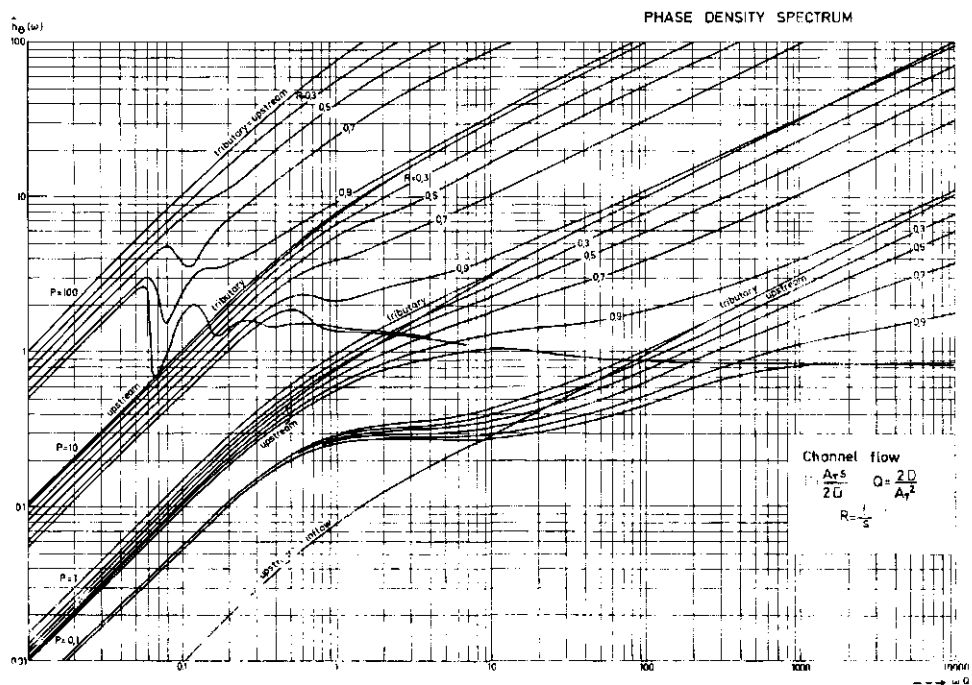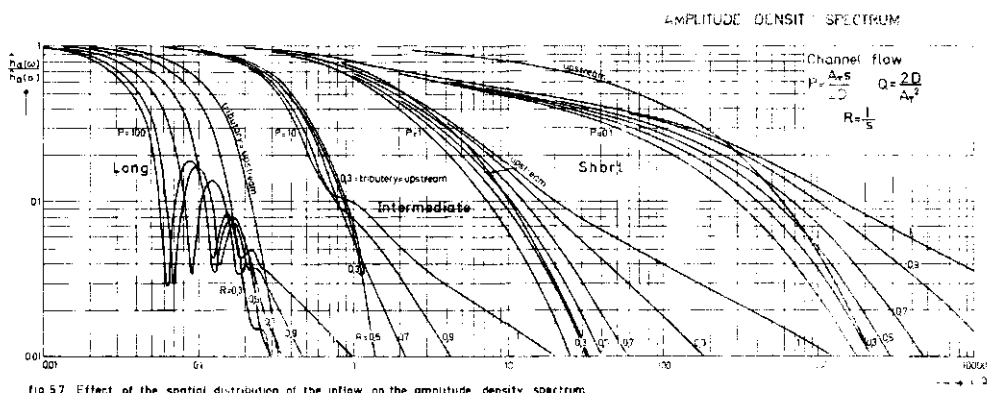
very sensitive to the spatial distribution of inflow, while for the long
reach the spatial distribution of inflow has a dominant effect on the shape of
the IUH's. In the short channel reach however the spectrum for the fully
lateral inflow ($R = 1$) lies above the spectrum for the tributary inflow ($R = 0$),
whereas in the long channel reach the reverse applies.

Apparently in the intermediate channel reach the spectra cross each other. This
is demonstrated for $P = 10$, where the spectrum for $R = 0.5$ lies just above the
tributary spectrum and the spectrum of $R = 1$ is just below the spectrum for the
tributary. Eq. 4.40 shows that for $R = \frac{P}{6}$ the attenuation of the tributary and
lateral inflow are equal. This is an agreement with the corresponding spectra.
The phase density spectra in Fig. 5.8 show for $P = 0.1$ (the short channel
reach) a large difference between tributary and upstream inflow. For the
lateral inflow the value of R has a small effect, which effect is increasing
with larger values of P. However for larger values of P the phase density
spectra for the tributary and upstream inflow converge. Because of similar
amplitude and phase spectra for the tributary and upstream inflow into a
long channel reach, both the shape and the time lag of the IUH are the same.
It has already been shown that in the intermediate reach the shape of the IUH's
was not very sensitivefor the type of inflow, which was demonstrated Fig. 5.2
for the example of a long 'Thomas' wave input into an intermediate channel
reach ($P = 10$)

The difference of translation of the tributary and the partial inflow (for $R = \frac{1}{2}$)
can be derived from the phase density spectra. (Fig. 5.8). This difference of
translation can be calculated using Eq. 2.17.
For $P = 10$ and $\omega Q = 1$:

$$\Delta \hat{h}_\Theta(\omega) = 8 - 5\tfrac{1}{2} = \frac{t_o}{Q}$$

For $Q = 4.9$ hours the difference of lag $t_o = 12.5$ hours.
The difference for fully lateral and tributary inflow is found to be:

$$8 - 1.5 = \frac{t_o}{Q} \quad , \text{ and } t_o = 32 \text{ hours}$$

These results are in agreement with the translations, measured from the
responses given in Fig. 5.2.

5.4. SPECIFIC ATTENUATION

As mentioned in Section 2.3. it is assumed that there is a relation between the specific attenuation of the inflow (Eq. 2.12) and the attenuation coefficient (Eq. 2.11). In Fig. 5.9 the specific attenuation is plotted as a function of the attenuation coefficient C_A for the different types of inflow problems. Although these results do not definitely prove the assumed relation they indicate however that further research could produce a practical rule for determining the attenuation of an inflow wave from the characteristics of a channel.

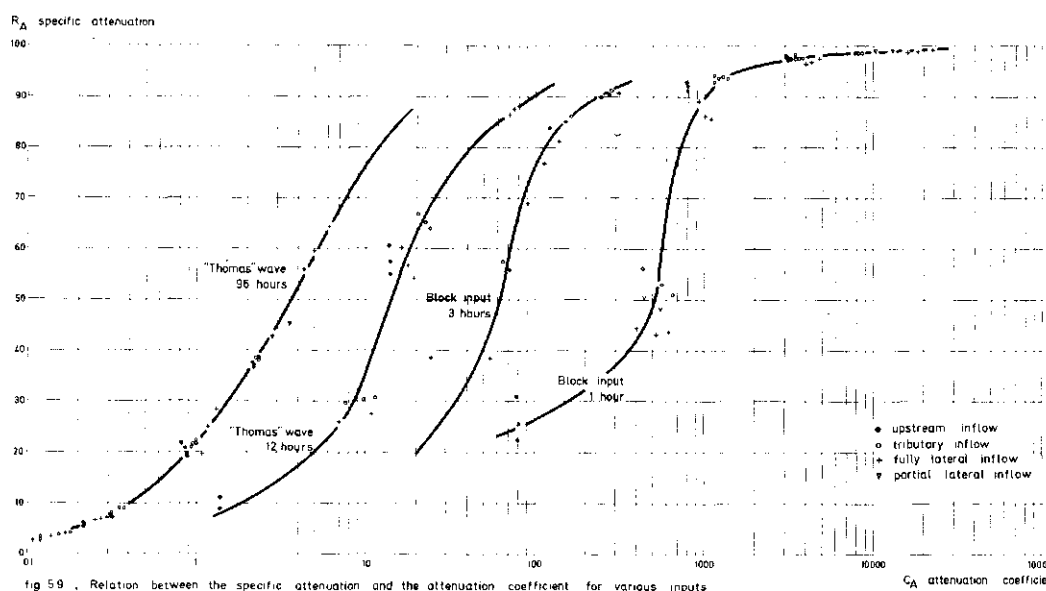

fig 5.9 . Relation between the specific attenuation and the attenuation coefficient for various inputs

5.5. SAMPLING INTERVAL

Section 2.4. explains how the interval duration Δt, for the measurement of the input can be derived from the amplitude density spectrum of the IUH's for the different types of conceptual elements by the following relation:

82

$$\Delta t \leqslant \frac{1}{\omega_c} \quad \text{for } \omega_p > \omega_c \tag{5.1}$$

If the channel is considered as a filter the upper limit of its passband is chosen where the relative amplitude equals 0.1. This subjective criterion should be verified in later work.

From the amplitude density spectrum for the lateral inflow problem can be concluded that:

$$\omega_c \ Q = f_1(R,P) \quad \text{radians} \tag{5.2}$$

for the upstream inflow problem:

$$\omega_c \ Q = f_2(P) \quad \text{radians} \tag{5.3}$$

The values for $\omega_c \ Q$ can be read from the amplitude density spectra.

A dimensionless sampling interval can be derived by introduction of Eq. 5.2 or 5.3 into Eq. 5.1. For the lateral inflow problem follows:

$$\Delta T = \frac{\Delta t}{Q} \leqslant \frac{1}{f_1(R,P)} \tag{5.4}$$

and for the upstream inflow problem

$$\Delta T = \frac{\Delta t}{Q} \leqslant \frac{1}{f_2(P)} \tag{5.5}$$

For the case $\omega_p < \omega_c$ however the entire band width of the input signal is of interest; then the filtering effect of the system is small and the following relation for the sampling interval is valid:

$$\Delta t \leqslant \frac{\pi}{\omega_p} \tag{5.6}$$

For the 'Thomas' wave the relative amplitude density spectrum (Fig. 5.10) can be expressed as follows:

$$\hat{x}_a(\omega) \Big/ \hat{x}_a(o) = \frac{8\pi^2}{|\omega t_F (4\pi^2 - \omega^2 t_F^2)|} \cdot |\sin \tfrac{1}{2}\omega t_F| \tag{5.7}$$

fig 5.10 Amplitude density spectrum for the Thomas wave
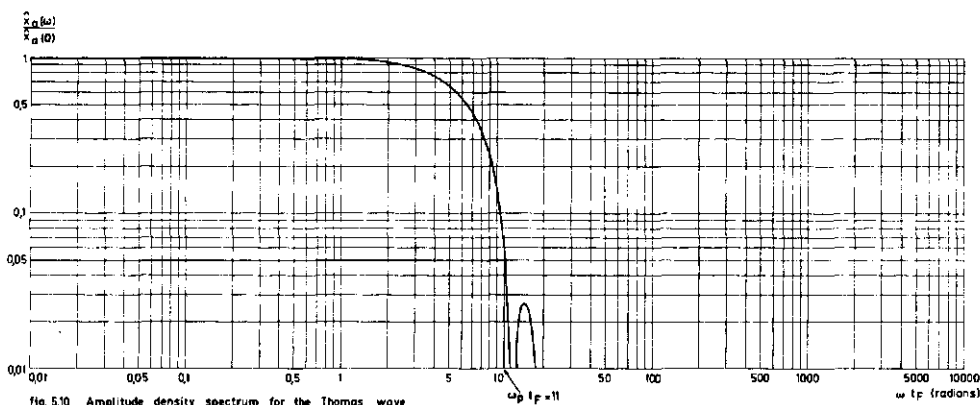
where t_F is the duration of this cosinus wave.

Using the criterion $\hat{x}_a(\omega_p) = 0.05 \, \hat{x}_a(\omega_o)$ yields $\omega_p = 11/t_F$.

So with the condition $\omega_p < \omega_c$ it follows from Eq 5.2 or 5.3:

$$\frac{11}{t_F} < \frac{f_1(P,R)}{Q} \quad \text{or} \quad \frac{11}{t_F} < \frac{f_2(P)}{Q}$$

and

$$\frac{t_F}{Q} > \frac{11}{f_1(P,R)} \quad \text{or} \quad \frac{t_F}{Q} > \frac{11}{f_2(P)} \tag{5.8a}$$

For $\omega_p > \omega_c$:

$$\frac{t_F}{Q} < \frac{11}{f_1(P,R)} \quad \text{or} \quad \frac{t_F}{Q} < \frac{11}{f_2(P)} \tag{5.8b}$$

For the example of the upstream inflow problem for the 500 miles reach (Section 4.4) where $P \approx 20$, $Q \approx 5$ hours Fig. 4.20 shows that $f_2(P) = 0.55$. The duration of the long 'Thomas' wave is $t_F = 96$ hours. With $Q = 5$ hours and $f_2(P) = 0.55$ it follows $t_F/Q < 11/f_2(P)$. Therefore $\omega_c < \omega_p$ and the sampling interval is to be derived from Eq. 5.5.

$$\Delta T \leqslant \sim 2$$

The same applies to the intermediate 'Thomas wave'.

For the 50 mile reach ($P \approx 2$, $Q \approx 5$ hours) $f_2(P) = 4$. Then for the intermediate 'Thomas wave' also $\omega_c < \omega_p$ and

84

$$\Delta T \leqslant \tfrac{1}{2}$$

For the long 'Thomas wave' however $\omega_c > \omega_p$ and since $\omega_p = 11/t_F$ it follows from Eq. 5.6

$$\Delta t \leqslant \frac{\pi t_F}{11} = 27.3 \text{ hours}$$

For the 5 mile reach $(P \approx 0.2,\ Q = 5 \text{ hours})$ $f_2(P) = 150$, so that for both waves $\omega_p < \omega_c$.
For the intermediate wave the sampling interval is:

$$\Delta t \leqslant \frac{\pi t_F}{11} = 3.42 \text{ hours}$$

The chosen values of Δt for the 'Thomas waves' input, with which the responses were calculated, are in agreement with this criterion. In this way the chosen time interval Δt have been checked for all types of inflow problems, so that it can be concluded that the sampling of the input did not effect the shape of the calculated responses.

The above calculations were based on the criterion $\omega_p = 11/t_F$ for a 'Thomas wave'.

Eagleson et al (1966) gave for a block input the cut off frequency $\omega_p = 39/t_F$ and for a triangular input $\omega_p = 10/t_F$.

If $\omega_c < \omega_p$, or $\dfrac{f_1(P,R)}{Q} < \dfrac{11}{t_F}P$ the system filters all frequencies $> \omega_c$. Eq. (5.8b) shows that this filtering effect of the system depends both on the ratio of the duration t_F of inflow and the characteristic time Q of the system and also on the ratio of a coefficient (11 radians), determined by the shape of the inflow and another shape coefficient, dependent on the dimensionless system parameters P and R corresponding with the shape of the IUH.

The classification of the channels in short, intermediate and long channel reaches is based on these parameters P and R.

The requirement for a short reach to act as a filter ($\omega_p > \omega_c$) is stated in Eq. 5.8b. Therefore $\dfrac{t_F}{Q}$ should be small. Fig. 5.7 shows that the sampling interval depends on R. In the calculated examples (Fig. 5.4) however $\omega_p < \omega_c$ so that the effect or R on the sampling interval was suppressed.

In Section 5.3 it has already been explained for the intermediate reach that R which represents the spatial distribution of the inflow, hardly affects the responses. This is in agreement with Fig. 5.7 which shows that in the inter-

mediate reach R hardly affects ω_c (0.75 < $\omega_c Q$ < 1.0) and therefore Δt is practically independent of R.

The amplitude spectrum for the long reach in Fig. 5.7 shows that $f_1(P,R)$ and $f_2(P)$ are smaller than 0.5. Therefore it follows from Eq. 5.8b that t_F/Q must be smaller than 20 for the reach to act as a filter ($\omega_p > \omega_c$).

Unlike the response of the intermediate reach, the response of the long reach is also determined by values of R between 0.5 and 1, so that these values also affect the sampling interval.

6. A LINEAR DISTRIBUTED MODEL OF SURFACE RUNOFF

A complex distributed surface run-off system can be composed of the linear elements as discussed and compared in Section 4 and 5.

Schematically this is represented in Fig. 3.1. In each series the output from one element is the input for the next element. To each element the convolution integral can be applied. The first three moments of the IUH for a series of elements can be obtained by adding the appropriate moments of the elements, while the amplitude density spectrum can be obtained by multiplication and the phase density spectrum can be obtained by summation. These moments and spectra are the characteristics of a series of linear elements.

By studying the change of these characteristics through the series of components it can be decided which component does not significantly affect the response and can therefore be neglected. Also a decision can be made with respect to the required sampling interval.

Because the whole complex system is linear and time-invariant the principle of superposition applies and the responses of all series can be added.

In this approach interactions between the elements cannot be studied, because no internal boundary conditions are built into the distributed model. A next step in the presented development of linear distributed models could be the introduction of such internal boundary conditions between linear elements.

6.1. COMPLEXITY OF THE SYSTEM

Bravo et al (1970) defined the problem of dealing with complex distributed systems as follows: 'Criteria for choosing the general arrangement of elements, size of elements and spatial distribution of rainfall inputs have not as yet been formally established. At present, judgement based on past experience and a feeling for the physical processes which are involved, tempered by the practical need to keep the number of elements reasonably small, has been used as a guide'.

In our linear systems approach to the surface run-off problem the size of the elements is expressed by the model parameter P, while the spatial distribution of rainfall inputs over these elements is expressed by the model parameter R. The filtering effect of each element determines its right to exist in the model. In this way the complexity of the model is determined. The actual filtering of each element follows from the spectra of the input and the impulse response. In Section 5 it was shown that the filtering effect of each system element depends on one hand on the ratio of the duration of inflow to the characteristic

time of the system and on the other hand on the ratio of a coefficient, deter-
mining the shape of inflow to a coefficient, determined by the dimensionless
model parameters P and R. In the short channel reach the spatial distribution
of the inflow can only influence the filtering effect of the model if t_F/Q is
very small, so that $\omega_c > \omega_p$.

In the intermediate channel reach the spatial distribution of the inflow has
little influence on the filtering effect of the system.

It is interesting to note that if the points for a number of British catchments
(Nash, 1960) are plotted in the shape factor diagram for the upstream inflow
problem (Fig. 5.6) these points fall within the range $2 < P < 5$. Nash expressed
the system's response of these catchments in gamma-distributions defined by a
dimensionless parameter n and a characteristic time k. The spectra of these
gamma-distributions and of the impulse responses of the upstream inflow problem
are very similar for $P = n$ and $Q = k$.

This illustrates the feasibility of Nash's lumped model to cope with the
intermediate channel reach where the spatial distribution (R) of inflow has
little effect on the response.

In a long channel reach (high values of P) the spatial distribution of the
inflow (R) strongly effects the system's response. Therefore it cannot be
considered as a lumped system. It can either be divided into a number of
intermediate reaches or the spatial distribution of the inflow must be taken
into account.

When composing a conceptual model for the surface run-off it is advisable to
start with estimates of P for the channel system beginning at the outlet of
the catchment.

In this way every channel section of the catchment can be analysed, so that
conclusions can be drawn about the required complexity of the system. Therefore
it is necessary to estimate the values of the model parameters and because these
depend on the physical characteristics of the system, physical information about
the system must be available.

6.2. COMPUTER PROGRAM

A computer program, written in Fortran IV, consisting of a master control
program and a number of subroutines, has been developed. In this computer
program not only the surface run-off component has been taken into account,
but also the base flow, which consists of flow through the unsaturated zone
followed by flow through the saturated zone, as shown in Fig. 2.1.

The separation of precipitation into precipitation excess and infiltration
has as yet not been achieved.

This report is however restricted to surface run-off.

The complex surface run-off system is composed of the spatially distributed
sub-systems of the catchment. These sub-systems are connected by channel
reaches (Fig. 3.1). The rainfall excess of each sub-system is routed separately
through the channel system to the outlet of the catchment. In this way the
conceptual model of the surface run-off system consists of a number of parallel
series of linear elements. The sequence of calculations for these parallel
series is carried out by a master control program according to the chosen
conceptual model.

Each subroutine calculates the ordinate of the TUH at the end of the intervals.
The histogram ordinates of the corresponding distribution graph are obtained
as the areas between adjacent ordinates of the TUH, using a straight line
approximation between these ordinate values. This distribution graph may
subsequently be convolved with the TUH of the following linear element. In
this way each conceptual element can be either studied separately or in a
series with other elements. The output of each series is stored in the memory
of the computer, so that the results of the whole complex surface run-off
system can be obtained by summation of the outputs of all series.

These results show how the TUH has been changed by the various conceptual
elements in a series, and by comparing the TUH for the various series it can
be clearly seen how the TUH of the whole complex system is composed of the
spatially distributed sub-systems of the catchment.

With the control Data 3200 computer of the Department of Mathematics at the
Agriculutral University, the calculations of TUH for a complex system,
consisting of 25 elements takes about 4 min. Also the convolution of the TUH
with an input in the form of a histogram takes a relatively short time, which
depending on the length of the input is of the order of seconds or minutes.

7. APPLICATIONS

This chapter will discuss some applications of the proposed linear distributed model. To verify this model the following pieces of experimental work were used: Takahashi (1971) on the Kizu River in Japan, Kellerhals (1969) on steep channel networks in Canada and finally a laboratory experiment of the Department of Hydraulics and Catchment Hydrology.

7.1. KIZU RIVER (JAPAN)

Takahashi studied unsteady flow in irrigular open channels. He considered both the effect of storage in regions abutting on the main channel and the effect of large scale horizontal mixing. Figure 7.1 shows the concepts of main channel and dead zone (storage region).
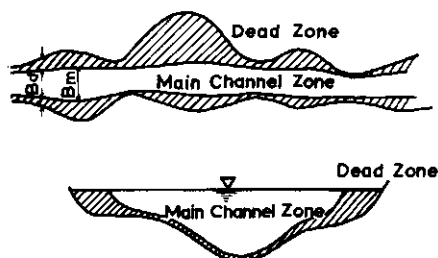
Fig. 7.1 Concept of main channel and dead zone.

Figure 7.2 is a plan of the Kizu River downstream of Kamo.

Fig. 7.2 Plan of the Kizu River downstream of Kano

The discharge has been measured in Kamo, Iloka ($\pm$ 14 km downstream of Kamo). The channel width in the reach from Kamo to Yawata ranges from 260 m to 860 m. In this reach no significant local inflow occurs. Takahashi assumed a Manning's roughness coefficient value $K_m = 25 \text{ m}^{1/3}\text{s}^{-1}$ and $S_o = 0.0008$.

90

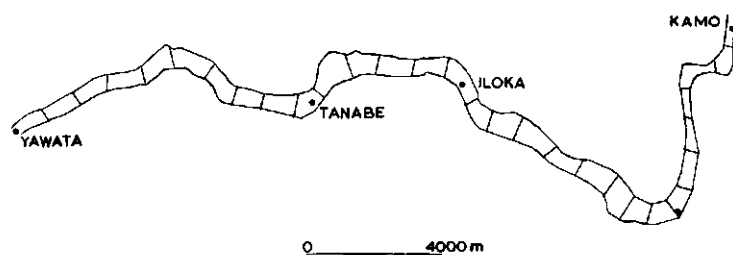From the recorded river hydrograph he further assumed a reference waterdepth of 5 m. In his calculations Takahashi accounted for the above inequality of channel width B_m and storage width $B_d + B_m$. In his study however, the channel profile is assumed to be wide and rectangular with a 5 m reference depth over the whole width. Notwithstanding this simplification, the calculated results compared favourably with those given by Takahashi. Figure 7.3 gives the recorded hydrographs of discharge at Kamo, Iloka and Yawata together with the calculated results for Iloka and Yawata.

Fig 7.3   Experimental results of Kizu River (Takahaski 1971)
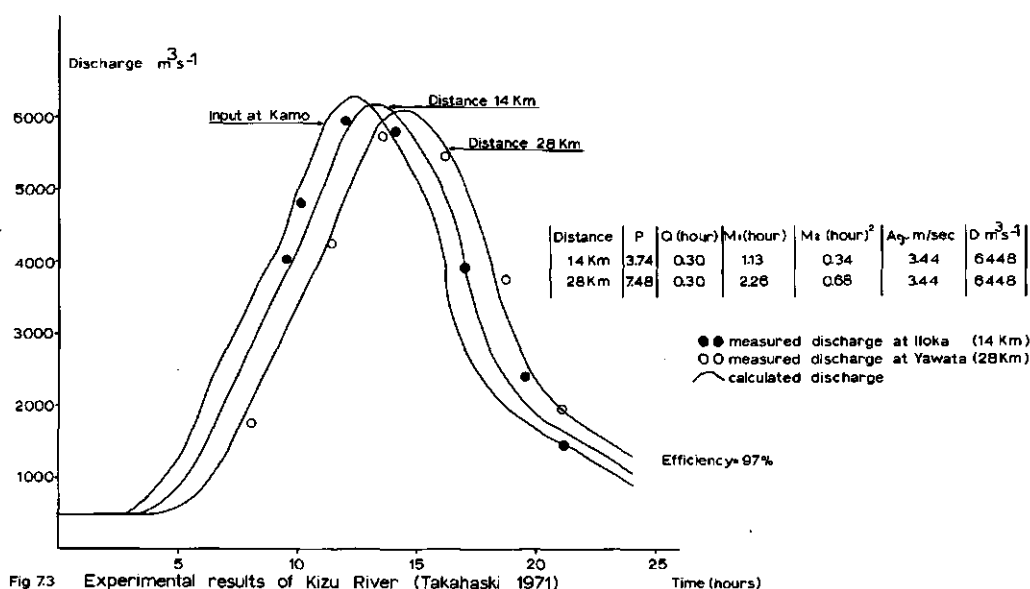
The hydrograph of Kamo was used as the input for a semi-infinite channel (Section 4.4.). The goodness of fit, expressed by the efficiency coefficient, was 97% for both downstream points.

For this upstream inflow problem the incoming wave can be considered as a "Thomas" cosine wave with a wave length $t_F = 25$ h and $\beta = 0.033$ in 4.17 where βt_F^2 is the second moment about the mean of the incoming wave. The second moment of the IUH reads PQ^2 and for the Kamo-Yawata reach $P = 7.48$ and $Q = 0.3$ h. It follows that the attenuation coefficient (Eq 4.17) is $C_A = 0.03$. Introducing this value in Fig. 5.10 we indeed find a negligible attenuation. The same conclusion can be drawn from the spectral analysis as follows:

In Fig 5.10 we find the cut-off frequency ω_p in $\omega_p t_F = 11$ so that $\omega_p = 11/25 = 0.44$ rad hour^{-1}.

In the considered reach the cut-off frequency of the IUH in Fig 4.20 is found

91

for $P = 7.48$ and $\omega_c Q = 1.5$ rad to be $\omega_c = 1.5/0.3 = 5$ rad hour^{-1}.
We find ω_p is much smaller than ω_c and this means (section 2.4.) that there
should indeed be very little attenuation.
The translation expressed in the lag of the model is $PQ = 7.48 \times 0.3 = 2.24$ hours.
This is also in agreement with Takahashi's experimental results.

7.2. PHYLLIS CREEK (ROCKY MOUNTAINS, CANADA)

Kellerhals (1969) combined a "flow equation" $A = a^b$ with a continuity equation
for a tumbling stream consisting of pools and riffles. For his parameters a and
b he found correlations with characteristics which could be derived directly
from the topography of the stream channel and the corresponding catchment area.
He tested his method in a number of mountainous stream-channels where he could
effect inputs of certain shapes and he could measure the resulting outputs.
His data of the Phyllis Creek, located below Marion Lake, have been used here to
find out if the present "diffusion type" model can also be used in this case
of a "tumbling stream". Obviously the normal wave equation 3.5 does not apply
and therefore the physical meaning of an "equivalent" formula like Manning's is
not real anymore. Nevertheless an equivalent Manning coefficient in a wide
rectangular channel derived from Kellerhals' flow equation with the values for
the coefficients a and b and the channel slope S_o as given in his thesis.
Subsequently the reference discharge q_o was used as a free parameter to determine
A and D in the diffusion type equation such that a good agreement between
calculated and observed outflow hydrographs was obtained (Fig 7.4).
Table 5 gives the Kellerhals' data and the derived K-Manning values for the
various channel reaches.

Table 5 : Physically characteristics.

	Length (m)	Width (m)	Slope	K_m (m$^{1/3}$s^{-1})
Gauge 1-2	770	11.48	0.0307	3.30
2-3	716	12.57	0.0488	2.40
3-4	617	12.64	0.0641	2.40
4-6	305	12.88	0.0995	1.90

Kellerhals ascribes the decreasing quality of his calculated results to a non-
linearity which should increase with the number of channel reaches. However the
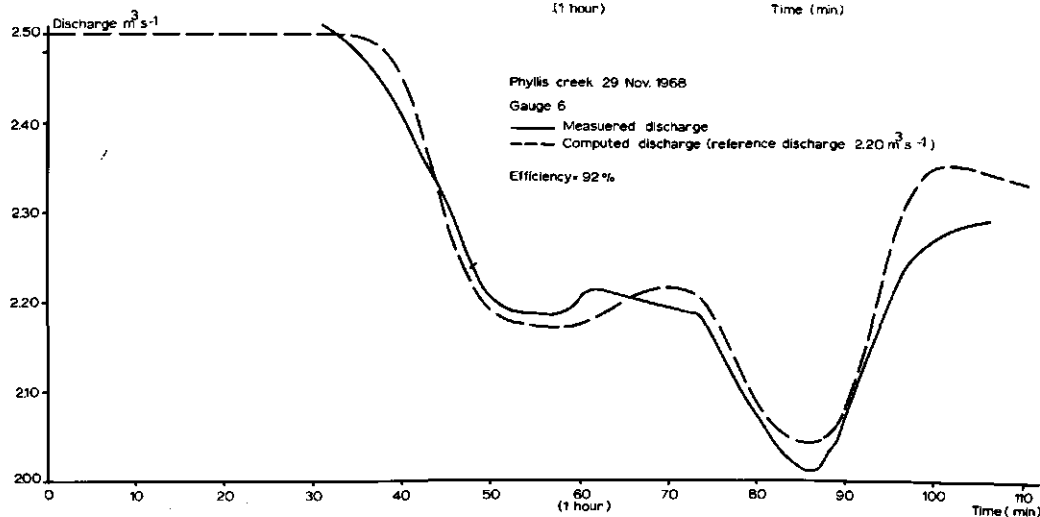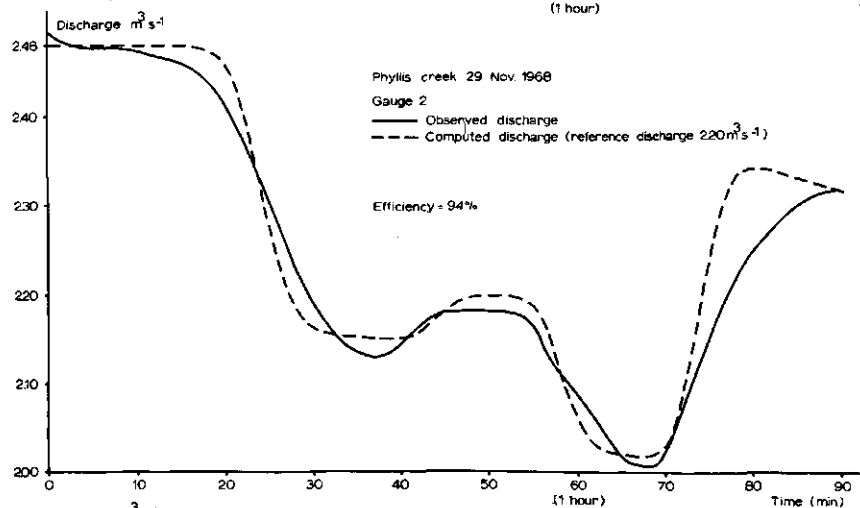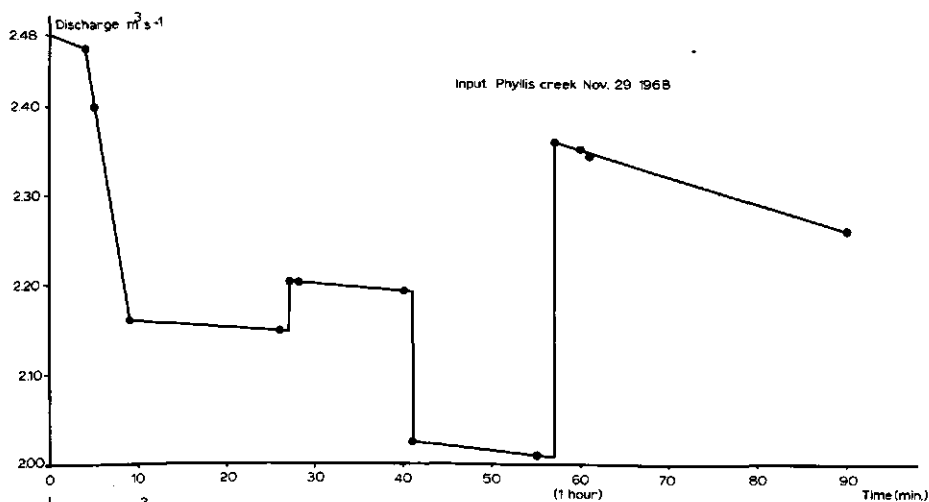linear diffusion type model for this upstream inflow problem appeared to be

Fig 74   Experimental results of Phillis creek (Kellerhals 1969)

93

successful both for short and long channels. The values obtained for the efficiency coefficient were 0.94 and 0.92, respectively against Kellerhals' values of 0.82 and 0.72.

The parameter values $P = 65$ and $Q = 0.3$ min in reach 1-2 yield $M_1' = PQ = 18.5$ min and $M_2 = PQ^2 = 5.3$ min^2 for the IUH. These values indicate the major effect of translation. The same applies for reach 1-6.

7.3. LABORATORY EXPERIMENT

At the Laboratory of Hydraulics and Catchment Hydrology a series of surface run-off experiments were done in a 15 m long tilting flume with rectangular cross-section of 1.02 m width. Over the flume a rainfall simulator, consisting of 184 elements, was constructed. In this way the inflow to the surface run-off system can be distributed in time and space with reasonable accuracy. The outflow was measured at the end of the flume. The hydrograph of outflow presented in Fig 7.5 shows a satisfactory sensitivity of the measurement equipment.

At the upstream end of the channel it was possible to introduce a constant initial flow, upon which the rainfall was superimposed.

An artificial uniform roughness was brought into the channel. From steady state experiments a mean Manning coefficient $K_m = 30.5$ m$^{1/3}$s^{-1} was chosen.

In the experiment the bottom slope of the flume was 0.0025 and the initial base flow was set up at 0.7×10^{-3} m^{3}s^{-1}. In Fig 7.5 the rainfall histogram has been given.

Theoretically this experiment must be represented by the model for fully lateral inflow into a wide rectangular channel (Section 4.3.). Both the results of the complete non-linear solution and of the linear solution with a reference discharge of 1.35×10^{-3} m^{-3}s^{-1} show an efficiency coefficient of about 96%. The computer took about 20 minutes to calculate the non-linear solution and half a minute for the linear solution.

The value of P, 5.2, and Q, 0.34, minute, follow from the physical parameters and it follows from Eq. 4.55 that $M_1' = 1.1$ minute and $M_2 = 0.69$ min^2 for the IUH, indicating both significant translations and attenuation.

For a block input in Section 5.5. the cut-off frequency was given as $\omega_p = \frac{39}{t_F}$, so that in this experiment where t_F varies between 2 and 3 minutes ω_p varies between 13 and 19 rad min^{-1}.

From Fig 4.10e it follows that $\omega_c Q = 2$ rad, so that for $Q = 0.34$ min $\omega_c = 5.9$ rad min^{-1}. In this case $\omega_p > \omega_c$, so the model acts as a filter, which is
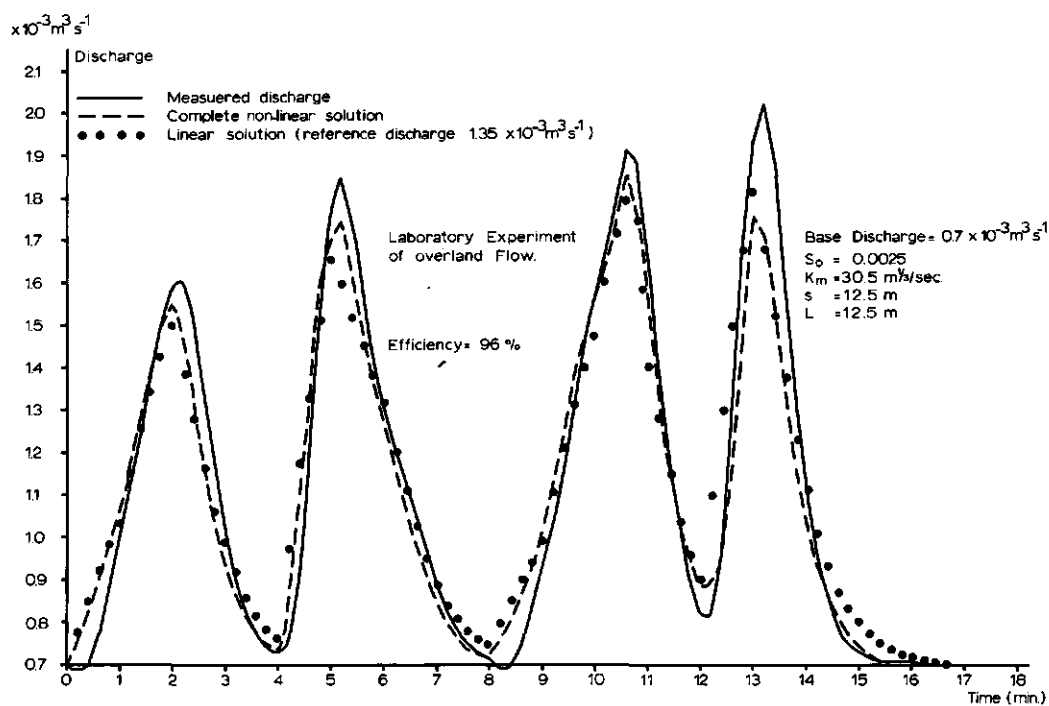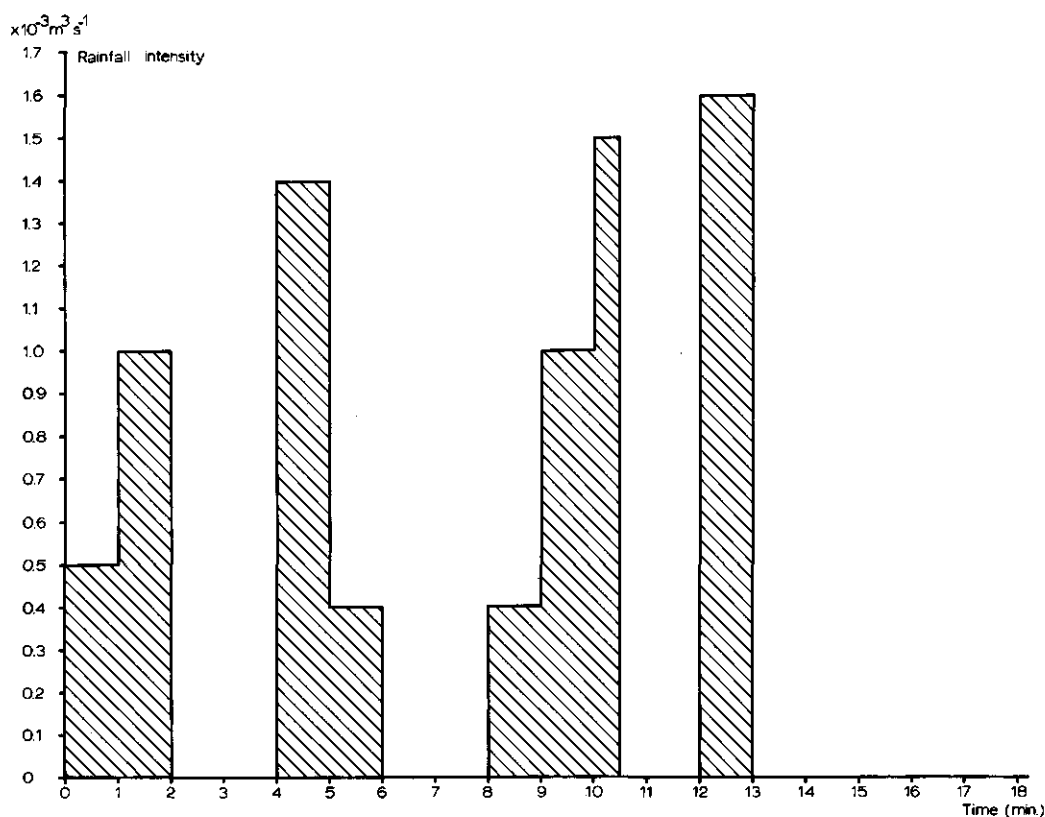
Fig. 7.5 Rainfall run-off relation from a Laboratory experiment

in agreement with the experiment that shows the attenuation of the rainfall histogram. Eq. 4.58 for the attenuation coefficient yields a value C_A 1 à 2, however from Fig 5.9 it is not yet possible to find the specific attenuation, because the empirical curves are not complete. More research has to be done to refine these curves.

In contrast to this experiment, a histogram describing a natural input, such as effective precipitation, will only approximate the true sequence of inflow rates. So the maximum duration of the histogram intervals to give an adequate description of events, should be determined. In this experiment the cut-off frequency ω_c was found to be 5.9 rad min^{-1}. Eq. 5.1 yields the corresponding sampling interval $\Delta t = \frac{1}{\omega} = 0.17$ min.

8. SUMMARY AND CONCLUSIONS

8.1. SUMMARY

A linear distributed model of surface run-off, consisting of a number of linear
conceptual elements, has been developed to calculate the discharge or stage
hydrograph of a complex catchment area from the rainfall excess data distributed
in time and space.

The run-off system is simulated by a network of overland flow and channel flow
elements similar to that proposed by Bravo, et al (1970). The present approach
however differs from the latter because 5 types of linear conceptual elements
have been introduced. Their behaviour is based on a linearized version of the
simplified one-dimensional equation of motion for flow in prismatic channels.
This approach leads to linear diffusion type equations, for the discharge and
water depth. The impulse response of each conceptual element is derived for
the appropriate boundary conditions.

In this way a link is made between the hydrodynamic approach and the linear
systems theory. The following conceptual elements are considered:

a. The overland flow component. This element is considered as an infinitely
   wide rectangular channel subjected to uniformly distributed lateral inflow.

b. The channel flow component, subdivided in the tributary, the partial lateral,
   the fully lateral and the upstream inflow problem.

In the systems approach to the surface run-off component where the model
parameters are expressed in physical characteristics two types of mathematical
models are used. First a two-parameter model for the upstream inflow problem,
where the model parameter P is a dimensionless length parameter and Q represents
the characteristic time of the model. Second a three parameter model for the
lateral inflow problem with the model parameters P, Q and R, where R is a
dimensionless inflow length parameter. For the tributary inflow problem $R = 0$
and for the fully lateral inflow problem and the overland flow problem $R = 1$.
For these special cases the three parameter model is reduced to a two parameter
model

The various conceptual elements, characterized by their impulse response
functions, are classified, analysed and compared according to their shape
factors and spectra.

With these techniques the effect of variations of the inflow in space and time
on the system's response are studied. These effects provide criteria for the
required complexity of the conceptual model and they also provide criteria for

the sampling interval of the input.

Because the hydrodynamic approach is linked to the linear systems theory the model parameters are expressed in the physical characteristics of the surface runoff system (channel length and cross section, bottom slope and friction coefficient) and a chosen reference discharge or water depth. The effect of the reference discharge or water depth on the response of 'Thomas wave' inputs of various durations has been studied. Some linear results were compared with the corresponding complete non-linear solution. An empirical relation between the attenuation coefficient C_A and the specific attenuation of the peak value of the input is suggested for the optimization procedure.

However if for a sub-system the input and output data are known the linear system analysis can be used to derive the model parameters without any knowledge of the physical characteristics, using the simple relation between the moments of input, output and impulse response.

The above theoretical aspects were demonstrated in some simple examples.

8.2. CONCLUSIONS

1. The complexity of a distributed model of surface run-off can be determined by techniques of linear system analysis. Physical information about the surface run-off system should be available.

2. The techniques of linear system analysis show the effect of the model parameters P (the dimensionless length parameter) Q (the characteristic time of the system) and R (the dimensionless inflow length parameter, expressing the spatial distribution of inflow) on the behaviour of each conceptual element in relation to a given input. The following channel classification is introduced:

   a. In the short channel reach the variation of both P and R have a dominant effect on the attenuation of the input.

   b. In the intermediate reach the variation of both P and R have relatively small attenuation and translation effects.

   c. In the long reach the variation of both P and R have dominant translation effects for $0 < R < 0.5$. For $0.5 < R < 1$ an important attenuation effect also occurs.

   The filtering effect of the model for a given input depends on the ratio of the duration of input to the characteristic time Q.

3. The sampling interval of the input depends on the filtering effect of the model and can be derived from the amplitude density spectrum of the impulse response.

4. For one input wave the linear diffusion type solutions were compared with the complete non-linear solutions for the various conceptual elements of the surface run-off model. The results showed good agreement for the presented examples with a proper choice of reference discharge or water depth. The goodness of fit, expressed by the efficiency coefficient R_E, is 90% for most examples.

5. The variation of the reference discharge has a dominant attenuation effect on the model's behaviour for the short reach, a relatively small attenuation and translation effect for the intermediate reach, and a dominant translation effect for the long reach for $0 < R < 0.5$, while for $0.5 < R < 1$ an important attenuation effect also occurs. The magnitude of these effects depends on the ratio of the duration of input to the characteristic time Q of the model.

6. The linear diffusion type solutions for the various conceptual elements, breaks down if the Froude number $F > \sim 2$, assuming Chezy friction and $F > \sim 1\frac{1}{2}$, assuming Manning friction, because then the parameter $D < 0$. Henderson (1966) has however shown that for the steady state for these values of the Froude number rolling waves occur, for which the hydrodynamic considerations, as presented in this report, are not valid. Moreover normally this situation will not occur.

7. The application of the linear theory on the results of experiments in a river in Japan, in a mountainous stream channel in Canada and in a tilting flume in the laboratory shows a good agreement between observed and computed hydrographs.

LIST OF SYMBOLS

dimension

A	= cross-sectional area of the channel	L^2
A_τ	= translation coefficient	L/T
B	= surface width of the channel	L
C	= Chezy coefficient	$L^{\frac{1}{2}}/T$
C_A	= attenuation coefficient	−
c	= celerity	L/T
D	= 'diffusion' coefficient	L^2/T
D_L	= term for the energy dissipation as the lateral inflow mixes with the water already in the channel	−
F	= local Froude number	−
$\tilde{f}(\lambda)$	= Laplace transform of the function $f(t)$	−
$\hat{f}(\omega)$	= Fourier transform of the function $f(t)$	−
$\hat{f}_a(\omega)$	= amplitude density spectrum of the function $f(t)$	−
$\hat{f}_\theta(\omega)$	= phase density spectrum of the function $f(t)$	−
g	= acceleration of gravity	L/T^2
h_q	= impulse response for the discharge	L^2/T
h_y	= impulse response for the water depth	L
$\overline{h}_q$	= dimensionless impulse response for the discharge	−
$\overline{h}_y$	= dimensionless impulse response for the water depth	−
I	= subscript for initial uniform flow	
$i(s,t)$	= lateral inflow per unit length of channel	L^2/T
K	= bottom width of the channel	L
K_m	= Manning coefficient	$L^{1/3}/T$
ℓ	= distance over which the lateral inflow takes place	L
$M'_n(f)$	= n^{th} moment of the function $f(t)$ relative to the origin	T^n
$M_n(f)$	= n^{th} moment of the function $f(t)$ relative to the mean	T^n
m^{-1}	= tangent of the side slope of a trapezoidal channel	−
o	= subscript for reference value	
P	= dimensionless length parameter of the system	−
p	= subscript for perturbation	
Q	= discharge rate	L^3/T
q	= discharge rate per unit width of channel	L^2/T
Q	= characteristic time of the system	T
R	= dimensionless inflow parameter of the system	−
R_A	= specific attenuation	−

100

R	= hydraulic radius	L
R_E	= coefficient of determination or efficiency coefficient	-
S	= slope of the water level	-
S_o	= bottom slope	-
S_f	= friction slope	-
S_n	= dimensionless shape factors	-
S_q	= summation curve for the discharge	L^2/T
S_y	= summation curve for the water depth	L
s	= distance in flow direction	L
T_p	= dimensionless time to peak	-
T	= dimensionless time parameter	-
t_F	= duration of inflow	T
Δt	= sampling interval	T
ΔT	= dimensionless sampling interval	-
t_o	= translation time	T
t	= time	T
u_L	= component of the inflow velocity vector in flow direction	L/T
v	= velocity	L/T
x	= input	
y	= output or waterdepth	
β	= coefficient determining the shape of the inflow graph	
$\delta(t)$ or $\delta(x)$	= Dirac function	
μ_c	= storage capacity	-
ω	= frequency (radian per time interval)	rad/T
ω_c	= upper limit of the filter characteristic	rad/T
ω_p	= cut-off frequency of the input signal	rad/T
Ψ	= unit volume per unit width of channel	L^2

REFERENCES

Abramowitz, M. and Stegun, I.A. (1965). Handbook of mathematical functions.
    Dover Publications, Inc., New York.

Amein, M. (1968). An impliciet method for numerical flood routing.
    Water Resources Research, vol. 4, no. 4, p. 719-726.

Bravo, C.A. et al. (1970). A linear distributed model of catchment run-off.
    M.I.T., Hydrodynamics Laboratory Techn. Report, no. 123.

Chen, C.L. and Chow, V.T. (1968). Hydrodynamics of mathematically simulated
    surface run-off. Department of civil engineering, University of Illinois,
    Hydraulic engineering series no. 18.

Chow, V.T. (1959). Open channel hydraulics. McGraw-Hill Book Company,
    New York.

Chow, V.T. (1964). Handbook of applied hydrology. McGraw-Hill Book Company,
    New York.

Daubert, A. (1964). Quelques aspects de la propagation des crues.
    La Houille Blanche, no. 3, p. 341-346.

Dawdy, D.R. (1969). Mathematical modelling in hydrology. Proceedings of the
    first international seminar for hydrology professores. University of
    Illinois, Urbana, U.S.A., vol. 1, p. 346-362.

Diskin, M.H. (1967). A Laplace transform proof of the theorem of moments for
    the instantaneous unit hydrograph. Water Resources Research, vol. 3, no. 2,
    p. 385-388.

Dooge, J.C.I. and Harley, B.M. (1967). Linear routing in uniform open channels.
    I.A.S.H. Hydrology Symposium, Fort Collins, Colorado, vol. 1, p. 57-63.

Dooge, J.C.I. (1967). The hydrologic system as a closed system. I.A.S.H. Hydro-
    logy Symposium, Fort Collins, Colorado, vol. 2, p. 241-256.

Eagleson, P.S. and Shack, W.J. (1966). Some criteria for the measurement of
    rainfall and run-off. Water Resources Research, vol. 2, no. 3, p. 427-436.

Eagleson, P.S. (1970). Dynamic hydrology. McGraw-Hill Book Company,
    New York.

Fiering, M.B. (1967). Stream flow synthesis. Harvard University Press,
    Cambridge, Mass., 139 p.

Gringorten, I.I. (1960). Extreme value statistics in meteorology, a method of
    application. Air Force Surv. Geophys., 125 p.

Grijsen, J.G. (1971). Een direkte impliciete methode voor de berekening van
    de niet-permanente stroming in open leidingen. Ingenieursscriptie, Afde-
    ling Hydraulica en Afvoerhydrologie, Landbouwhogeschool, Wageningen.

Hamming, R.W. (1962). Numerical methods for scientists and engineers.
    McGraw-Hill Book Company, New York, 303 p.

Harley, B.M. (1967). Linear routing in uniform open channels. M.Eng.Science
    Thesis, National University of Ireland, Dept. of Civil Engineering.

Harley, B.M. and Dooge, J.C.I. (1968). Problems in simulating and evaluating
    various methods of linear flood routing using a small digital computer.
    I.A.S.H. Hydrology Symposium, University of Arizona, Tucson, vol. 2,
    p. 417-426.

Harley, B.M. et al (1970). A modular distributed model of catchment dynamics.
    M.I.T., Hydrodynamics Laboratory Techn. Report no. 133.

Hayami, S. (1951). On the propagation of floodwaves, Disaster Prevent Res. Inst.
    Bull. 1, Kyoto University.

Henderson, F.M. and Wooding, R.A. (1964). Overland flow and groundwater flow
    from a steady rainfall of finite duration. J.Geophys.Res., vol. 69, no. 8,
    p. 1531-1540.

Henderson, F.M. (1966). Open channel flow. Macmillan Company,
    New York.

Kellerhals, R. (1969). Runoff concentration in steep channel networks. Ph.D.
    Thesis, The University of British Columbia, Dept. of Geography.

Nash, J.E. (1959). Systematic determination of unit hydrographs. J.Geophys.
    Res., vol. 64, no. 1, p. 111-115.

Nash, J.E. (1960). A unit hydrograph study, with particular reference to
    British catchments. Proceedings Inst. of Civil Engineers p. 17-249.

Nash, J.E. (1968). A course of lectures on parametric or analytical hydrology
    as delivered at the Universities of Guelph, Ottawa and Queen's University.

Nash, J.E. and Sutcliffe, J.V. (1970). Riverflow forecasting through conceptual
    models, Part 1 - A discussion of principles. Journal of Hydrology, no. 10,
    p. 282-290.

Nes, Th.J. van de and Hendriks, M.H. (1971). Analysis of a linear distributed
    model of surface runoff. Laboratorium voor Hydraulica en Afvoerhydrologie,
    Landbouwhogeschool, Wageningen, Rapport 1.

O'Meara, B.E. (1968). Linear routing of lateral inflow in uniform open channel.
    M.Eng. Science Thesis, National University of Ireland, Dept. of Civil
    Engineering.

Sherman, L.K. (1932). Stream flow from rainfall by the unit-graph method.
    Engineering – News Record, April 7.

Schermerhorn, V.P. and Kuehl, D.W. (1968). Operational stream flow forecasting
    with the SSARR model. I.A.S.H. Pub., no. 80, p. 317-328.

Schönfeld, J.C. (1948). Voortplanting en verzwakking van hoogwatergolven op
    een rivier. Ingenieur, B., Jan. p. 1-7.

Strelkoff, Th. (1970). Numerical solution of Saint-Venant equations. Journal
    of the Hydraulics Division, vol. 96, no. HY3, p. 861-876.

Takahashi, T. (1970). Flood low in an irregular channel. Disaster Prevent Res.
    Inst., Bull. 13 B, March, Kyoto University, p. 299-310.

Vemuri, V. and Vemuri, N. (1970). On the systems approach in hydrology.
    Bulletin of the I.A.S.H., XV, 2 6/(1970), p. 17-38.

Wooding, R.A. (1965). A hydraulic model for the catchment stream flow, part 1.
    Kinematic wave theory. Journal of Hydrology 3, p. 254-267.

Wooding, R.A. (1965). A hydraulic model for the catchment stream flow, part 2.
    Numerical solutions. Journal of Hydrology 3, p. 268-282.

Wooding, R.A. (1966). A hydraulic model for the catchment stream flow, part 3.
    Comparison with run-off observations. Journal of Hydrology 4, p. 21-37.